Lawrence Berkeley National Laboratory
Recent Work

Title

ACTIVE SITES IN HETEROGENEOUS CATALYSIS

Permalink

https://escholarship.org/uc/item/5kf5d44v

Author

Somorjai, G.A.

Publication Date

1976

U U J J 4 4 J / / J 9

ACTIVE SITES IN HETEROGENEOUS CATALYSIS

G. A. Somorjai

January 7, 1976

DISCLAIMER

ACTIVE SITES IN HETEROGENEOUS CATALYSIS

G. A. Somorjai
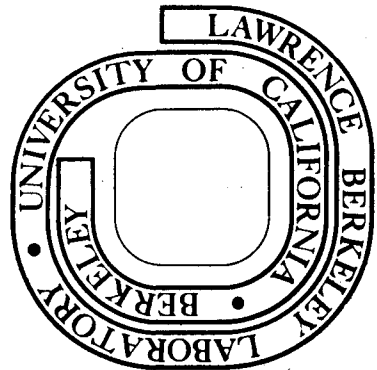
Materials and Molecular Research Division, Lawrence Berkeley Laboratory
and Department of Chemistry, University of California,
Berkeley, California 94720

1. Introduction

The catalytic function of surfaces is exhibited in two ways. The catalyst reduces the potential energy barrier (activation energy) in the path of the chemical reaction, that is otherwise thermodynamically feasible, by forming, temporarily, chemical bonds with the adsorbing molecules. The ability of the surface to break some of the strong chemical bonds of the reactant molecules (for example, H-H, C-H, C-C, C=O, N≡N bonds), bind them with strong enough surface bonds so that the residence time of the adsorbate is sufficiently long for the necessary chemical rearrangement to occur, and then permit the release of the product molecules to make the various active surface sites available for new reactions is one of the essential features of heterogeneous catalysis. It is well known that too strong chemical bonds between the surface atom and the reaction intermediate leads to permanent blocking of the catalyst surface, i.e., poisoning. Too weak chemical bonds between the reactant molecules and the surface will either not permit the crucial bond breaking processes to occur or the adsorbate residence time becomes too short for the necessary and sometimes complex chemical rearrangements to take place.

There is another and equally important function of a good catalyst surface that leads to selectivity. A proper catalyst will facilitate the formation of only one out of many possible reaction products. There may be many thermodynamically possible paths that could yield a wide variety of product molecules. However, the proper catalyst may produce only one product, selectively. This enzyme-like characteristic of heterogeneous catalysis has not been receiving as wide attention as the ability of the catalyst to lower the activation energy of the chemical reaction by forming temporary chemical bonds with the

reactants. Both of these features are the properties of most technologic-
ally important working catalysts, especially those that exhibit ability to
catalyze the production of structurally complex molecules or catalyze
complex molecular rearrangement.

Identification and study of the "active sites" where chemical bond
scission or rearrangement occurs, so crucial to the working of a catalyst,
requires that <u>we investigate the structure and the chemical composition of
the working catalyst on the atomic scale.</u> Ideally, we would like to inspect
each non-identical surface site and determine its structure and chemical
composition while the chemical reaction is taking place.

Over the past 10 years a multitude of new techniques has been developed
to permit characterization of catalyst surfaces on the atomic scale. Low-
energy electron diffraction (LEED) can determine the atomic surface
structure of the topmost layer of the clean catalyst or of the adsorbed
intermediate.[1] Auger electron spectroscopy[2](AES) and other electron spectro-
scopy techniques (X-ray photoelectron, ultra-violet photoelectron, electron
loss spectroscopies, etc.) can be used to determine the chemical composition
of the surface with the sensitivity of 1% of a monolayer (approximately
10^{13} atoms/cm^2). In addition to qualitative and quantitative chemical
analysis of the surface layer, electron spectroscopy can also be utilized
to determine the valency of surface atoms and the nature of the surface
chemical bond. These are static techniques but using a suitable apparatus,
that will be described later, one can monitor the atomic structure and
composition during catalytic reactions at low pressures (less than 10^{-4}
torr). <u>As a result we can determine reaction rates and product distri-
butions in catalytic surface reactions as a function of surface structure
and surface chemical composition.</u> These relations permit the exploration

of the mechanistic details of catalysis on the molecular level to optimize catalyst preparation and to build new catalyst systems by employing the knowledge gained.

Ideally, we would like to study the structure and composition of supported, dispersed catalyst particles in the same configuration

used in/chemical technology. However, the determination of the atomic
surface structure of the/particle that is situated inside the pores of

the high surface area support by low-energy electron diffraction, for

example, is not possible. This technique requires the presence of

ordered domains of 200 Å or larger to obtain sharp diffraction features

necessary to define the surface structure. Even Auger electron emission

that is the property of individual atoms can be obtained even from liquid
surfaces and can only be employed for studies of supported/surfaces with

difficulty. Identification of the active sites does require the deter-
mination of the structure and composition of the/surface, however. To

avoid the difficulties of carrying out these experiments on supported

catalyst surfaces, we have adopted the strategy in our studies of catalyst

surfaces that is used successfully in synthetic organic chemistry and many

other fields of chemistry as well.

We shall prepare the various building blocks of the catalyst surface

and study them separately. Then we put the parts together and the re-

sultant structure should have all of the properties of the working

catalyst particle. Just as in the case of synthetic insulin or the B_{12}

molecule the proof that the synthesis was successful is in the identical

performance of the synthesized and "natural" products. Our building

blocks are crystal surfaces with well-characterized atomic surface structure

and composition. Cutting these crystals in various directions permits us

to systematically vary their surface structure and to study the chemical

reactivity associated with each surface structure. If we do it properly,

all of the surface sites and microstructures with unique chemical activity

could be identified this way. Then, by preparing a surface where all of

these sites are simultaneously present in the correct configurations and concentrations the chemical behavior of the catalyst particle could be reproduced. The real value of this synthetic approach is that ultimately, one should be able to synthesize a catalyst that is much more selective since we build into it only the desirable active sites in a controlled manner.

In our modelling approach to heterogeneous catalysis we carry out studies on well-characterized crystal surfaces first in the following sequence:

Structure of Crystal Surfaces and of Adsorbed Gases

$\uparrow\downarrow$

Surface Reactions on Crystals at Low Pressures ($\leq 10^{-4}$ torr)

$\uparrow\downarrow$

Surface Reactions on Crystals at High Pressures ($10^3 - 10^5$ torr)

$\uparrow\downarrow$

Reactions on Dispersed Catalysts

First we study the surface structure and chemisorption characteristics of crystals cut along different crystallographic orientations. Then a well chosen chemical reaction is studied at low pressure to establish correlations between reactivity and surface structure and composition. Below 10^{-4} torr the surface can be monitored continuously during the reaction with various electron spectroscopy techniques. Then the same catalytic reaction is studied at high pressures (1 - 100 atmospheres) and the pressure dependence of the reaction rate is determined using the same sample over the 9 orders of magnitude range. Finally, the rates and product distributions that were determined at high pressures on single

crystal surfaces are compared with the reactivity of polydispersed small particle catalyst systems. At low pressures a quadrupole mass spectrometer is used as a detector of both the chemical reaction rates and the product distributions.[3] At high pressures a gas chromatograph is employed that is as sensitive as a mass spectrometer that is used at low pressures.[4] Our experiment indicates that small surface area (approximately 1 cm^2) single crystal catalyst samples can readily be used in studies as long as the reaction rate is greater than 10^{-6} product molecules/surface atom/ second. The rate so defined is commonly called "turnover number" in the field of catalysis. Most of the important catalytic reactions — hydrogenation, dehydrogenation, oxidation, isomerization, dehydrocyclization, hydrogenolysis -- have rates usually greater than the detection limit, even at low pressures.

Using this approach to study heterogeneous catalysis on the atomic scale, we have investigated the mechanism of hydrocarbon catalysis by platinum surfaces. We shall describe in detail the results of these studies that are pertinent in determining the nature of the active sites on the surface of this metal. We shall show how the results obtained for platinum may be extrapolated to other catalyst systems. Finally we shall present a model of metal catalysis that has been emerging from our studies of platinum surfaces.

2. The Atomic Structure of Surfaces. Structures of Low and High Miller Index Crystal Surfaces.

Figure 1 shows the schematic diagram of a solid surface. The surface

is clearly heterogeneous on an atomic scale. There are atoms in various positions that are distinguishable by their number of nearest neighbors, atoms in steps and in kinks; there are adatoms and there are point defects, vacancies in the surface. Experimental evidence to the existence of all of these surface species has come mostly from low-energy electron diffraction and field ion microscopy studies. Of these surface sites that are shown schematically in Figure 1, the terrace sites, the kink and step sites are perhaps the most important for purposes of heterogeneous catalysis. The concentration of these sites can be large from 5 to over 50% of a monolayer (10^{13} - 10^{15} sites/cm^2), while the concentration of adatoms and vacancies are very small, less than 10^{-2}%, even at the melting point of most metals.

By cutting single crystals in various crystallographic directions, we can change the relative concentrations of atoms in terraces and steps and kinks. Figure 2 shows a stereographic triangle of a face-centered cubic metal. At the corners the (111), (100) and (110) crystal faces are shown. These are the lowest surface free energy, highest atomic density crystal orientations. When crystals are cut to these low Miller Index orientations, most of the surface atoms will be in terrace positions. The surface will be relatively smooth on the atomic scale and most of the surface atoms have the highest coordination number or number of nearest neighbors possible. One of these surfaces, the (111) face of platinum, is shown/in Figure 3a. schematically

On cutting high Miller Index surfaces at some angle with respect to the low Miller Index surface, the atomic surface structure changes completely. A (557) surface, for example, exhibits periodic steps of monatomic height separated by terraces that are 6 atoms wide. This is shown/in Figure 3b. schematically

The terraces have (111) orientations since they are cut closest to the (111) crystal face while the steps have (100) orientation since the high Miller Index surface is in the direction of the ($\bar{1}$00) crystal face. The high and low Miller Index surfaces, their atomic structure and chemistry will be discussed in some detail below.

On cutting a crystal surface in the middle of the stereographic triangle, a surface structure that exhibits a large density of kinks in the steps will be produced. | One of these high kink density surfaces
[New Paragraph]
is shown schematically in Figure 3c. Platinum crystal surfaces that were prepared in the zones indicated by the arrows at the sides of the triangle, are thermally unstable. These surfaces, on heating, will rearrange to yield the two surfaces that appear at the end of the arrows.

There is reason to believe that the thermal stability exhibited by various low and high Miller Index platinum surfaces are the same for other face-centered cubic metals. There are, of course, differences expected for surfaces of body-centered cubic solids or for surfaces of solids with other crystal structures.

We have found that the chemical reactivity of low Miller Index surfaces of platinum are very different from the reactivity of high Miller Index stepped or kinked surfaces and that the reactivities of surfaces with steps and with kinks in the steps are very different from each other.[5] Thus, it is appropriate to discuss these various surfaces separately. First we shall discuss the atomic structure of low Miller Index surfaces, then we shall discuss the atomic surface structures of high Miller Index stepped and kinked surfaces.

The Atomic Surface Structure of the Clean (111) Platinum Crystal Face

Low-energy electron diffraction studies have revealed that the atoms in this platinum surface are in positions as expected from the projection of the X-ray unit cell to the surface.[5] The diffraction pattern that is exhibited (Figure 4) clearly indicates a six-fold rotational symmetry that is expected in such a surface. Calculations of surface structure from low-energy electron diffraction beam intensities indicate that atoms are in those positions in the surface layer (with respect to the second layer) as indicated by the X-ray unit cell within 5% of the interlayer distance.[6,7]

The Atomic Surface Structure of the Clean (100) Platinum Crystal Face

Figure 5 shows the diffraction pattern associated with the clean (100) platinum surface. There are extra diffraction features in addition to those expected for this surface structure from the X-ray unit cell. This surface exhibits a so-called (5x1) surface structure.[8] There are two perpendicular domains of this structure and there are 1/5, 2/5, 3/5 and 4/5 order spots between the (00) and (10) diffraction beams. The surface structure is not quite as simple as the shorthand notation indicates as is shown by the splitting of the fractional order beams. The surface structure appears to be stable at all temperatures from 25°C to the melting point, although at elevated temperatures carbon can diffuse to the surface and cause transformation of the structure to the impurity stabilized (1x1) surface structure. The same structure is observed for other 5d transition metals that are neighbors of platinum in the periodic table, such as gold and iridium.

The diffraction beam intensities of the (5x1) surface structure are under close investigation in many laboratories. Preliminary calculations favor a model in which the surface atoms assume a distorted, hexagonal configuration by out-of-plane buckling. The apparent (5x1) unit cell is the result of coincidence of the atomic positions of atoms in the surface with atoms of the undistorted second layer below. It has been suggested that the surface reconstruction arises from the high polarizability of these metal atoms which intensifies the driving force towards reconstruction under action of the surface electric field.[9]

We call this Pt(100) surface reconstructed. Surface reconstruction

is defined as the state of the clean surface when it's low-energy electron

diffraction pattern indicates the presence of a surface unit mesh that is

different from the bulk-like (1x1) unit mesh that is expected from the

projection of the bulk X-ray unit cell. Conversely, an unreconstructed

surface has a surface structure and a/(1x1) $\overset{\text{so-called}}{}$ diffraction pattern that is

expected from the projection of the X-ray unit cell for that particular

surface. Such a definition of surface reconstruction does not tell us

anything about possible changes in the interlayer distances between the

first and the second layers of atoms at the surface. Contraction or

expansion in the direction perpendicular to the surface can take place

without changing the (1x1) two dimensional surface unit cell size or

orientation. Indeed, several low Miller Index surfaces of clean monatomic

and diatomic solids exhibit unreconstrcted surfaces but the surface

structure also exhibits contraction or expansion perpendicular to the

surface plane in the first layer of atoms.[9a]

The Atomic Surface Structure of the Clean (110) Platinum Crystal Face

The (110) crystal face, just like the (100) crystal face, is recon-

structed.[10] The surface unit cell is an apparent (1x2) unit mesh indicating

that the lattice unit cell vector is twice as large in one direction while

the same in the other direction as that expected from the projection of

the bulk X-ray unit cell to this surface. Thus, the rectangular surface

unit mesh that would be expected from the projection of the X-ray unit

cell is elongated in one direction while remaining unchanged in the other

direction. This surface has not been investigated to such an extent as

the (111) and (100) crystal faces of platinum. The chemisorption characteristics of various adsorbates
/are certainly less explored than those on the other two low Miller Index

surfaces. However adsorbates which have been investigated, CO and O_2,[10, 10aa] are more strongly bound than on other low index surfaces, thus the valley and ridge structure make this surface adsorb similarly to high Miller Index step surfaces.

The Atomic Surface Structure of High Miller Index Surfaces

Studies of surfaces of high Miller Index and higher surface free energies are important in their own right. It is important to elucidate their atomic structure and stability under a variety of experimental conditions in the presence of reactive and inert gases and in vacuum. Recent low-energy electron diffraction investigations of copper,[11] germanium,[12] gallium arsenide[12] and platinum[13] surfaces indicate that the surfaces of crystals characterized by high Miller Index consist of terraces of low Index planes separated by steps often one atom in height. The ordered stepped surfaces display varying degrees of thermal stability. Figure 6 shows a stereographic triangle of a face-centered cubic crystal depicting the various high Miller Index surfaces of platinum that were studied. The diffraction patter from a high Miller Index surface exhibits diffraction beam doublets that appear at well-defined electron beam energies. Some of the diffraction patterns that are obtained from the high Miller Index surfaces and the surface structures that can be derived from these diffraction patterns are indicated in Figure 7. The terrace widths are calculated from the doublet separation. The step height is obtained from the variation of the intensity maximum of the doublet diffraction beam features with electron energy. The detailed analysis of the surface structure based on these diffraction patterns are described elsewhere.[13] The terrace width does not have to be uniform to obtain satisfactory diffraction patterns. Houston and Park[14] in a theoretical study have shown that there may be a great deal of variation in the step width about an average value still, one obtains a diffraction pattern of

satisfactory quality. That is, if the diffraction pattern indicates that the terrace width is six atoms wide, that does not rule out the presence of a large number of terraces of five or seven atoms wide. Since the re-arrangements of high Miller Index surfaces to ordered low Index terraces separated by periodic steps, takes place regardless of the chemical bonding in the crystal, it may be regarded as a general structural property of high Index surfaces. It is therefore of value to have a standardized nomenclature to identify stepped surface structures.

Stepped surfaces are indicated by the postscirpts, S, so that Pt(S) indicates a stepped platinum crystal surface. The ordered step array can then be completely designated by the widths and the orientations of the terraces and the height and the orientation of the steps. The stepped surface may be designated as Pt(S)-[M(111)xN(100)](where M(111) designates a terrace of (111) orientation and M atomic rows in width and N(100) indicates a stepped (100) orientation and N atomic layers high). Pt(S)-[M(111)x(100)] indicates the structure of various high Miller Index platinum stepped surfaces having step heights of one atomic layer. (The one is not shown in front of the step orientation.) A more detailed description of the nomenclature of more complex stepped structures is given elsewhere.[13]   In Figure 6 the stereographic triangle indicates both the high Miller Index notation as well as the step notation that is more descriptive of the real atomic structure of high Miller Index surfaces.

The thermal stability of the steps is of great interest. We have found that for platinum high Miller Index surfaces show extraordinary thermal stability away from the arrows indicated in Figure 6. These surfaces may be heated above 1200°C where they may disorder. However,

on cooling to 800°C or in that temperature range the ordered step structure
is re-established. Because of the high thermal stability of these surfaces
they must play important roles in catalytic surface reactions that take
place at temperatures appreciably below the temperature at which the sur-
face structure orders by annealing. However,

high Miller Index surfaces in the range of the arrows indicated in Figure 6 facet to crystal surfaces at the end of the arrows. Thus, on heating, a (510) surface will / re-structure into a (100) and (210) surface. This faceting is easily detectable and monitored by low-energy electron diffraction.

Perhaps the most significant property of stepped platinum surfaces is their great reactivity as compared to low Index crystal surfaces. The chemisorption of hydrogen, oxygen and carbon monoxide was studied by low-energy electon diffraction on ordered stepped surfaces of platinum.[15] The stepped surfaces behave very differently during chemisorption from those of low Index platinum surfaces and the various stepped surfaces also behave differently from each other.[15] Hydrogen and oxygen that do not chemisorb easily on the (111) and (100) crystal faces of platinum, chemisorb readily at relatively low temperatures on the stepped platinum surfaces. All in all, these surfaces play important roles in breaking large binding energy chemical bonds (H-H, C-H, C-C, etc.) that would not break readily on low Miller Index surfaces. It appears that steps and kinks are active sites and their chemical properties play an important role in catalytic surface reactions. Much of our discussions of chemisorption and reactivity associated with catalyst surfaces are centered on discussions of properties of atomic sites (steps and kinks) of low coordination number. These properties will be discussed shortly.

3.   Techniques to Study the Relationship Between Reactivity and the Structure and Composition of Surfaces in the Atomic Scale.

Static Techniques

A. Low-energy electron diffraction. A typical low-energy electron diffraction experiment consists of a monoenergetic beam of electrons,

10 to 500 eV in energy, incident on one face on a single crystal (Figure 8). Roughly 5% of the electrons are elastically back-scattered and this fraction is allowed to impinge on a fluorescent screen. If the crystal surface is well-ordered, a diffraction pattern consisting of bright well-defined spots will be displayed on the screen. The sharpness and overall intensity of the spots is related to the degree of order on surfaces.[1] Although the surface may be irregular on a microscopic and submicroscopic scale, the presence of sharp diffraction features indicates that the surface is ordered on an atomic scale, the atoms lying in a plane parallel to the surface characterized by a two-dimensional lattice structure. The size of these ordered domains determines the quality of the diffraction pattern. Because of experimental limitations on the coherence width of the electron beam, ordered domains larger than approximately 500 Å in diameter are not / distinguishable from smaller ones . However, if the ordered domains become significantly smaller than 500 Å, diffraction spots broaden and become less intense. The presence of sharp diffraction features in low-energy electron diffraction/ (Figure 9) establishes that the surfaces are ordered on the atomic scale. In addition, the positions and symmetry of the diffraction spots can be used to determine the two-dimensional periodicity of the surface structure. We can imagine for the moment that the surface structure will be rather like the determination of the bulk structure along the crystal plane, although there may be a rearrangement or reconstruction of the surface atoms from the bulk structure. The presence of the surface destroys the bulk translational periodicity in the direction normal to the presumed planar surface while the translational periodicity of the solid parallel to the surface is retained. The

diffraction pattern gives a representation of the surface reciprocal lattice and the unit cell vectors may be determined from measurement of the beam angles.

The basic complication of surface structure analysis by low-energy electron diffraction comes from the fact that observation of the diffraction pattern geometry serves only to determine the size and shape of the two-dimensional unit cell which characterizes the translational periodicity parallel to the surface.[1] Critical information relating to structural variation in the direction normal to the surface must be extracted from the analysis of the intensity of the diffracted beams. Such an intensity analysis is in priciple required, for example, to determine the packing sequence and interlayer spacing of the top few atomic layers of a single crystal surface.

Low-energy electron diffraction studies of clean surfaces have revealed that most of these surfaces, if prepared under proper conditions, are ordered on an atomic scale and exhibit sharp diffraction beams and high diffraction beam intensities. Metal, semiconductors, alkali halide, inert gas and organic crystal surfaces have been studied this way, and all of these exhibit ordered surface structures.

One of the most exciting observations of low-energy electron diffraction studies of adsorbed monolayers on low Miller Index crystal surfaces is the predominance of ordering within these layers.[18] These studies have detected a large number of surface structures formed upon adsorption of different atoms and molecules on a variety of solid surfaces. Conditions range from low temperature, inert gas physisorption to the chemisorption of reactive diatomic gas molecules and hydrocarbons at room temperature and above. A listing of over 200 adsorbed surface structures, mostly of

small molecules, adsorbed on low Miller Index surfaces can be found in a recent review.[1]

There are two systems to denote the unit mesh of ordered monolayer structures formed upon adsorption. The first system originally proposed by Wood[19] is probably the most commonly used and can be applied to systems in which the angle between the vectors $\vec{a}$ and $\vec{b}$ is the same for the adsorbed structure as for the substrate. The structure is labeled by the general form $p(nxm)R\phi°$ or $c(nxm)R\phi°$, depending on whether the unit mesh is primitive or centered. For example, in Figure 10 the diffraction pattern of a clean platinum (111) surface and a pattern with adsorbed acetylene (C_2H_2) on the (111) crystal face are shown. The structure deduced from this figure is thus labeled p(2x2) having unit cell vectors twice as large as the unit cell of the platinum substrate and pointing in the same direction. The total system is then referred to as $Pt(111)-(2x2)-C_2H_2$.

For cases in which the angle between the unit mesh vectors of the/substrate ordered[2] and the/adsorbate is different, ordered a matrix notation is generally used.[13a] The unit mesh vectors or the adsorbed structure are related to substrate mesh vectors by the transformation

$$\vec{a}' = m_{11}\vec{a} + m_{12}\vec{b}$$
$$\vec{b}' = m_{21}\vec{a} + m_{22}\vec{b}$$

These equations define the transformation matrix, $M = \begin{pmatrix} m_{11} & m_{12} \\ m_{21} & m_{22} \end{pmatrix}$ which is used to characterize the structure. For the structure illustrated in Figure 10 the transformation matrix is $M = \begin{pmatrix} 2 & 0 \\ 0 & 2 \end{pmatrix}$. Using this notation the reciprocal lattice transformation matrix and thus the diffraction pattern can be obtained by taking the inverse transpose of M, $M^* = \tilde{M}^{-1}$ and this

equation can obviously also be used in the reverse direction to obtain the real space unit mesh from the diffraction pattern.

Over the past several years, low-energy electron diffraction theory has been developed that allows us to compute from the diffraction beam intensities the precise locations of atoms or molecules on surfaces. The basic experimental data is the measured intensity of the diffraction beams as a function of electron energy, and the only adjustable parameters are the surface atomic geometry itself. Once the intensity vs. voltage curve (I vs. V) is computed, assuming a certain atomic location in the surface, they are compated with experiments. The computation is repeated using various locations for surface atoms until the best agreement between experiment and theory is obtained. Figure 11 shows the computed and experimental intensities of diffraction beams from platinum (111) clean surface where best agreement between experiment and theory has been obtained. For this surface the atoms appears to be positioned according to the predictable projection of the X-ray unit cell to that particular surface.

There are two major features of the electron-solid interaction evidenced in the I-V profiles and in other scattering data in low-energy electron diffraction that the theory must provide for. 1) In contrast to the case of X-ray scattering, cross-sections for low-energy electrons from atoms are large (on the order of 10 $\mathring{A}^2$/atom) and 2) the incident electrons interact strongly with the valence electrons in the solids resulting in a high probability of inelastic scattering. Features 1 and 2, taken together with the wave-like behavior of the electrons, make low-energy electron diffraction a sensitive probe of the surface atomic

structure. Feature 1, however, renders the use of the simple kinematical, since scattering theory that is used so successfully in X-ray diffraction inadequate in low-energy electron diffraction and necessitates the use of multiple scattering or so-called dynamical theories. Feature 2, on the other hand, means that the electrons are removed from the elastic electron beam due to inelastic collision damping with a characteristic mean free path of 3 to 10 Å. The inelastic collision damping tends to reduce though by no means eliminates the effect of multiple scattering. The presence of multiple scattering introduces secondary maxima in the I-V profiles in addition to the Bragg peaks that are also observed in X-ray diffraction and anticipated from kinematical theory.

Over the past several years the surface structures of several clean monatomic solid surfaces and a variety of adsorbed atoms on solid surfaces have been determined by low-energy electron diffraction.[1] This field of study is now called surface crystallography and it is one of the most rapidly growing field of surface science. By studying the atomic surface structure of clean surfaces and adsorbed molecules, the nature of the surface chemical bond can be explored in a systematic manner.

B. <u>Auger Electron Spectroscopy</u>. If a high energy electron beam $(10^3 - 10^5$ eV) or high energy electromagnetic radiation (X-rays) is allowed to strike a solid surface in addition to electron emission from the valence band, electrons are excited from inner electron shells as well. The two primary electron shell excitation processes that lead to the production of a free electron that can be collected by a suitable detector is illustrated

in Figure 12. The notation we have adopted to designate the electron

energy levels in the atoms is that most commonly used in atomic spectroscopy.

The K, L, M shells refer to those with principle quantum number 1, 2, 3,
respectively,
/ and the subscripts (L_1, L_2, L_3) indicate the multiplicity $\vec{J}$ which is a

vector sum of the angular momentus, $\vec{L}$ and the spin quantum number $\vec{S}$,

$\vec{J} = \vec{L} \pm \vec{S}$.

The electron, upon excitation, is ejected from an inner shell into

vacuum and the energy of the free electron is then measured. This techni-

que is called X-ray photoelectron spectroscopy. If the electron is ejected

from the valence band by ultaviolet radiation, the technique is called

ultraviolet phoroelectron spectroscopy. Excitation energies not greater

than those provided by ultraviolet radiation are necessary for electron

excitation from the valence ban or of electrons from the valence shell of

adsorbed molecules.

Let us turn our attention to the dominant recombination or de-

excitation processes which follow the excitation of electrons from the
(Figure 13)
inner shell or from the valence shell/. The first mode of de-excitation is

the Auger process which leads to further electron emission. The second

mode of de-excitation may result in the emission of electromagnetic

radiation and it is commonly called X-ray fluorescence. In the Auger

transition, the electron vacancy in an inner shell is filled by an electron

from an outer band. The energy released by this transition is transferred

to another electron in any of the electron levels which is then ejected.

Energy analysis of the emitted electrons will give differences in binding

energy between electronic bands participating in the Auger process that

are characteristic of a given element. Analysis of the X-ray fluorescence

spectra gives similar information. It has been found, however, that for light elements the probability of Auger transitions is much greater than the probability of X-ray fluorescence.

In recent years Auger electron spectroscopy,[2] ultraviolet photoelectron spectroscopy[20] and X-ray photoelectron spectroscopy[21] have come to play prominent roles in studies analyzing the composition and bonding at surfaces. These techniques can conveniently be used to determine nondestructively the composition of the surface and changes of the surface composition under a variety of experimental conditions. Since the Auger transition probabilities are large, especially for elements of low atomic number, surface impurities in quantities as little as 1% of a monolayer ($\sim 10^{13}$ atoms/cm^2) may be detected.

The experimental apparatus to detect Auger electron emission that is frequently used at present utilized the goemetry of the low-energy electron diffraction apparatus. Thus, both Auger electron spectroscopy and low-energy electron diffraction studies can be carried out on the same crystal surface by using the same electron optics in two different modes alternately in the same experimental system. In the Auger mode, however, we analyze the energy distribution of the inelastically scattered electrons. Separation of the Auger peaks from the background of secondary electrons is carried out by superposing a small ac signal on a retarding dc potential.[2] Suitable detection | allows the monitoring of the first and second derivative of the electric current as a function of the retarding potential $\frac{dI}{dV}$ and $\frac{dI^2}{dV^2}$. In this way, the Auger peaks or other characteristic energy loss peaks can easily be distinguished from the background of other electron emission processes. The energy at which the Auger peak is detected in

such a spectrum, E (observed), is actually the binding energy difference
of the electronic shells that participate in the process/. (Figure 14) Since the

electronic binding energies are tabulated in most cases inspection of these

tables allows one to determine the element responsible for the energy loss

and the particular electronic transitions that took place. By suitable

calibration with known standards, the intensities of the peaks can be

used for quanitative as well as qualitative surface analysis. 21a A typical

Auger spectrum from platinum   surfaces is displayed in Figure 15.

The presence of small concentrations of carbon   , the most common

impurities on surfaces, are easily discernable. Since both Auger electron

and photoelectron emission are atomic properties, these techniques can be

applied to studies of solid surfaces with various degrees of crystallinity

(foil, crystal, dispersed particles, etc.) and to studies of liquid surfaces

as well.

Transport Techniques

A. <u>Studies of surface reaction rates at low (10^{-7} - 10^{-4} torr) and</u>

<u>at high (10^{3} - 10^{5} torr) pressures.</u> During the past five years new in-

struments have been developed in our laboratory to permit in situ studies

of the reactivity of crystal surfaces at both low and at high pressures. 22a

In all of these experiments small surface area, approximately 1 cm^2 single

crystal or polycrystalline catalyst samples, can readily be used

as long as the reaction rate is greater than 10^{-6} product molecules/

surface atom/second. The scheme of one of these apparati is shown in

Figure 16. At low pressures (10^{-7} - 10^{-4} torr) the reaction rate and

product distributions are monitored by quadrupole mass spectrometer while

the surface structure and composition are determined by low-energy electron

diffraction and Auger electron spectroscopy, respectively, during the surface reaction if desired. Then, a small cup (total volume approximately 10 cm^3) can be placed around the crystal sample that isolates it from the rest of the chamber that can be pressurized to over 100 atmospheres, if desired, during the mixture of gaseous reactants. The high pressure reaction chamber is connected to a gas chromatograph that serves to monitor both rate and product distribution in this circumstance. The structure and composition can be determined in situ by LEED and Auger electron spectroscopy before and after the high pressure experiment once the cup is removed. Crystal samples may be heated during both low and high pressure experiments and a vacuum of 10^{-8} torr can be maintained outside the pressurized cup in the reaction chamber. The effect of adding an impurity or a second constituent (alloying) to the surface on the reactivity, can also be studied in this system. The second constituent may be vaporized at low ambient pressure onto the surface of the crystalline sample from an external vapor source until the desired surface composition is obtained. The crystal surface can be cleaned by ion bombardment that is also available as an attachment on the reaction chamber.

This and similar instruments[34] that allow one to study reaction rates and product distributions on small area crystal surfaces and catalyst surfaces have been used in our studies of the mechanism of heterogeneous catalysis and the nature of active sites. The studies that are primarily concentrated on hydrocarbon reaction as catalyzed by platinum crystal surfaces, will be reviewed below.

B. __Molecular Beam Surface Scattering.__ Another apparatus that is very useful in studies of the mechanism of catalytic surface

reactions is shown in Figure 17. This is/a molecular beam-surface scattering
experiment[22] in which a well-collimated beam of the reactant gas or gas

mixture is scattered from a crystal surface and the products that are

desorbed after a single scattering at a given solid angle are detected

by mass spectrometry. By rotation of the mass spectrometer around the

sample, the angular distribution of the scattered products can be determined.

If the incident molecular beam is chopped at well-defined frequencies,

the time of flight of the incident molecules between the chopper and the

detector is determined by phase shift measurements.[23] This information

yields the residence time of molecules on the surface. Chopping the

product molecules that desorb from the surface permit determination of

their volocity. The experimental variables of this system are the

temperature, atomic structure and composition of the surface and the

velocity and the angle of incidence of the molecular beam. In reactive

scattering experiments the mass spectrometer detects the product distri-

bution and rates of formation of product molecules (reaction probabilities

or single scattering) as a function of the system variables. From the

dependence of the reaction rate on the incident beam velocity (or "beam

temperature") the activation energy for adsorption, if any, is deter-

mined. From the surface temperature dependence of the rate of activation

energy of the surface reaction is obtained. The surface residence time

of the molecules, the kinetic energy and angular distribution of the

products reveals the nature of energy transfer during the gas-surface

interactions.[23]

A detailed description of molecular beam-surface scattering experi-

ments and the results of these studies are given elsewhere.[22,23] Here

we shall discuss only those studies that are important in verifying the
nature of active sites in heterogeneous catalysis.

Cleaning and Preparation of Single Crystal Surfaces

The catalyst crystal samples are generally cut from single crystal
rods that are electron beam zone-refined to obtain low impurity concen-
trations (in the ten parts per million range). The common impurities in
platinum samples are carbon, calcium, phosphorus and sulfur; these must
be removed before commencing with the studies of catalytic reactions.
The catalyst samples were prepared by orienting with a Laue back-reflection
X-ray technique, spark cutting an approximately 1 mm thick slice with the
proper crystallographic orientation exposed and polishing both sides and
etching. The carbon, phosphorus and sulfur impurities can be removed by
oxidation in $5x10^{-8}$ torr of oxygen at ~1000K. The adsorbed oxygen is
removed by heating the sample to 1300K in vacuum. The high concentration
of calcium impurity which possibly remained in the sample from the reduction
of the platinum ore, could only be removed by extensive oxidative heat
treatments. The sample was oxidized at 1500K in 10^{-5} torr of oxygen for
24-48 hours. This treatment fixes calcium on the surface in the form of
a stable oxide which will decompose with calcium vaporization from the
surface upon heating to 1800K. A small amount of calcium impurity may be
removed also by argon ion bombardment at 1100K. The clean platinum sur-
face structure can be identified by both low-energy electron diffraction
pattern and the Laue X-ray diffraction pattern.

The cleaning of the various catalyst samples has to be scrutinized
for each materials studied. For iron, the major impurity is sulfur and
its removal has to be carried out outside the vacuum system in a furnace

in a constant hydrogen flow for a long period of time (days). Trace metallic impurities or nonmetallic impurities may be removed either by argon ion bombardment in the vacuum chamber or by chemical treatment using gas-surface interactions of different types.

We shall restrict our discussion of studies on platinum surfaces that will serve as a model of surface studies of other catalysts.

4.   Chemisorption of Hydrocarbons on Low and High Miller Index Surfaces of Platinum, Iridium and Gold.

Chemisorption of Hydrocarbons on the Platinum(111) and (100) Crystal Faces

The adsorption and ordering characteristics of a large group of organic compounds has been studied on the platinum (100) and (111) single crystal surfaces.[24] Low-energy electron diffraction has been used to determine the surface structures. Work function change measurements have been made to determine the charge redistribution which occurs on adsorption. The molecules which have been studied are acetylene, aniline, benzene, biphenyl, n-butybenzene, t-butylbenzene, cyanobenzene, 1,3-cyclohexadiene, cyclohexane, cyclohexene, cyclopentane, ethylene, n-hexane, mesitylene, 2-methylnaphthalene, napthalene, nitrobenzene, propylene, pyridine, toluene and m-xylene.   The shape and the bonding characteristics of the organic molecules have been varied systematically so that correlations can be made between these properties and their interaction with the metal surface. The two   platinum crystal faces, (111) and (100), that were used as substrates in this study have six-fold and four-fold rotational symmetry, respectively. Thus, we can find out how the atomic surface structure of

the metal influences the nature of chemisorption of the various organic molecules. The adsorption of molecules with molecular dimensions smaller than substrate interatomic distances usually gives rise to the formation of ordered adsorbed structures with the rotational symmetry of the substrate such that the unit vectors of the overlayer are closely related to the substrate unit cell vectors.[25] Thus in most cases local interactions between substrate and adsorbate seems to play a dominant role in determining their adsorption characteristics. However, as the surface density of small molecules is increased adsorbate-adsorbate interactions often become increasingly important as evidenced by continuous two dimensional compressions in the unit cell size for some of the adsorbates.[26]

Studies of the adsorption of large molecules where the molecular size is larger than the interatomic distances in the substrate is especially interesting because of the possibility that localized surface atom-adsorbed molecule interaction may not play a dominant role in the interaction between the substrate and the adsorbate. Large molecules may interact simultaneously with several surface atoms upon adsorption so that the characteristics of the adsorbed layers may be less controlled by the local substrate bond while the adsorbate-adsorbate interaction becomes more predominant. In the extreme, the interaction of these large molecules with metal substrates may be similar to the interaction of large polarizable rare gas stoms, such as xenon with metal substrates.[27,23] The surface structure of adsorbed xenon at high coverage is independent of the atomic structure of the substrate.

We have found that most of the monolayers of organic molecules that were studied did not undergo chemical change on these low Miller Index

platinum surfaces during the adsorption studies that were carried out at low pressures (10^{-9} - 10^{-6} torr) and in the temperature range of 300 - 500 K, but remained intact so that their ordering characteristics and surface structure could readily be studied.

Summary of Experimental Findings

All the organic molecules studied adsorb on both the Pt(111) and Pt(100)-(5x1) surface. The results of adsorption experiments are shown in Tables I. | . Ordering in the adsorbed layer was more pronounced on the Pt(111) surface than on the Pt(100)-(5x1) surface. One of these ordered surface structures, the structure of adsorbed monolayer of benzene on the Pt(111) face is shown in Figure 18. In general, the adsorbed layer is more ordered and causes a larger work function change (WFC, $\Delta\phi$) on adsorption if the incident flux is lower. The work function decreases with adsorption for all the organic molecules studied. This implies that the adsorbed molecules are acting as electron donors to the metal surface. This might be expected since the metal has a high work function (~5.7 V) and all of the molecules studied are polarizable.

The magnitude of the work function change associated with the adsorption of unsaturated hydrocarbons where π-electrons make major contributions to the bonding is in the range of -1.3 to 2.0 volts. Saturated hydrocarbons that were studied produce much smaller work function changes, in the range of -0.9 to -1.2 volts. The largest work function changes was observed during the adsorption of pyridine (-2.7 volts) and reflects the large contribution of the nitrogen lone electron pair and/or the permanent dipole moment to the charge transfer.

The work function change on adsorption for most of the molecules

studied varies approximately inversely with the first ionization potential of the adsorbate.[24] The data is scattered, however there are many types of molecules represented, some in fact have sizable permanent dipole moments.

Several compounds undergo pressure dependent transformations (usually above 10^{-6} torr adsorbate pressure) on the platinum surfaces studied; in fact the transformations occur over unexpectedly long time periods, For instance, at a surface pressure of 10^{-6} torr typical transformation times involve several thousand seconds of exposure. The compound studied which undergoes transition at 20°C as indicated by changes in WFC and diffraction information are benzene, 1,3-cyclohexadiene (dehydrated to benzene on the surface), cyclohexane, n-hexane, cyclopentane, and mesitylene. These transitions are changes in the chemistry of the adsorbate-surface interaction since they occur with only a few of the molecules studied.

The adsorption and ordering characteristics of the various hydrocarbon molecules on the low Miller Index platinum surfaces are discussed in great detail elsewhere. These two surfaces appear to be excellent substrates for ordered chemisorption of hydrocarbons that permit one to study the surface crystallography of these important organic molecules. The conspicuous absence of C-H and C-C bond breaking during the chemisorption of hydrocarbons below 500K and at low adsorbate pressures (10^{-9} - 10^{-6} torr) clearly indicates that these crystal faces are poor catalysts and they lack the active sites that can break the important C-C and C-H chemical bonds with near zero activation energy.

Upon heating the adsorbed organic layers above 550K partial desorption

and partial thermal decomposition of the molecules take place. Thus C-H
and C-C bond breaking on the terrace sites require considerable activation
energy that can be overcome at higher surface temperatures or by the
application of higher reactant pressures. Heating the surface above 900K
results in the formation of a graphitic overlayer that exhibits a diffraction
pattern characteristic of the basal plane of graphite.

Hydrocarbon Chemisorption on High Miller Index(Stepped)Platinum Surfaces

The chemisorption of over 25 hydrocarbons has been studied by low-

energy electron diffraction on four different stepped crystal faces of platinum,[5] the Pt(S)-[9(111)x(100)], Pt(S)-[6(111)x(100)], Pt(S)-[7(111)x (310)] and Pt(S)-[4(111)x(100)] structures.   These surface structures are shown in Figure 7 . The chemisorption of hydrocarbons produces carbonaceous deposits with characteristics which depend on the substrate structure, the type of hydrocarbon chemisorbed, the rate of adsorption, and the surface temperature. Thus, in contast with the chemisorption behavior on low Miller Index surfaces, breaking of carbon-hydrogen and even at 300K and at low adsorbate pressures (10^{-9}-10^{-6} torr), carbon-carbon bonds can readily take place at stepped surfaces of platinum/ Hydrocarbons on the [9(100)x(100)] and [6(111)x(100)] crystal faces form mostly ordered partially dehydrogenated carbonaceous deposits while disordered carbonaceous layers are formed on the [7(111)x(310)] surface, which has a high concentration of kinks in the steps. The distinctly different chemisorption characteristics of these stepped platinum surfaces can be explained by considering the interplay of four competing processes: (1) the nucleation and growth of ordered carbonaceous surface structures, (2) dehydrogenation, i.e., breaking of carbon-hydrogen bonds in the adsorbed organic molecules, (3) decomposition of the organic molecules, i.e., breaking of both carbon-hydrogen and carbon-carbon bonds at steps, and finally, (4) rearrangement of the substrate by faceting. On the [9(111)x(100)] and [6(111)x(100)] crystal faces, processes (1) and (2) predominate. On the [7(111)x(310)] face process (3) predominates, while process (4) is the most important on the [4(111)x(100)] face. The lack of reactivity of low Miller Index surfaces in hydrocarbon reactions indicates the importance of steps in breaking carbon-hydrogen and carbon-carbon bonds so important in various surface reactions of hydrocarbons.

Atomic steps and kinks, i.e. low coordination number sites, are responsible
for decomposition via dehydrogenation and C-C bond breaking of hydrocarbon
molecules that can take place at these sites with near zero activation energy.
In the absence of a large concentration of the low coordination number sites,
the hydrocarbon molecules remain intact below ~450K and at low pressures
(~10^{-6} torr) and their surface crystallography may be readily studied.
However, in the presence of atomic steps and kinks only carbonaceous re-
sidues remain on the surface that are the products of decomposition of the
various hydrocarbon molecules that participate in chemisorption or in surface
chemical reactions. The properties of this carbonaceous residue is also
important in heterogeneous catalysis as will be shown below. Platinum dis-
plays a unique surface chemistry in that low coordination number sites are
predominantly responsible for bond-breaking processes. In the absence of
these sites the low Miller Index surfaces do not exhibit bond breaking at
low temperatures (~450K) and pressures (<10^{-6} torr). Such a marked change
in the chemical activity from surface site to surface site is one of the
major attributes of platinum that is responsible for its unique catalytic
activity. On iridium surfaces as will be discussed later even on low Miller
Index surfaces partial decomposition of hydrocarbons may occur even at low
temperatures and pressures due to the stronger adsorbate-substrate, hydro-
carbon-metal bonds. Even though for other transition metals the chemistry
of low coordination number surface sites is likely to be different from the
terrace atom sites that are predominant on low Miller Index surfaces, the
hydrocarbon molecules may not remain intact on either high or low Miller
Index crystal paces. Platinum and perhaps palladium and nickel are the ele-
ments to show this drastic variation of reactivity when one compares low and
high Miller Index crystal faces at low temperatures and reactant pressures.

The Chemisorption of Hydrocarbons on Gold and Iridium Crystal Surfaces

The chemisorption of hydrocarbons, ethelyene, cyclohexene, n-heptane, benzene and napthalene at room temperature and above, were studied on both the gold (111) and gold [6(111)x(100)] stepped surfaces.[29] The difference in the adsorption characteristics of hydrocarbons on gold surfaces and on platinum surfaces is striking. The various light hydrocarbons studied (ethylene, cyclohexene, n-heptane and benzene) chemisorb readily on the platinum (111) surface. These molecules on the other hand do not adsorb on the gold (111) surface under identical experimental conditions as far as can be judged by changes that occur in the Auger spectra. Napthalene that forms an ordered surface structure on the (111) face of platinum, forms a disordered layer on adsorption on the gold (111) surface.

The stepped [6(111)x(100)] face of platinum reacts readily with all of the adsorbed hydrocarbons and certainly/those that are listed here. with The partially dehydrogenated carbonaceous layers that form as a result of dissociated hydrocarbon chemisorption are larely disordered. In contrast, stepped gold surfaces of the same atomic structure remain inert to adsorption of the light hydrocarbon molecules just as the gold (111) crystal face and the chemisorption behavior of the two types of gold surfaces, low and high Miller Index surfaces, are indistinguishable. Napthalene, however, adsorbs on both gold surfaces and the adsorption behavior indicates dissociative chemisorption. The hydrocarbon fragments that form are strongly bound.

These results indicate that while chemisorption of hydrocarbons on platinum surfaces requires little or no activation energy, chemisorption on gold has large enough activation energy for most hydrocarbons to prevent

adsorption at the studied low pressures (10^{-6} torr) and temperatures (less than 550°C). While the activation energy for surface reactions such as the rupture of C-H and C-C bonds is greatly reduced at atomic steps on the platinum surface, this effect is not at all apparent on gold surfaces.

The chemisorption of acetylene, ethylene, benzene, and cyclohexane were also studied on the (111) and stepped [6(111)x(100)] iridium crystal surfaces.[30] Chemisorption characteristics of the iridium (111) and platinum (111) surface are markedly different. Also, the chemisorption characteristics of the iridium low Miller Index (111) surface and the stepped iridium [6(111)x(100)] surface are markedly different for each of the molecules that was studied. The hydrocarbon molecules form only poorly ordered surface structures on either the (111) or stepped iridium surfaces. Acetylene and ethylene (C_2H_2 and C_2H_4) form surface structures that are somewhat better ordered on the stepped iridium than on the low Miller Index (111) iridium metal surface. The lack of ordering on iridium surfaces as compared to the excellent ordering characteristics of these molecules on the platinum (111) surface indicates either the lack of mobility of hydrocarbon molecules necessary for ordering at these temperatures or a chemical reaction, i.e., decomposition. The observation that C_2H_2, C_2H_4 and C_6H_{12} all yield the same diffraction pattern on the stepped iridium surface regardless of molecular size would suggest that decomposition occurs on iridium substrates even at 200K on stepped iridium surfaces. The degree of decomposition appears to be different on the two crystal

faces at room temperature, being higher on stepped iridium surfaces than on the (111) iridium surface as the differences in surface structure and flash desorption studies indicate.[30] The poorly ordered (2x2) structure which has been observed on Ir[6(111)x(100)] surfaces after adsorption of C_2H_2 and C_2H_4 at room temperature is not found on the iridium (111) surface below 500K. This could indicate a higher degree of dehydrogenation on the stepped surface than on the (111) surfaces .

The difference between the iridium (111) and platinum (111) surfaces in their reactivity to C-H bond breaking as indicated by flash desorption spectra is striking. From the platinum (111) crystal face, ethylene, acetylene and benzene can all be desorbed in large quantities, upon heating. On the iridium (111) surface, however, benzene is the only adsorbate that can be desorbed upon flash desorption. Ethylene remains largely on the surface, only a few percent of it is removed by heating and acetylene cannot be desorbed at all. Only hydrogen evolution is observed under conditions of flash desorption.

The differences between the ordering characteristics of the platinum and iridium (111) surfaces after heating to high temperature (above 800°C) following hydrocarbon adsorption, are marked. Iridium (111) yields an ordered (9x9) coincidence carbon structure. This structure can be attributed to hexagonal overlayers of carbon similar to that of the basal plane of graphite or benzene, deposited on the (111) surface. A similar structure was found on the platinum [6(111)x(100)] surface when this surface was heated to high temperature in the presence of various hydrocarbons. However, on the platinum (111) surface under similar experimental conditions, one observes a ring-like diffraction feature that is characteristic of a

graphite overlayer with rotationally disordered domains.

It appears that the stronger metal-carbon interaction on iridium surfaces imposes the periodicity on the carbon atoms in the overlayer while the structure of the graphite overlayer on the platinum (111) face is independent of the substrate periodicity and rotational symmetry. Ordering of the dehydrogenated carbonaceous residue on the stepped iridium surface is absent when the surface is heated to above 1100K. Atomic steps of (100) orientation appear to prevent the formation of ordered domains that are predominant on the iridium (111) crystal face. The reasons for this are not clear. Perhaps the rate of carbon-carbon bond breaking on account of the steps is too rapid to allow nucleation and growth of the ordered overlayer. On the (111) face, the slower dehydrogenation allows ordering as observed. It is tempting to list the stepped and (111) iridium and platinum surfaces according to their ability of breaking C-H and C-C bonds as $Ir[6(111)x(100)] > Ir(111) \approx Pt[6(111)x(100)] > Pt(111)$. The surfaces at the two ends of this series are not likely to be versatile catalysts in reactions where C-H and C-C bond dissociations are necessary. The stepped iridium surface would decompose the reactants too rapidly and the residue that forms would block the surface rather well to further chemical reaction. The platinum (111) surface interacts with the reactants too weakly and would not efficiently break the chemical bonds. The surfaces in the middle of the series would likely be very versatile catalysts. This contention is, of course, subjected to experimental scrutiny at the present.

5. Chemical Reactions on Platinum Crystal Surfaces

The H_2-D_2 Exchange on Platinum Crystal Surfaces at Low Pressures

·One of the fundamental questions of heterogeneous catalysis is how
surfaces lower the activation energy for simple reactions on an atomic
scale so that they proceed readily on the surface while the same reaction
in the gas phase is improbable. The reaction of hydrogen and deuterium
molecules to form hydrogen deuteride is one of the simple reactions that
takes place readily on metal surfaces even at temperatures below 100K.
The same reaction is completely inhibited in the gas phase by the large
dissociation energy of H_2 or D_2 (103 kcal/mole). Once the H_2 molecule
is dissociated, the successive atom-molecule reaction ($H + D_2 = HD + D$)
in the gas phase still has a potential energy barrier of roughly 10 kcal/
mole. The H_2-D_2 exchange reaction was studied by Bernasek et al.[31]
using platinum single crystal surfaces of low and high Miller Index.
Under conditions of the experiments which put strict limitations on the
residence time of the detected molecules, the reaction product HD could not
be detected from the (111) crystal face. However, the reaction product
was readily detectable from the high Miller Index stepped surface. The
integrated reaction probability (defined as total desorbed HD flux divided
by H_2 flux incident on the surface) is approximately 10^{-1} while HD formation
was below the limit of detectability on the platinum (111) surface (re-
action probability less than 10^{-5}). Thus, atomic steps at the platinum
surface must play controlling roles in dissociating the diatomic molecules.
Figure 19 shows the scattering distributions from both the (111) and the
stepped platinum surfaces. Varying the chopping frequency of
the incident molecular beam has yielded

HD residence times of about 25 milliseconds on a stepped platinum surface at 700K surface temperature. Such long residence time should result in complete thermal equilibration between the surface and the reaction products. Indeed, it was found by experiments that the desorbing HD beam exhibits, cosine angular distribution as seen in Figure 19.

The pressure dependence of the exchange reaction indicates than an atom-molecule reaction or possibly an atom-atom reaction on the surface is the rate limiting step. The absence of beam kinetic energy dependence of the rate indicates that the adsorption of hydrogen does not require activation energy. The surface is able to store a sufficiently large concentration of atoms which react with the molecules by a two branch mechanism. The rate constants for the H_2-D_2 reaction were also determined under conditions of constant hydrogen atom coverage. At lower temperatures (below 600K) the rate constant for this exchange is $k_1 = 2 \times 10^5 \exp(-4.5 \text{ kcal/Rt}) \text{sec}^{-1}$. The rate determining step appears to be a Langmuir-Hinschelwood type reaction between the diffusing D_2 molecules on the surface to a step site where the hydrogen atom is located, where HD is formed by a three center or a two center reaction (subsequent to D_2 dissociation at the step). At higher temperatures, (above 600K) the reaction between an adsorbed hydrogen atom and an incident D_2 gas molecules competes with the low temperature branch. This reaction, thus, appears to follow Eley-Rideal mechanism. The rate constant for this branch is $k_2 = 10^2 x \exp(-0.6 \text{ kcal/Rt}) \text{sec}^{-1}$. The catalyst action of the platinum surface for the exchange reaction is due to its ability to adsorb and dissociate hydrogen molecules with near zero activation energy and to store atomic hydrogen on the surface thereby converting the gas phase molecule-molecule reaction to atom-molecule or an

atom-atom reaction of low activation energy. The detailed mechanism of H_2-D_2 exchange on platinum crystal faces is described elsewhere.[31] Similar techniques are being used to study deuterium exchange with methane and other hydrocarbon molecules to test the C-H bond breaking process on a variety of metal crystal surfaces.

The H_2-D_2 exhange reaction was also studied by Palmer et al.[32] on platinum and nickel surfaces that were prepared as evaporated thin films. They observed angular distributions that are peaked near the surface normal following a cosine $^n\theta_R$ relationship, where θ_R is the angle of desorption from the surface relative to the surface normal. The value of n varies from 2.5 to 4.0 on the different surfaces studied. This angular distribution instead of cosine θ, indicates perhaps incomplete accommodation of the reaction product with the surface. The peaked angular distribution could be related to the presence of impurities such as carbon and sulfur contamination on the metal surfaces. There is evidence from the experiments of Stickney et al.[33] that as the surface is cleaned of sulfur, oxygen or carbon, n approaches unity. Copper, on the other hand, shows noncosine angular distribution for scattered HD even from a clean surface. Unlike for platinum, the adsorption of H_2 or D_2 is activated on a copper surface. The activation energy of adsorption is about 5 kcal/mole as determined by Balooch et al.[34] from the beam temperature dependence of the reaction probability. It would be of importance to measure the velocity of the scattered products in addition to their angular distribution in order to determine the nature of energy transfer between the HD product molecules and the surface prior to desorption. These studies are in progress in several laboratories.

Dehydrogenation and Hydrogenolysis of Cyclohexane on Platinum Crystal
Surfaces at Low Pressures (less than 10^{-4} torr)

In a series of studies, the variation of the turnover number for this reaction (the number of product molecules/platinum surface atoms/second) with the hydrogen to hydrocarbon ratio at a constant hydrocarbon pressure of $4x8^{-8}$ torr was determined. The results are shown in Figure 20 for the several stepped surfaces studied. The reaction rates increase with increasing hydrogen to hydrocarbon ratio. If no hydrogen is introduced into the reaction chamber the catalyst behaves very differently. No benzene is produced and cyclohexene production is reduced greatly. There is also a higher than normal amount of carbon residue on the surface, approximately one monolayer. Pretreating the catalyst in hydrogen and then removing it prior to hydrocarbon introduction does not increase the activity for dehydrogenation or hydrogenolysis.

We shall present the results of the reaction rate studies for dehydrogenation and hydrogenolysis that were obtained on stepped platinum surfaces first.[35] Then we shall present the same rate data obtained for stepped surfaces which have a large concentration of kinks in the step. In Figure 21A the turnover number for dehydrogenation to benzene and hydrogenolysis to n-hexane are shown as a function of step density at 423K. The dehydrogenation rate is independent of step density, while the hydrogenolysis rate increases with increased step density. The hydrogenolysis rate that was measured via the rate of formation of n-hexane, one of the hydrogenolysis products was lower than the rate of dehydrogenation to benzene. The molar hydrogenolysis product distribution, (saturated aliphatic hydrocarbons only), appears to be a $C_6:C_3:C_1 = 1:1:4$. Even though n-hexane is a

minority hydrogenolysis product, it is a reliable measure of the degree

of hydrogenolysis because of its ease of mass spectrometric detection and

it is not formed in a background reaction with the walls of the reaction

chamber. Besides the saturated hydrogenolysis products and benzene, we

found the olefinic products cyclohexene, ethylene, and propylene. Cyclo-

hexene is an intermediate in the dehydrogenation to benzene and its

various reactions will be discussed separately in the next section. The

olefinic product distribution of ethylene: propylene: cyclohexene: benzene

is 10 :1:0.5:1.

The turnover numbers for dehydrogenation and hydrogenolysis on kinked

surfaces are shown in Figure 21B. The kink density is defined as the

number of kink sites per square centimeter (the total number of atoms on

the surface is approximately $1.5 \times 10^{15}/cm^2$). For example, on the Pt(S)-

[7(111)x(310)] surface every third atom along the step should, on the

average, be in a kink position. Therefore, for this surface the step

density is $2.0 \times 10^{14}/cm^2$ and the kink density is approximately $7 \times 10^{13}/cm^2$.

By comparing the turnover numbers with those obtained from stepped surfaces

that were shown in Figure 21A, it appears that the rate of hydrogenolysis

is markedly higher in the presence of kinks. The dehydrogenation rate

is approximately constant and remains unaffected by variation of kink

density while the hydrogenolysis rate increases by an order of magnitude

from a surface that is almost free of steps, Pt(111). The kinks in the

stepped surface appear to be very effective in breaking C-C bonds leading

to much enhanced hydrogenolysis rates. The hydrogenolysis product distri-

butions do not change appreciably with step or kink density, only the rate

increases. The independence of the dehydrogenation rate from the step

and kink density shows that this reaction is indeed structure-insensitive. The hydrogenolysis rate increases with kink density just as with increasing step density, thus, hydrogenolysis appears to be structure-sensitive.

There was always an induction period of 10 to 20 minutes before the benzene product reached its steady state rate of production as detected by the mass spectrometer after the introduction of cyclohexane onto the crystal surface. This is shown in Figure 22 for several catalyst temperatures. The catalyst was initially at 300K. When steady state reaction rates were obtained, the catalyst temperature was rapidly increased (in approximately 30 seconds) to 423K and the reaction rate monitored. This was repeated with heating to 573K and 723K. The benzene desorbed during rapid heating of the catalyst surface is approximately $1x10^{13}$ molecules or less and represents only a small fraction of the carbon on the surface. The steady state reaction rates at a given temperature are the same whether the catalyst was initially at that temperature or another. This induction period coincides with a higher than steady state uptake of cyclohexane. A mass balance calculation on carbon, utilizing the known adsorption and desorption rates of reactants and products during the induction period indicated that carbon was deposited on the surface. The amount calculated agreed reasonably well with that determined by the Auger electron spectra taken after the reaction mixture was pumped from the chamber, since the electron beam may induce polymerization of hydrocarbons and further carbon deposition. The formation of the adsorbed carbon layer always precedes the desorption of benzene and olefinic products. However, the amount of adsorbate changes as a function of temperature. This is shown in Figure 23 . A 4:1 ratio of the carbon 274 eV Auger peak to the platinum

238 eV Auger peak corresponds to a complete monolayer of carbon by calibration with acetylene. The carbon coverage ranges from 0.1 monolayer at 300K to almost 1.0 monolayer at 723K. The line has a slope of 2±0.2 kcal/mole. During and after the reaction this carbon deposit was always present on the surface not only at our low pressure reaction conditions, but also after reactions that were carried out in another apparatus at higher pressures (approximately 200 torr total pressure).

The temperature dependence of the dehydrogenation and hydrogenolysis rates for the various crystal faces at a fixed hydrogen to hydrocarbon ratio of 20:1 is shown in Figure 24. The dehydrogenation rate to benzene decreases slightly at 723K. The rate of formation of olefinic products have a similar temperature dependence as that of the rate of formation of benzene. The hydrogenolysis rate to saturated products increases with increasing temperature and an Arrhenius plot gives an activation energy of 3±0.3 kcal/mole that is the same for all of the crystal faces within our experimental accuracy.

We have found that the dehydrogenation reaction of cyclohexane to form benzene was sensitive to the ordering of the carbonaceous overlayer as shown in Figure 25. Initially, the overlayer was ordered on all of the stepped surfaces that were studied and dehydrogenation yielded more benzene than cyclohexene. The low-energy electron diffraction pattern from the carbon deposit formed on stepped surfaces in 20:1 hydrogen to hydrocarbon reaction mixture at 423K and above has a hexagonal unit cell approximately 5.1 Å on a side. This is about 5% larger than the next nearest neighbor distance of Pt and considerably smaller than the Van der Waal's radius of either benzene (7.3 Å) or cyclohexane (7.6 Å) indicating

that the adsorbed layer is at least partially dehydrogenated and the
diffraction pattern is certainly not due to the intact reactant or product
molecules. Complete dehydrogenation that occurs on heating the adsorbed
layer to above 1000K yields graphitic deposits characterized by ring-like
diffraction features of 2.46 Å unit cell size.   After several hours of
reaction time, the carbonaceous overlayer slowly disorders. Simultaneously,
the rate of production of cyclohexene increases while the rate of benzene
formation decreases until the product becomes predominantly cyclohexene.
As shown in Figure 25 for the Pt(S)-[6(111)x(100)] surface at 423K, the
initial 2:1 benzene to cyclohexene product ratio typical for dehydrogenation
on ordered carbonaceous overlayers becomes 1:3 on a disordered overlayer.
Thus, for all practical purposes, the dehydrogenation on disordered over-
layers produces cyclohexene as further dehydrogenation to benzene is
poisoned.

A small amount of oxygen on a stepped surface is an effective poison
for dehydrogenation. If the catalyst sample was not vacuum reduced at
1375K after oxygen cleaning, approximately 0.1 of a monolayer of oxygen
(by Auger electron spectroscopy) would be left on the catalyst. This
was enough to completely stop the production of benzene and decrease the
cyclohexene production by 50% at 423K on the Pt(S)-[6(111)x(100)]. The
0.1 monolayer coverage would be less than one oxygen atom/step atom if
all the oxygen was adsorbed at the steps. The oxygen was still present
on the surface after 1 hour of reaction at 423K and standard pressure
conditions.

The Dehydrogenation and Hydrogenolysis of Cyclohexene on Platinum Crystal
Surfaces at Low Pressures[35]

The turnover number for the dehydrogenation of cyclohexene to benzene is about two orders of magnitude greater than for the dehydrogenation of cyclohexane. In Figure 26A we plot the dehydrogenation rate as a function of step density. The turnover number increases rapidly with step density indicating that unlike the slower dehydrogenation reaction of cyclohexane, this reaction is structure-sensitive. In Figure 26B the turnover number is plotted as a function of kink density. Although there is a small increase in the dehydrogenation rate, it may be considered insignificant compared to the marked change of rate with step density.

Unlike the dehydrogenation of cyclohexane, the cyclohexene dehydrogenation reaction poisons rapidly on many catalyst surfaces. Using a hydrogen to cyclohexene mixture of 20:1, the rate of dehydrogenation reaches a maximum, then it decreases rapidly as poisoning occurs, the catalysts losing approximately one-half of their activity in 10-12 minutes. Figure 27 shows a representative plot of the turnover number as a function of time. On many catalyst surfaces, particularly on those with (111) orientation terraces, a disordered carbonaceous overlayer forms which poisons further dehydrogenation of cyclohexene. The poisoning is greatly decreased, however, if the carbonaceous overlayer is ordered.

The overlayer is disordered on (111) orientation terraced stepped surfaces while the overlayer orders on surfaces with (100) orientation terraces upon cyclohexene-hydrogen adsorption at 423K. With an ordered overlayer, the rate of dehydrogenation remains high for hours and there is only slow deactivation of these catalysts. On both types of catalyst surfaces the coverage is approximately 1.0 monolayer of carbon after the induction period during the chemical reactions.

Hydrocarbon Reactions on Platinum Crystal Surfaces at High Pressures

(1 to 10^3 torr). Cyclopropane, Cyclohexane and n-Heptane

Perhaps the most significant step in bridging the gap between catalytic reaction studies on crystal surfaces at low pressues on the one hand and on dispersed metal particles at high pressures on the other is represented by high pressure studies of chemical reactions on crystal surfaces. A series of experimental apparatus have been developed that permit us to study catalytic reactions on crystal surfaces at high pressures after suitable cleaning by ultrahigh vacuum techniques and analyzing the surface structure and surface composition by LEED and Auger electron spectroscopy. Detailed descriptions of these equipments are given elsewhere [36a] and a brief description of the most versatile apparatus that allows the study of the reactivity of the crystal surface at both low and high pressures, in situ, is in the experimental part of this paper. Using these various apparati for high pressure studies on crystal surfaces, the turnover numbers and product distributions have been determined for the hydrogenolysis of cyclopropane and cyclohexane, the dehydrogenation of cyclohexane and for the dehydrocyclization of n-heptane. [36b] The purpose of these investigations is to determine the rate equations that govern these reactions at high pressures and compare to the rate rate equations that were determined at much lower pressures on the same crystal surface. This way the mechanism of the same reaction at low and high pressures are compared and attempts are made to analyze the chemical changes that occur over nine orders of magnitude reactant pressure range.

These studies are beginning to produce important kinetic information only in recent years. We shall summarize the experimental information

available from studies of these reactions on the stepped [6(111)x(100)] and low Miller Index (111) crystal surfaces and compare the low and high pressure rates when these data are available.

The hydrogenolysis of cyclopropane was studied at one atmosphere total pressure on the stepped single crystal surface of platinum.[4] The hydrogenolysis of cyclopropane was chosen as the test reaction because of the considerable amount of data and experience which has been collected in studies of this reaction in various laboratories. The rate is relatively high even at room temperature on supported platinum catalysts and only one product, propane, is formed below 150°C, thereby simplifying the analysis of the results. Table II summarizes the results that were obtained and compares our results on stepped single crystal surfaces at atmospheric pressure with those of others obtained using supported platinum catalysts. It appears that at one atmosphere pressure the platinum stepped single crystal behaves very much like a highly dispersed supported platinum catalyst for the cyclopropane hydrogenolysis. In addition, the same studies that were carried out on the platinum (111) crystal face result in identical reaction rates as those found on stepped crystal surfaces of platinum. These observations support the contention that well-defined crystal surfaces can be excellent models for polycrystalline supported metal catalysts. It also tends to verify Boudart's hypothesis that cyclopropane hydrogenolysis is an example of a structure insensitive reaction. The initial specific reaction rates that were reproducible within 10% are within a factor of two identical to published values for this reaction on highly dispersed platinum catalysts. The activation energies that were observed for this reaction, in addition to

the turnover number, are similar enough on the various platinum surfaces that we may call the agreement excellent.

In a series of studies the dehydrogenation and hydrogenolysis of cyclohexane was studied on both the stepped and low Miller Index (111) crystal faces of platinum at a surface temperature of 300°C and a hydrogen to cyclohexane ratio of 20:1. While the rates on the stepped and low Miller Index surfaces were not very different for the formation of benzene and hexane. The formation of cyclohexene was very structure sensitive; its rate being 100 times greater on the stepped surface than on the (111) crystal face. In Table III we compare the initial turnover numbers for the various reactions at low and high pressures that have been studied so far. The reaction rates may change from 3 to 5 orders of magnitude upon changing the total reactant pressure by about 9 orders of magnitude. Work is in progress to determine the rate equation, both at low and high pressures, and to determine the rate constants under these two widely different experimental conditions. These studies should lead to a complete picture of the mechanism of hydrocarbon reactions on platinum surfaces at both low and high pressures.

6. Active Sites for C-H, H-H and C-C Bond Breaking on Platinum Crystal Surfaces

Dehydrogenation of cyclohexane and cyclohexene to benzene occurs readily at low pressures (less than 10^{-6} torr) on stepped platinum catalyst surfaces.[35] This is in contrast with the very slow or negligible dehydrogenation rate of these molecules on the Pt(111) catalyst surface.[36] Thus,

C-H bond breaking takes place at atomic steps, the same steps that are effective in breaking H-H bonds as revealed by studies in this laboratory of the hydrogen-deuterium exchange reaction at low pressures, using molecular beam scattering techniques.[31] Atomic steps on platinum surfaces appear to be the active sites for C-H and H-H bond scissions.

We have been able to identify another active site by studying the ratio of the dehydrogenation rate to hydrogenolysis rate of cyclohexane to benzene and n-hexane, respectively. While the benzene:n-hexane ratio is 3:1 on a stepped surface (with roughly 17% of the surface atoms in step positions), the ratio decreases rapidly with increasing kink density (Figure 21B). Using a set of catalyst surfaces that were cut to maintain the same terrace width (step density equal to $2.5 \times 10^{14}/cm^{2}$), but with variable kink density in the steps, we have found that the hydrogenolysis rate increases linearly with kink density while the dehydrogenation rate remains unaffected. On a Pt(S)-[7(111)x(310)] catalyst surface approximately 30% of the atoms in the step are in kink positions, (in addition to the thermally generated kinks). For this surface the benzene to n-hexane ratio has reached unity. Thus, the microstructure of kinks in the steps is effective in breaking C-C bonds in addition to C-C and H-H bonds. The selectivity of these bond breaking processes at different atomic surface sites on platinum is certainly significant in that the atomic surface structure of platinum may be properly tailored to provide selectivity in chemical reactions where C-H and C-C bond breaking processes are to be separated.

7. <u>The Role of the Carbonaceous Overlayer in Hydrocarbon Reactions on Platinum Surfaces.</u>

During dehydrogenation of cyclohexane and cyclohexene, the platinum crystal surfaces are always covered with a carbonaceous deposit of 0.1-1.0 monolayer judged by the carbon to platinum Auger peak intensity ratio. The coverage appears to increase with increasing reaction temperature, but is rather independent of pressure as indicated by recent high pressure studies on the Pt(S)-[6(111)x(100)] catalyst surfaces in this laboratory. The overlayer coverage also depends on the particular surface reaction, higher molecular weight reactants and products (cyclohexene, benzene, n-heptane, toluene) yield greater coverage than low molecular weight reactants and products (cyclopropane, propane, etc.). Low molecular weight hydrocarbons (cyclopropane, ethane) which do not form carbonaceous overlayers do not readily react on platinum surfaces at low pressures. The build-up of adsorbates during the induction period for cyclohexane and cyclohexene dehydrogenation to benzene indicates the need for the formation of carbonaceous overlayer to obtain the products. This is not a build-up of the product benzene since it will desorb at a two orders of magnitude higher rate as evidenced by the rate of cyclohexene dehydrogenation.

During the dehydrogenation of cyclohexane the carbonaceous overlayer is ordered initially. After a few hours of reaction at 423K, however, the overlayer becomes successively more disordered as judged by its low-energy electron diffraction pattern. The amount of carbon in the over-layer, however, remains constant at approximately 0.3 monolayers as determined by Auger electron spectroscopy. Simultaneously the product distribution in the dehydrogenation reaction changes as well. While benzene is the dominant product in the presence of the ordered overlayer, cyclohexene becomes the major product of the dehydrogenation reaction in

the presence of the disordered overlayer. This is shown in Figure 25. Thus, the disordering of the carbonaceous overlayer poisons the formation of benzene, i.e. the dehydrogenation of cyclohexene, and under the reaction conditions the cyclohexene intermediate becomes the final product. It should be noted that the turnover number for the cyclohexene-benzene reaction is two orders of magnitude higher (approximately 10^{-3}/second) than for the cyclohexane-benzene reaction (approximately 10^{-5}/second). Thus, the presence of the disordered overlayers poisons the fast second step, but not the first slow step in the dehydrogenation of cyclohexane to benzene.

The marked effect of the ordering characteristics of the carbonaceous deposit on the reaction rate is also clearly displayed during our studies of the dehydrogenation of cyclohexene. As shown in Figure 27, there is rapid poisoning of the dehydrogenation rate within minutes as the disordered carbonaceous overlayer forms. However, when the overlayer is ordered (on (100) orientation terraced surfaces), the catalytic activity decreases much more slowly. Again, the poisoning of benzene production is prevented by the formation of an ordered overlayer. Since the platinum catalyst surface is covered with a carbonaceous layer at low as well as at high pressures, we must consider this layer an important part of the surface reaction.

Carbonaceous overlayers can have an important effect in both the catalytic activity and selectivity of a metal surface. Weinberg, Deans and Merrill[37] postulated that the carbonaceous overlayer is the catalytic site for the hydrogenation of ethylene on the Pt(111) surface and similarly by Gardner and Hansen[33] for tungsten stepped surfaces. Yasumori

et al.[39] found preadsorbing acetylene prevents poisoning or restores the activity of a palladium film for the hydrogenation of ethylene. In all three cases, the structure of the carbonaceous overlayer has a marked effect on the catalytic activity in a manner which is not simple site blockage poisoning. Holbrook and Wise[40] found a specific pretreatment of their Pd catalyst which involved oxygen activation and hydrocarbon preadsorption could markedly affect the electivity of an isomerization reaction. The rate of dehydrocyclization of n-heptane, as well as the selectivity to isomerization and hydrogenolysis, was observed in this laboratory[41] to be dependent on the ordering of the carbonaceous over-layer. These observations, in addition to the data presented in this paper indicate that the formation of the carbonaceous overlayer on the catalyst surface can affect the selectivity as well as activity of a catalytic reaction. The presence of these effects at both atmospheric and low pressures and on a variety of metals indicates the importance of the carbonaceous overlayers and the need for their further characterization. This leads to the conclusion that not all carbon on a catalyst surface is deleterious and only amorphous forms cause site blockage poisoning.

8. The Mechanism of the Dehydrogenation of Cyclohexane and Cyclohexene: Expanded Classification of Reactions According to Their Structure Sensitivity.

In dispersed metal catalysts, the metal is dispersed into small particles, the order of 5-500 Å in diameter, which are generally located in the micropores (20-1000 Å) of a high surface area support. This provides a large metal surface area per gram for high, easily measurable reaction rates, but hides much of the structural surface chemistry of the

catalytic reaction. The surface structure of the small particles is unknown; only their mean diameter can be measured and the pore structure could hide reactive intermediates from characterization. Some of the same difficulties also hold for thin films. However, we can accurately characterize and vary the surface structure of our single crystal catalysts and in our reactor the surface composition can also be readily measured; both are prerequisites for the mechanistic study of the catalysis on the atomic scale.

We have been able to identify two types of structural features of platinum surfaces that influence the catalytic surface reactions: (a) atomic steps and kinks, i.e. sites of low metal coordination number and (b) carbonaceous overlayers, ordered or disordered. The surface reaction may be sensitive to both or just one of these structural features or it may be totally insensitive to the surface structure. The dehydrogenation of cyclohexane to cyclohexene appears to be a structure-insensitive reaction. It takes place even on the Pt(111) crystal face that has a very low density of steps and proceeds even in the presence of a disordered overlayer. The dehydrogenation of cyclohexene to benzene is very structure-sensitive. It requires the presence of atomic steps (does not occur on the Pt(111) crystal face) and the presence of an ordered overlayer (it is poisoned by disorder). Others have found the dehydrogenation of cyclohexane to benzene to be a structure-insensitive[42, 43] on dispersed metal catalysts. On our catalyst, surfaces which contain steps, this is also true, but on the Pt(111) catalyst surface, benzene formation is much slower. Dispersed particles of any size will always contain many step-like atoms of low coordination, and therefore, the reaction will display

structure-insensitivity. Based on our findings, we may write a mechanism

for these reactions by identifying the sequence of reaction steps:

$$C_6H_{12}(gas) \quad \text{ordered or} \quad C_6H_{12}(gas) \quad C_6H_6(gas)$$

$$\text{disordered}$$
$$\text{overlayer}$$

$$C_6H_{12}(ads) \xrightarrow{\text{slow}} C_6H_{10}(ads) \xrightarrow[\substack{\text{ordered} \\ \text{overlayer}}]{\text{step}} C_6H_6(ads)$$
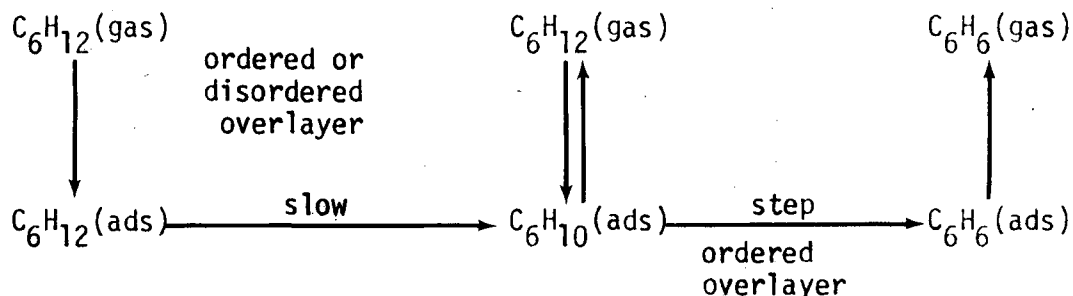
The slow step in the dehydrogenation of cyclohexane to benzene is

the production of the cyclohexene intermediate at these low pressures

on stepped surfaces. Cyclohexene dehydrogenates very rapidly at a step

to form benzene; approximately 1 in every 3 collisions of a cyclohexene

molecule with an unpoisoned step results in the formation of a benzene

molecule. However, on the Pt(111) surface, which is practically free of

steps, the rate of dehydrogenation of cyclohexene had become slow

enough to be rate-limiting.[36] Sinfelt, Hurwitz and Shulman[44] concluded

the dehydrogenation of methylcyclohexane to toluene, a very similar

reaction to cyclohexane dehydrogenation to benzene, was rate limited by

the desorption to toluene. Their arguments are equally valid if the slow

step was the desorption of methylcyclohexene, followed by its very rapid

dehydrogenation to toluene which would be hidden by the pore structure.

Maatman, et al.,[44a] postulated the slow step,,in agreement with out results,

as the formation of an intermediate species. Haensel, et al.,[45] have

observed the intermediate cyclohexene species at very high (approximately

30,000 LHSV) space velocities. This indicates the intermediate is also

found at atmospheric pressure reaction conditions and is very reactive

at the step and edge atoms which must exist on the dispersed metal particles.

In addition to dehydrogenation reactions, hydrogenolysis is also taking place on the platinum surfaces. By monitoring the benzene to n-hexane ratio on the various catalysts as a function of surface structure, we have identified steps as primarily responsible for C-H and H-H bond breaking and kinks for C-C bond breaking in addition to C-H and H-H bond scissions. Thus, hydrogenolysis is initiated at kinks in the atomic steps. Since we need specific surface sites for hydrogenolysis to occur this is also a structure-sensitive reaction. However, hydrogenolysis is insensitive to the state of ordering of the carbonaceous overlayer. It proceeds whether the carbonaceous overlayer is ordered or disordered.

It appears that the classification of structure-sensitive reactions should be expanded to separate those reactions that exhibit step (or kink) sensitivity into one group and those that are also sensitive to the structure of the overlayer, into another group. This expanded classification is shown in Table IV . In addition to the dehydrogenation and hydrogenolysis reactions described in this paper we have included two other reactions that were studied recently. It would be of great value to include in this classification several other hydrocarbon reactions (isomerization, hydrogenation, exchange). More reactions are presently being studied to expand these results on characterized surfaces. Monogue and Katzer[46] Have proposed a subdivision of structure-sensitive (demanding) reactions along very similar lines. 'Primary structure-sensitivity' is the effect of changing particle size or step and kink density. Their 'secondary structure-sensitivity' includes effects of self-poisoning and oxygen impurity on reaction rate. The self-poisoning phenomena is, for hydrocarbon reactions on platinum, at least at low

pressure, the sensitivity of a reaction to the order in the carbonaceous
overlayer. However, caution must be exercised in studies of structure-
sensitivity as the reaction mechanism or the surface structure may change
markedly with pressure, temperature and reactant ratio. Most of the sur-
face structure-sensitivity of various catalytic reactions was derived
from the particle size dependence of the reaction rate on polydispersed
metal catalyst systems. Although there is excellent agreement between
the classifications of the various reactions based on studies using supported
metal catalysts with variable particle size and our studies using various
single crystal surfaces, this may not be the case for all reactions.
Perhaps the step density or the kink density is proportional to particle
size while the ordering characteristics of the carbonaceous overlayer may
or may not be affected by changes of particle size. In addition, studies
similar to those reported on platinum must be carried out using crystal
surfaces of other transition metals to ascertain that these arguments are
more broadly applicable to describe the catalytic chemistry of transition
elements. There is evidence that the heat of adsorption of hydrogen on
palladium crystal surfaces varies markedly with step density[47] while gold
crystal surfaces exhibit chemisorption behavior that is independent of
step density.[29]

9. A Descriptive Model of Hydrocarbon Catalysis on Platinum Surfaces.

Studies to correlate the reactivity and the surface structure and
composition of platinum surfaces indicate that the active platinum crystal
surface must be heterogeneous. The heterogeneity involves the presence
of various atomic sites that are distinguishable by their number of

nearest neighbors (atoms in terraces, in steps and in kinks), and also variation in surface chemical composition. A model that depicts the active platinum surface is shown schematically in Figure 2ₐ. Part of the surface is covered with a partially dehydrogenated carbonaceous overlayer, ordered or disordered, from which 'islands' of platinum clusters protrude. These are the platinum atoms in steps and at kinks that are active in various C-C, C-H an H-H bond breaking activity. Perhaps because of the ease of dissociation and higher binding energy of hydrogen at the steps, these sites and their vicinity remain clean (as long as there is excess hydrogen) and represent areas of high turnover number. The species that form as a result of bond scission at these clusters may rearrange and then diffuse away onto the terrace that is covered with the overlayer, where desorption takes place. Alternately, rearrangement takes place on the ordered carbonaceous overlayer prior to desorption. The heat of desorption should be lower on the portion of the surface that is covered with the overlayer than at an exposed step.

It should be noted that the presence of excess hydrogen is always necessary during hydrocarbon reactions even in those circumstances when the reaction is hydrogen producing (dehydrogenation, dehydrocyclization, etc). It appears that the main role of excess hydrogen is to keep the step and kink sites clean. The reduction of the hydrogen pressure can lead to immediate deactivation as it is frequently experienced in reactor studies.

The discovery that kink sites in steps are effective in breaking C-C bonds in addition to C-H and H-H bonds, thereby initiating hydrogenolysis reactions may also explain the effect of trace impurities or second

component metals that introduce selectivity. Since these kink sites have fewer nearest neighbors than step or terrace sites, they are likely to bind impurities or other metal atoms with stronger chemical bonds. Thus, these sites are readily blocked by impurities. As a result selective 'poisoning" of hydrogenolysis may be obtained by minute concentrations of well-chosen impurities or another metal component.

10. Theory of Low Coordination Number Active Sites on Surfaces

The large difference in the bond breaking ability between various surface sites that are distinguishable by the number of nearest neighbors must be the result of their unique local structural environment and charge density. The charge density at a corner on the surface has been calculated by Kesmodel and Falicov[48] employing the configuration that is depicted in Figure 19 . Their calculations utilized the jellium model for the metal that permits computations of the charge density at the surface self-consistently and also utilized the free electron gas properties of tungsten. At the corner site there is enhanced amplitude of the charged density fluctuation (Friedel oscillation) that leads to an increased potential energy, $\Delta\phi$, for electrons on the corner atom. The magnitude of this potential energy difference for free electrons between the corner sites and away from it depends on the local atomic structure at the surface irregularity. As a result some of the free electrons are displaced away from the corner site leaving there behind a net positive charge. The number of electrons, ΔN, that are removed from the corner sites is proportional to $\Delta N \alpha - \Delta\phi \cdot D(E_f)$ where $D(E_f)$ is the density of states at the Fermi level while the magnitude of $\Delta\phi$ is determined by the local step structure. Thus, there is a large local electric field present at the

corner sites of the order of 0.38 V/$\overset{\circ}{A}$ that should help to further polarize

the incoming molecules that have well-defined polarizabilities and break

them apart. The higher the density of states of the Fermi level, the

larger is the positive charge at the corner site. For transition metals

the density of states at the Fermi level is very large indeed while for

nontransition metals $D(E_f)$ can be quite small. Some of the values of

$D(E_f)$ that have been determined are Pt: 2.1 e/V/atom, Ni: 1.1, W: 0.7,

Cu: 0.4, Au: 0.3. These values yield ΔN of -0.6, -0.3 and -0.2 for Pt, Ni

and W taking $\Delta\phi = 0.3$ volts. Thus, for metals with large values of $D(E_f)$

there are large variations of charge density at surface irregularities

(i.e., low coordination number sites). For gold, on the other hand, ΔN

is about -0.09. Thus, surface irregularities do not show much charge

density variation with respect to atoms at surface sites away from steps.

Therefore the surface is likely to present uniform charge density to the

incoming reactants and is homogeneous regardless of variations of surface

sites. These conclusions are certainly supported by our experiments of

chemisorption and chemical reactions on platinum, gold and iridium sur-

faces. While surface irregularities like atomic steps have different

chemistry for platinum and iridium, both metals with high density of

states, gold surfaces show the same chemical behavior regardless of surface

atomic structure.

For platinum C-H, H-H and C-C bond breaking occurs predominantly at

low coordination number sites (steps and kinks) at low pressures and

temperatures while atoms in terraces are relatively inactive under these

experimental conditions. Thus, the bond scission activities for these

three bond breaking processes could be identified by experiments on low

and high Miller Index surface with relative ease due to the marked change in reactivity with step and kink density. For iridium and for that matter for most transition metals to the left of platinum, in the periodic table, C-H, H-H and C-C bonds may be broken on atomic terraces as well due to the increased M-C and M-H bond energies. Thus, distinguishing between the chemical activities of surface sites of different coordination number may be somewhat more difficult. Detailed experimental analysis of the chemical behavior of different surface sites on cobalt, iron, rhodium and ruthenium, etc. surfaces is yet to be carried out. It is likely that larger binding energy diatomic molecules, CO and N_2, should perhaps be more sensitive probes of the bond breaking abilities associated with different low coordination number sites of these elements than hydrocarbons with weaker chemical bonds.

While low coordination number sites, steps and kinks, are the active sites for bond breaking in platinum, the atomic terrace sites with larger coordination numbers may also become active sites with unique chemistry. for other elements. It will perhaps become possible to identify the bond breaking ability of various coordination number sites of a given metal in breaking H-H, C-H, C-C, C=O, N≡N, etc. chemical bonds. By variation of the atomic surface structure that would change the relative contentrations of the different coordination number surface sites, the product distribution in surface chemical reactions may be markedly varied.

Falicov and Tsang[9] have calculated the charge density distribution at corner sites in ionic and rare gas crystal surfaces. For ionic solids, low coordination number surface sites should have large charge density variations and even changes in interionic distances at steps when compared to sites away from steps. On rare gas crystal surfaces, the charge density

appears to be uniform independent of atomic irregularities. These calculations, no doubt, will be subjected to experimental scrutiny in the not too distant future. Results similar to that obtained by Falicov et al. for corners on metal surfaces were obtained by K. Johnson using $X\alpha$ computational methods. Calculations are also being carried out to determine the lattice vibrational spectrum (phonon spectrum) and the mean square displacement associated with surface atoms in steps and kinks. [52a]

One would expect that the local field experienced by a transition metal ion deriving from (1) the self-consistent field of the s-electrons and (2) the crystal field from the lattice to be different depending on the ion's position; in the bulk, on the plane surface or near a step corner. This local field has two major effects: (1) causing a sizable electron transfer from the stepped corner to the bulk or vice versa, (2) producing different d-orbital level splittings and different d-orbital occupations depending on the position of the metal ion. Tsang and Falicov[50] have calculated the energy levels of d-electrons at different corner sites when the crystal field is turned on. These calculations made across the periodic table for ions with different number of d-electrons namesly V^{2+}, Cr^{2+}, Fe^{2+}, Co^{2+}, Ni^{2+} and Cu^{2+}. The d-electron wave function is a product of the radial and the angular part. Assuming that the radial part is constant, they display the resultant constant contour of the angular part for these various ions. These contours clearly indicate that the stereo-chemistry of the corner atom can be quite different from that of a surface atom therefore a different kind of bonding is favored at different sites. The results of their calculations have been applied to explain the large differences between the catalytic activity of platinum

and gold at atomic steps.

Studies of the charge density, the energy and the spatial arrangement of localized electronic orbitals at low coordination number surface sites (i.e, steps and kinks) appears to be an important and challenging area of theoretical surface chemistry. The effect of surface irregularities on orbital symmetry considerations, so important in chemical reactions, may further elucidate the unique chemical activity of these assymetric sites. Although potential energy surface calculations either by trajectory or by transition state methods for surface reactions are in their infancy, these computations should be of great value to obtain theoretical insight into the dynamics of surface reactions. Experimental determination of surface reaction rate constants, activation energies and pre-exponential factors are slow in coming; however, there are enough data available at present to provide tests for surface reaction theories. This is certainly the case for the H_2-D_2 exchange reaction on various surfaces as the data for this reaction and for others has been reviewed and tabulated recently. It is hoped that theoretical models that will be developed will take into account the heterogeneity of the surface and the unique chemical activity associated with low coordination number surface sites of various local atomic structure and symmetry.

Perhaps one of the important conclusions of these studies that point to the unique chemistry of surface irregularities; steps and kinks that appear to be active sites, is the controlling influence of the local atomic structure, local surface composition and local bonding between absorbates and surface sites. The microstructure of the metal surface controls bond scission and thus the rate and path of chemical reactions. Calculations taking into account this local bonding picture should help

to unravel the elementary bond breaking steps in catalytic surface reactions.

Active Sites on Non-Metallic Surfaces

On transition metal surfaces much of the chemical activity that results in the breaking of large binding energy chemical bonds (C-H, C-C, etc.) is likely to be associated with surface sites of low coordination number (steps and kinks). The question arises to what extent these low coordination number sites are responsible for bond scission in non-metallic catalyst surfaces such as oxides and various other semiconductors. Experimental studies over the past several years indicate that low coordination number surface sites are also chemically active in non-metallic surfaces. Stone et al.[51] have studied the decomposition of methanol and formic acid on doped MgO surfaces. Doping with cobalt and other metals changes the surface composition and introduces excess vacancies at tetrahedral sites. The decomposition of hydrocarbons has been markedly enhanced with increasing concentrations of these low coordination number defect sites. Cimino and Indovina[51a] in a similar study found doping MgO with Mn increased the concentration of surface defect sites and increased the rate of N_2O decomposition and CO oxidation. Boudart et al.[51b] found H_2-D_2 exchange occurs at specially prepared defect sites on an MgO surface. Thus defect sites on oxide surfaces, similar to steps on metal surfaces, have greater catalytic activity.

Studies of the sticking probability of oxygen on silicon surfaces revealed a change from 10^{-5} to 1 with increasing density of surface steps.[52] Crystals with large density of steps may be prepared by cleavage and their chemistry can be readily studied. Ibach has associated the increased activity of dissociatively chemisorbed oxygen to the presence of electron orbitals that became available on silicon atoms at low coordination number step sites on surfaces.

Even in the absence of a free electron gas that causes charge redistribution at low coordination number sites on metal surfaces there are strong chemical effects associated with atoms in surface irregularities.

The rehybridization of localized electron orbitals should have a marked
effect on the chemical bonding at these sites. These are indicated by
experiments on MgO and silicon surfaces as well as by calculations of
crystal field splitting of metal ions in steps and charge distribution at
corners or ionic crystal surfaces. It is likely that low coordination
number sites are active sites for breaking of chemical bonds of various
strength and types of non-metallic surfaces as well. Clearly, studies
of the surface chemistry associated with low coordination number sites in
non-metallic surface is an important area of exploration of catalysis
science.

11. Aspects of Enzyme Catalysis on Metal Surfaces

Our studies of hydrocarbon reactions on platinum surfaces when
coupled with Auger electron spectroscopy determinations of the composition
of the reactive surface indicate that the catalyst surface is covered
with a carbonaceous deposit during the surface reaction either at low or
at high pressure. Thus the reaction intermediates and products form in
the presence of, or perhaps with the participation of, these carbonaceous
residues. Studies by Hansen et al.[53] of ammonia decomposition on tungsten
surfaces also indicate that the reactive metal catalyst surface is covered
with nitrogen or nitrogen-tungsten compounds during the surface reaction.
During the oxidation of ammonia on platinum surfaces there is evidence by
Auger electron spectroscopy that tenaciously held chemisorbed nitrogen or
nitride is present on the surface during the chemical reaction.[54] It is not
too difficult to rationalize the necessary presence of such an overlayer
by surface thermodynamic arguments. The total surface free energy of
metal surfaces would be lowered by the presence of carbon or nitrogen

contamination or other deposits. The surface segregation of impurities such as calcium, carbon or sulfur are well demonstrated by electron spectroscopy studies. The driving force for surface segregation of these impurities on metal surfaces largely comes from the lowering of the surface free energy of the metal catalyst system due to their presence. Thus, the catalyst activity is associated <u>not</u> with the metal surface but with the metal-carbon on metal-nitrogen, i.e., the metal-adsorbate system. It is perhaps misleading to consider the metal alone as providing the catalytic surface as one ought to scrutinize the surface properties of the catalyst in the presence of the reaction mixture. In this circumstance the surface carbonaceous overlayer or other deposit attributable to the reactant is likely to be an active participant in creating the active catalyst surface.

More importantly, the carbonaceous deposit on the platinum catalyst surfaces was often ordered, and ordering imparted to it unique properties. The presence of an ordered overlayer eliminated the poisoning of dehydrogenation reactions (C_6H_{10} to C_6H_6). The dehydrocyclization of n-heptane to toluene would only occur in the presence of the ordered carbonaceous overlayer that must form during the course of the reaction. On platinum crystal surfaces where ordering of the hydrocarbon residue was inhibited by either the atomic surface structure of platinum or by the reaction conditions, dehydrocyclization could not occur at all in competition with the much more facile hydrogenolysis or isomerization reactions.

It appears that complex molecular rearrangements on the surface require the presence of an ordered overlayer or template to compete successfully with other simpler reactions that take place at an appreciably

faster rate. The rates of hydrogenolysis or isomerization reactions are about one order of magnitude faster than the denyarocyclization rate of n-heptane to toluene at low pressures and also markedly more facile at high pressures. It is not unreasonable to suggest that the ordered overlayer provides the template for slower, more complex chemical re-arrangements during the course of the surface reactions by providing sites at proper distances and symmetry communsurate with the molecular dimensions and structure of the complex product to be formed. Future studies must explore the precise experimental conditions for ordering of the carbon-aceous overlayer, its composition and the unique relationship between its structure and that of the product molecules. It is likely that this simple mechanism for product selectivity is also the property of other catalyst surfaces that are employed in hydrocarbon reactions or in re-actions of nitrogen and oxygen containing compounds both in reducing and oxidizing environments. Perhaps these overlayer structures provide the bridge between heterogeneous catalysis and enzyme catalysis.

12. Possible Correlations Between Homogeneous and Heterogeneous Catalysis

Heterogeneous catalyst surfaces with their multitude of irregularities, steps and kinks, of various configurations provide ready sites for bond-breaking processes of many types that may occur simultaneously. Homogeneous catalysts that consist of a single metal atom surrounded by ligands cannot easily match the varied reactivity of the heterogeneous surface especially in breaking strong chemical bonds of different types. However, there are similarities between the homogeneous and heterogeneous systems that are already apparent. Internal rearrangement of the molecule that results in exchange among the surrounding ligands is much faster, and takes place on

a time scale much shorter than the exchange of the ligand with external molecules. Likewise, rearrangement of adsorbed molecules takes place much faster than desorption of the final product on heterogeneous surfaces. Thus, rearrangement on the surface of both heterogeneous and homogeneous systems is fast compared to external chemical exchange. We should increase the surface area of the homogeneous system and provide metal-metal bonds to further increase the similarity. Metal clusters, i.e., molecules with several metal atoms joined together and then stabilized by suitable ligands, are likely to approximate the catalyst activity of the heterogeneous systems. Clusters of this type, even bimetallic clusters, have already been synthesized. It appears that the assymetric structure of a step or kink is important in providing the charge density distribution and orbital configuration necessary to break strong chemical bonds. Assymetric clusters might be able to exhibit bond breaking acitivty similar to that of steps and kinks on metal surfaces.

We may then view the relationship between homogeneous, heterogeneous and enzyme catalysis as depicted in Figure 29. The two dominant features of heterogeneous metal catalysis, the importance of low coordination number sites to break chemical bonds and the structural properties of overlayers that control the path of more complex surface reactions, are the bridges between these fields. Future studies will verify how well these views are justified.

Acknowledgement

References

1. L. L. Kesmodel and G. A. Somorjai. MTP International Review of Science, 1975.

2. F. J. Szalkowski and G. A. Somorjai, Adv. High Temp. Chem., 4, 137 (1971).

3. B. Lang, R. W. Joyner and G. A. Somorjai, J. Catalysis, 27, 405 (1972).

4. D. R. Kahn, E. E. Petersen and G. A. Somorjai, J. Catalysis, 34, 294 (1974).

5. K. Baron, D. W. Blakely and G. A. Somorjai, Surface Sci., 41, 45 (1974).

6. L. L. Kesmodel and G. A. Somorjai, Phys. Rev. B. 11, 630 (1975).

7. P. C. Stair, T. J. Kaminska, L. L. Kesmodel and G. A. Somorjai, Phys. Rev. B. 11, 623 (1975).

8. A. E. Morgan and G. A. Somorjai, Surface Sci., 12, 405 (1968).

9. D. G. Fedak and N. A. Gjorstern, Surface Sci., 3, 77 (1967) and A. Ignatiev, A. V. Jones and T. N. Rhodin, Surface Sci., 30, 573 (1972).

9a. M. R. Martin and G. A. Somorjai, Phys. Rev. B. 7, 3607 (1973).

10. C. W. Tucker, J. Am. Phys., 35, 1897 (1964).

10a. W. P. Ellis and R. L. Schwoebel, Surface Sci., 11, 82 (1968) and Surface Sci., 30, 573 (1972).

10aa. H. Bonzel and R. Ku, Surface Sci., 33, 91 (1972).

11. J. Perdereau and G. E. Rhead, Surface Sci., 24, 555 (1971).

12. M. Henzler, Surface Sci., 19, 159 (1970) and Surface Sci., 22, 12 (1970).

13. B. Lang, R. W. Joyner and G. A. Somorjai, Surface Sci., 30, 440 (1972).

14. J. E. Houston and R. L. Park, Surface Sci., 26, 269 (1971).

15. B. Lang, R. W. Joyner and G. A. Somorjai, Surface Sci., 30, 454 (1972).

16. G. A. Somorjai, Proc. of the Battelle Cong. on Heterogeneous
     Catalysis. To be published 1976.

17. H. H. Farrell and G. A. Somorjai, Adv. Chem. Phys., 20, 215 (1971).

18. G. A. Somorjai, Surface Sci., 34, 156 (1973).

19. E. A. Wood, J. Appl. Phys., 35, 1306 (1964).

19a. R. L. Park and H. H. Madden, Surface Sci., 11, 188 (1968).

20. D. E. Eastman, Phys. Rev. B. 3, 1769 (1971).

21. K. Siegbahn et al. ESCA. Almquist and Wiksells, Uppsala, 1967.

21a. P. Palmberg, et al. Handbook of Auger Electron Spectra. Physical
     Electronic Industries, Edna, Minn., 1972.

22. S. B. Brumbach and G. A. Somorjai, Crit. Revs. in Solid State Sciences,
     4, 429 (1974).

22a. D. W. Blakely, B. A. Sexton, E. Kozak and G. A. Somorjai, To be
     published 1976.

23. S. L. Bernasek and G. A. Somorjai, Prog. in Surface Sci., 5, 377 (1975).

24. J. L. Gland and G. A. Somorjai, Adv. in Colloid and Interface Sci.,
     To be published 1976.

25. F. J. Szalkowski and G. A. Somorjai, J. Chem. Phys., 54, 389 (1971).

26. J. C. Tracy and P. W. Palmberg, J. Chem. Phys., 51, 4852
     (1969).

27. M. A. Chesters and J. Pritchard, Surface Sci., 28, 460 (1971).

28. A. Ignatiev, A. V. Jones and T. N. Rhodin, Surface Sci., 30, 573 (1972).

29.   M. A. Chesters and G. A. Somorjai, Surface Sci., 52, 21 (1975).

30.   B. E. Nieuwenhuys, G. F. Rovida and G. A. Somorjai, Surface Sci.,
      To be published 1976.

31.   S. L. Bernasek and G. A. Somorjai, J. Chem. Phys., 62, 3149 (1975).

32.   R. L. Palmer, J. N. Smith, H. Saltsburg and D. R. O'Keefe, J. Chem.
      Phys., 53, 1666 (1970).

33.   T. L. Bradley, A. E. Dabiri and R. E. Stickney, Surface Sci., 29,
      590 (1972).

34.   M. Balooch and R. E. Stickney, Surface Sci., 44, 310 (1974).

35.   D. W. Blakely and G. A. Somorjai, Surface Sci., To be published 1976.

36.   J. L. Gland, K. Baron and G. A. Somorjai, J. Catalysis, 36, 305 (1975).

36a. D. W. Blakely, B. A. Sexton, E. Kozak and G. A. Somorjai, To be
      published.

36aa. R. Herz, D. W. Blakely and G. A. Somorjai, To be published.

37.   W. H. Weinberg, H. A. Deans and R. P. Merrill, Surface Sci., 41, 312
      (1974).

38.   N. C. Gardner and R. S. Hansen, J. Phys. Chem., 74, 3298 (1970).

39.   I. Yasumori, H. Shinohara and Y. Inoue, in "Catalysis," Ed. J.
      Hightower, North Holland PUblishers, Amsterdam (1972).

40.   C. M. Holbrook and H. Wise, To be published.

41.   B. Lang, R. W. Joyner and G. A. Somorjai, Proc. Yor. Soc. A, 331,
      335 (1972).

42.   O. M. Poltorak and V. S. Boronin, Zh. Fiz. Khim., 40, 2671 (1966) and
      A. N. Mitrofanova, V. S. Boronin and O. M. Poltorak, Zh. Fiz. Khim.,
      46, 32 (1972).

43.   R. W. Maatman, P. Mahaffy, P. Hoekstra and C. Addink, J. Catalysis,

<u>23</u>, 105 (1971; J. A. Cusamano, G. W. Dembinski and J. H. Sinfelt, J. Catalysis J. Catalysis, <u>5</u>, 471 (1966) and M. Kraft and H. Spindler, in "Proceedings of the Fourth International Congress on Catalysis," Vol. 2, p. 286, Akademiai Kiado, Budapest, 1971.

44. J. H. Sinfelt, H. Hurwitz and R. A. Shulman, J. Phys. Chem., <u>64</u>, 1559 (1960).

45.. V. Haensel, G. R. Donaldson and F. J. Riedl, in "Proceedings of the International Congress on Catalysis, 3rd, 1964," Vol. 1, p. 294 (1965).

46. W. H. Manogue and J. R. Katzer, J. Catalysis, <u>32</u>, 166 (1974).

47. H. Conrad, G. Ertl and E. E. Latta, Surface Sci., <u>40</u>, 435 (1974).

48. L. L. Kesmodel and L. M. Falicov, Solid State Comm., <u>16</u>, 1201 (1975).

49. Y. W. Tsang and L. M. Falicov, Phys. Rev., To be published 1976.

50. Y. W. Tsang and L. M. Falicov, Phys. Rev., <u>12</u>, 2441 (1975).

51. F. S. Stone, To be published.

51a. A. Cimino and V. Indovina, J. Catalysis, <u>33</u>, 493 (1974).

51aa. M. Boudart, A. Delbouille, E. G. Derouane, V. Indovina and A. B. Walters, J. Am. Chem. Soc., <u>94</u>, 6622 (1972).

52. H. Ibach, K. Horn, R. Dorn and H. Luth, Surface Sci., <u>38</u>, 433 (1973).

52a. A. Maradudin and R. Wallis, Private communication.

53.

54. L. D. Schmidt and D. Luss, J. Catalysis, <u>22</u>, 269 (1971).

Figure Captions

1. Model of a heterogeneous solid surface depicting different surface
    sites. These sites are distinguishable by their number of nearest
    neighbors.

2. Stereographic triangle indicating various crystallographic orientations
    of face centered cubic solid surfaces using Miller Index notations.

3. Low-energy electron diffraction patterns and schematic representations
    of the surface configurations of platinum single crystal surfaces.
    (a) Pt (111) containing less than 10^{12} defects/cm^2; (b) Pt(557) sur-
    face containing 2.5×10^{14} step atoms/cm^2 with an average spacing between
    steps of 6 atoms and (c) Pt(679) surface containing 2.3×10^{14} step
    atoms/cm^2 and 7×10^{14} kink atoms/cm^2 with an average spacing between
    steps of 7 atoms and between kinks of 3 atoms.

4. Diffraction pattern and cnematic representation of the Pt(111)
    crystal face.

5. a) Diffraction pattern from the Pt(100)-(5x1) structure. b) Schematic re-
    presentation of the (100) surface with hexagonal overlayer. c) Diffraction
    pattern from the Pt(100)-(1x1) structure. d) Schematic representation
    of the (100) surface.

6. A stereographic triangle of a platinum crystal depicting the various
    high Miller Index surfaces of platinum that were studied.

7. Diffraction patterns and schematic representations of additional platinum
    stepped surfaces used in these studies: (a) Pt(S)-[9(111)x(100) at
    84 V, (b) Pt(S)-[4(111)x(100) at 34 V, and (c) Pt(S)-[7(111)x(310)
    at 49 V.

8. Scheme of the low-energy electron diffraction technique.

9. Typical diffraction patterns from the (111) face of a platinum single crystal at four different incident electron beam energies: (a) 51 eV, (b) 63.5 eV, (c) 160 eV and (d) 181 eV.

10. Diffraction patterns of a clean Pt(111) surface and from a surface with adsorbed ordered acetylene exhibiting a (2x2) structure.

11. Comparisons of theory and experiment for intensity-energy profiles from Pt(111) at room temperature for (a) the (00) beam and (b) the ($\bar{1}$0) beam at three angles of incidence. The verticle scales are of relative intensity in arbitrary units and are not necessarily compatible from one curve to the next. The theoretical results were calculated on the assumption of the bulk interplanar spacing for all atomic layers parallel to the surface.

12. Energy-level-diagram representation of (a) photoelectron emission and (b) X-ray absorption.

13. Energy-level-diagram representation of the excitations by a) Auger electron emission and (b) X-ray fluorescence.

14. Auger electron spectroscopy; experimental configuration and energy diagram.

a)

15. Auger spectra of platinum in the presence of carbon and carbon monoxide

b) in the clean state.

16. Scheme of the experimental apparatus to carry out catalytic reaction rate studies on single crystal surfaces at low and at high pressures in the range of 10^{-7} torr to 10^{-} torr.

17. Schematic of the ultrahigh vacuum molecular beam surface scattering apparatus.

18. Diffraction patterns for the benzene surface structure of the Pt(111) crystal face taken at several voltages and a schematic diagram of the unit cell. The benzene is shown in two orientations. All dimensions are in Å.

19. Scattering distribution of H_2, D_2 and HD formed at the surface from platinum (111) and platinum single crystal surfaces. On single scattering, HD signal from the Pt(111) surface is not observable.

20. The steady state rate of production of benzene and cyclohexene from cyclohexane as a function of hydrogen to hydrocarbon ratio. The reaction conditions are $4x10^{-8}$ torr of cyclohexane and 423K catalyst temperature. Δ - Pt(S)-[7(100)x(111)]; ☐ - Pt(S)-[3(111)x(100)]; O - Pt(S)-[6(111)x(100)]; ❶ - Pt(S)-[6(111)x(710)]; ● - Pt(S)-[7(111)x(310)]

21. (A) Cyclohexane dehydrogenation to benzene (-O-) and hydrogenolysis to n-hexane (-Δ-) as a function of step density. (B) Cyclohexane dehydrogenation to benzene and hydrogenolysis to n-hexane as a function of kink density at a constant step density of $2.0x10^{14}/cm^2$.

22. Induction period for the production of benzene (——) and cyclohexene (- - -) from cyclohexane. Hydrogen to cyclohexane ratio of 20:1; cyclohexane pressure $4x10^{-8}$ torr.

23. The amount of carbon on the catalyst surface at steady state reaction under standard conditions. An Auger peak height ratio of 4.0 corresponds to approximately 1.0 monolayers of carbon. Line through points at a 2 kcal/mole slope.

24. Temperature dependence of dehydrogenation of cyclohexane to benzene (-O-) and hydrogenolysis (-Δ-). The overall activation energy for hydrogenolysis

is 3±.5 kcal/mole. Standard reaction conditions, data for Pt(S)-[6(111)x(100)].

25. Inhibition of benzene (-0-) from cyclohexane and increasing cyclohexene formation (-□-) with time on Pt(S)-[6(111)x(100)] surface. All catalysts with (111) orientation terraces behave similarly.

26. Cyclohexene dehydrogenation to benzene as a function of ιAι step density and (Bᴵ kink density. Standard reaction conditions.

27. Inhibition of benzene formation from cyclohexene on disordered carbonaceous overlayers (——), Pt(S)-[6(111)x(100)] and Pt(S)-[13 (111)x(100)]; and lack of inhibition of ordered carbonaceous overlayers (---), Pt(S)-[7(100)x(111)].

28. Schematic representation of a platinum catalyst with a monolayer of carbonaceous overlayer showing the exposed platinum clusters.

29. Relationship between homogeneous, heterogeneous and enzyme catalysis as inferred from the experimental studies of hydrocarbon catalysis on platinum surfaces.

Table I

Work function changes and structural information for adsorption of
organic compounds on the Pt(111) and Pt(100)-(5x1) surfaces.

TABLE I

Work Function Changes and Structural Information for Adsorption of Organic Compounds
on the Pt(111) and Pt(100)-(5×1) Surfaces

Adsorbate	Temp °C	Pt(111) Work Function Change Pres (Torr)	WFC (Volts)	Pt(111) Adsorbate Diffraction Features or Surface Structure	Pt(100)-(5×1) Work Function Change Pres (Torr)	WFC (Volts)	Substrate Structure after Adsorption	Pt(100)-(5×1) Adsorbate Diffraction Features or Surface Structures
Acetylene	20°	1×10^{-8}	-1.5	(2×2)	6×10^{-7}	-1.65	(1×1)	$(\sqrt{2}\times\sqrt{2})\mathrm{R}45°$
	70°	1×10^{-8} (10 min)	-1.65	disordered				
	150°	4×10^{-7}	-1.8	disordered	6×10^{-7}	-1.7	(1×1)	$(\sqrt{2}\times\sqrt{2})\mathrm{R}45°$
Aniline	20°	1×10^{-8}	-1.8	Streaks at 1/3 order diffuse (1/2 n) features	1×10^{-8}	-1.75	(1×1)	disordered
Benzene	20°	4×10^{-7}	-1.8	poorly ordered	3×10^{-7}	-1.6	(1×1)	diffuse ring-like 1/2 order streak
	20°	6×10^{-7} (5 min)	-1.4	$\begin{vmatrix} -2 & 2 \\ 4 & 4 \end{vmatrix}$				
	20°	4×10^{-7} (40 min)	-.7	$\begin{vmatrix} -2 & 2 \\ 5 & 5 \end{vmatrix}$	3×10^{-7} (2 hrs)	-1.3	(1×1)	diffuse 1/2 order streak
Biphenyl	20°	2×10^{-9}	-1.85	very poorly ordered	2×10^{-9}	-1.8	(1×1)	disordered
n-Butylbenzene	20°	8×10^{-8}	-1.5	disordered	8×10^{-8}	-1.5	(1×1)	disordered
t-Butylbenzene	20°	5×10^{-8}	-1.7	disordered	5×10^{-8}	-1.75	(1×1)	disordered
Cyanobenzene	20°	1×10^{-8}	-1.6	diffuse (1/3 0) features	1×10^{-8}	-1.5	faint (5×1)	disordered
1,3-Cyclohexadiene	20°	2×10^{-8}	-1.75	poorly ordered	2×10^{-8}	-1.7	(1×1)	diffuse 1/2 order streak
	20°C	2×10^{-8} (1 hr)	-1.3	$\begin{vmatrix} -2 & 2 \\ 4 & 4 \end{vmatrix}$	2×10^{-8} (1 hr)	-1.6	(2×1)	diffuse 1/2 order streak
	20°C	3×10^{-7} (5 hrs)	-.8	$\begin{vmatrix} -2 & 2 \\ 5 & 5 \end{vmatrix}$	2×10^{-8} (5 hrs)	-1.4	(1×1)	diffuse 1/2 order streak
Cyclohexane	20°	6×10^{-9}	-1.2	(1×1) low background	6×10^{-9}	-.75	(5×1)	low background
	20°	4×10^{-7}	-.7	very poorly ordered	4×10^{-7}	-.4	(1×1)	diffuse streaked (2×1) pattern
	150°	4×10^{-7}	-1.1	apparent (2×2)	4×10^{-7}	-1.2	(1×1)	streaked (2×1) pattern
	300°	6×10^{-7}	-1.4	disordered	4×10^{-7}	-1.5	(1×1)	disordered
Cyclohexene	20°	6×10^{-7}	-1.7	$\begin{vmatrix} 2 & 2 \\ 4 & -2 \end{vmatrix}$	6×10^{-7}	-1.6	(1×1)	diffuse (1/2 0) features
	150°	6×10^{-7}	-1.6	apparent (2×2)	6×10^{-7}	-1.5	(1×1)	streaked (2×1) pattern
Cyclopentane	20°	7×10^{-9}	-.95	(1×1) low background	7×10^{-9}	-.4	(5×1)	low background
	20°	4×10^{-7}	-.7	disordered	4×10^{-7}	-.3	(1×1)	diffuse features at 1/2 order
Cyclopentene	20°	-	-	—	2×10^{-7}	-1.4	(1×1)	diffuse streaked (1/2 0) features
2,6-Dimethyl-pyridine	20°	4×10^{-8}	-1.6	diffuse 1/3,2, 2/3,2 order streaks	4×10^{-8}	-1.5	faint (5×1)	disordered
3,5-Dimethyl-pyridine	20°	4×10^{-8}	-2.1	diffuse 1/2 order streak	4×10^{-8}	-2.2	(1×1)	disordered

TABLE I, con't.

Work Function Changes and Structural Information for Adsorption of Organic Compounds
on the Pt(111) and Pt(100)-(5×1) Surfaces

Adsorbate	Temp °C	Pt(111) Work Function Change Press (Torr)	WFC (Volts)	Adsorbate Diffraction Features or Surface Structure	Pt(100)-(5×1) Work Function Change Press (Torr)	WFC (Volts)	Substrate Structure after Adsorption	Adsorbate Diffraction Features or Surface Structures
Ethylene	20°	1×10^{-8}	- 1.5	diffuse (1/2 0) features	1×10^{-8}	- 1.2	(1×1)	$(\sqrt{2} \times \sqrt{2})$R45°
	250°	1×10^{-8}	- 1.7	disordered	1×10^{-8}	- 1.5	(1×1)	disordered
Graphitic Overlayer	950°		- 1.1	ringlike diffraction features		- 1.0	(1×1)	ringlike diffraction features
n-Hexane	20°	5×10^{-8}	- 1.1	disordered	5×10^{-8}	- .8	(1×1)	disordered
	20°	5×10^{-8} (5 hrs)	- .9	disordered	5×10^{-8} (5 hrs)	- .6	(1×1)	disordered
	250°	5×10^{-8}	- 1.5	disordered	5×10^{-8}	- 1.2	(1×1)	disordered
Isoquinoline	20°	6×10^{-8}	- 1.9	diffuse (1/3 0) and (2/3 0) features	6×10^{-8}	- 2.1	(1×1)	disordered
Mesitylene	20°	4×10^{-8}	- 1.7	Streaks at 1/3.4 order diffuse (2/3.4 0) features	4×10^{-8}	- 1.7	(5×1)	1/3 order streaks
	20°	4×10^{-7}	- 1.35	disordered	4×10^{-7}	- 1.2	(1×1)	disordered
2-Methyl-naphthalene	20°	6×10^{-8}	- 2.0	very poorly ordered	4×10^{-9}	- 1.6	faint (5×1)	disordered
Naphthalene	20°	9×10^{-9}	- 1.95	apparent (3×1)	9×10^{-9}	- 1.7	(1×1)	disordered
	150°	9×10^{-9}	- 2.0	(6×6)	9×10^{-9}	- 1.65	(1×1)	disordered
Nitrobenzene	20°	9×10^{-9}	- 1.5	diffuse (1/3 0) features (pattern electron beam sensitive)	9×10^{-9}	- 2.4	(1×1)	disordered
Piperidine	20°	8×10^{-8}	- 2.1	disordered	8×10^{-8}	- 2.05	faint (5×1)	disordered
Propylene	20°	2×10^{-8}	- 1.3	(2×2) (pattern electron beam sensitive)	2×10^{-8}	- 1.2	(1×1)	1/2 order streaks (pattern electron beam sensitive)
Pyridine	20°	1×10^{-8}	- 2.7	diffuse (1/2 0) features	1×10^{-8}	- 2.4	(1×1)	disordered
	250°	1×10^{-8}	- 1.7	well defined streaks at 1/3, 2/3, 3/3 order	1×10^{-8}	-	(1×1)	$(\sqrt{2} \times \sqrt{2})$R45°
Pyrrole	20°	6×10^{-8}	- 1.45	diffuse (1/2 0) features (pattern electron beam sensitive)	6×10^{-8}	- 1.6	(1×1)	diffuse (1/2 0) features
Quinoline	20°	3×10^{-8}	- 1.65	diffuse 1/3 order streaks	3×10^{-8} (6 min)	-	(5×1)	diffuse 1/3 order streaks
					3×10^{-8} (14 min)	- 2.7	(1×1)	disordered
Styrene	20°	6×10^{-8}	- 1.7	streaks at 1/3 order	6×10^{-8}	- 1.65	(1×1)	very poorly ordered
Toluene	20°	1×10^{-9}	- 1.7	streaks at 1/3 order	1×10^{-9}	- 1.55	(5×1)	streaks at 1/3 order
	150°	1×10^{-9}	- 1.65	(4×2)	1×10^{-9}	- 1.5	(1×1)	disordered
o-Xylene	20°	1×10^{-8}	- 1.8	streaks at 1/2.6 order	1×10^{-8}	- 1.65	(5×1)	streaks at 1/3 order

Table II

Comparison on initial specific rate data for the cyclopropane hydro-
genolysis on platinum catalysts.

TABLE II

Comparison of Initial Specific Rate Data for the Cyclopropane
Hydrogenolysis on Platinum Catalysts

Data source	Type of Catalyst	Calculated specific reaction rate @ $P°_{CP}$ = 135 torr and T = 75°C	
		$\left(\dfrac{\text{moles } C_3H_8}{\text{min} \cdot \text{cm}^2 Pt}\right)$	$\left(\dfrac{\text{molecules } C_3H_8}{\text{min} \cdot \text{Pt site}}\right)$
Present study	Run 10A	2.1×10^{-6}	
	Run 12A	1.8×10^{-6}	
	Run 15	1.8×10^{-6}	
	Run 16	2.1×10^{-6}	
	Average	1.95×10^{-6}	312
Hegedus[30,49]	0.04 Wt%Pt on η – Al_2O_3	7.7×10^{-7} based on 100% Pt dispersion	410
Boudart et al.[17] and Dougharty[28]	0.3% and 2.0% Pt on η – Al_2O_3;	8.9×10^{-7}	480
	0.3% and 0.6% Pt on γ – Al_2O_3	2.5×10^{-6}	1340

Table III

Initial turnover numbers on platinum crystal surfaces for various hydrocarbon reactions at high pressures and at low pressures.

INITIAL TURNOVER NUMBER (sec⁻¹) ON Pt CRYSTAL SURFACES

REACTION	HIGH PRESSURE (total pressure 215 torr, reactant pressure 15 torr)	LOW PRESSURE (total pressure 8×10^{-7} torr, reactant pressure 4×10^{-8} torr)
$C_6H_{12} \rightarrow C_6H_6$	3	6.3×10^{-5}
$C_6H_{12} \rightarrow C_6H_{10}$	2×10^{-2}	2.0×10^{-5}
$C_6H_{10} \rightarrow C_6H_6$	100	4×10^{-3}
n-heptane $\rightarrow$ toluene	10^{-2}	10^{-5}
n-heptane $\rightarrow$ methyl cyclohexane	10^{-1}	—
cyclopropane $\rightarrow$ propane	150	10^{-3} (total pressure 7×10^{-5} torr)

The table is titled "INITIAL TURNOVER NUMBER (sec⁻¹) ON Pt CRYSTAL SURFACES (300° C)".

XBL 756-3161

Table IV

Classification of reactions by step density and carbonaceous overlayer
dependence.

STEP SENSITIVE		STEP INSENSITIVE	
Overlayer Sensitive	Overlayer Insensitive	Overlayer Sensitive	Overlayer Insensitive
Cyclohexene → Benzene n-heptane → Toluene	Cyclohexane → Hexane		Cyclohexane → Cyclohexene Cyclopropane → Propane

TERRACE   KINK   MONATOMIC STEP
                ADATOM   STEP - ADATOM

TERRACE
VACANCY
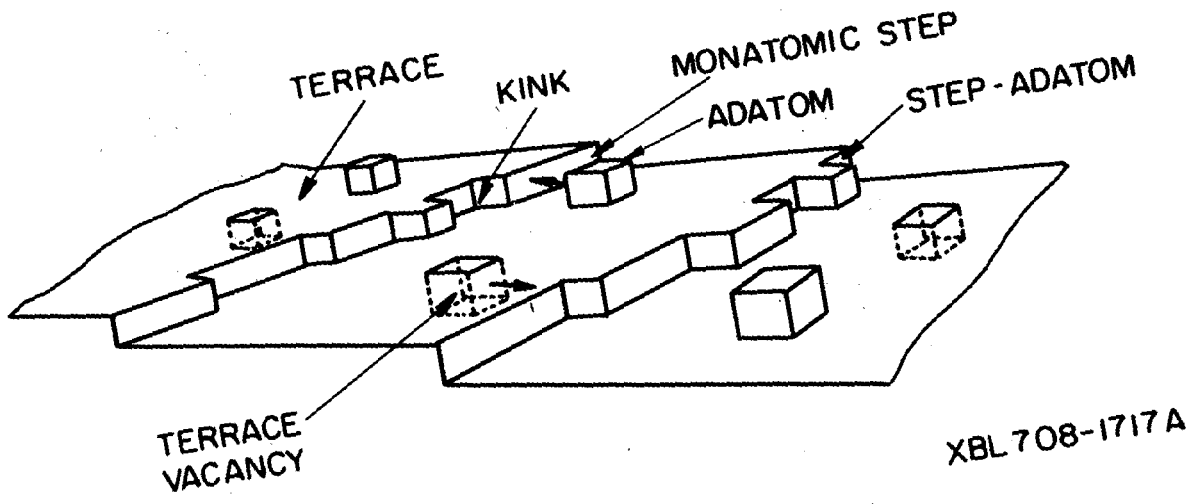
XBL 708-1717A

Fig. 1
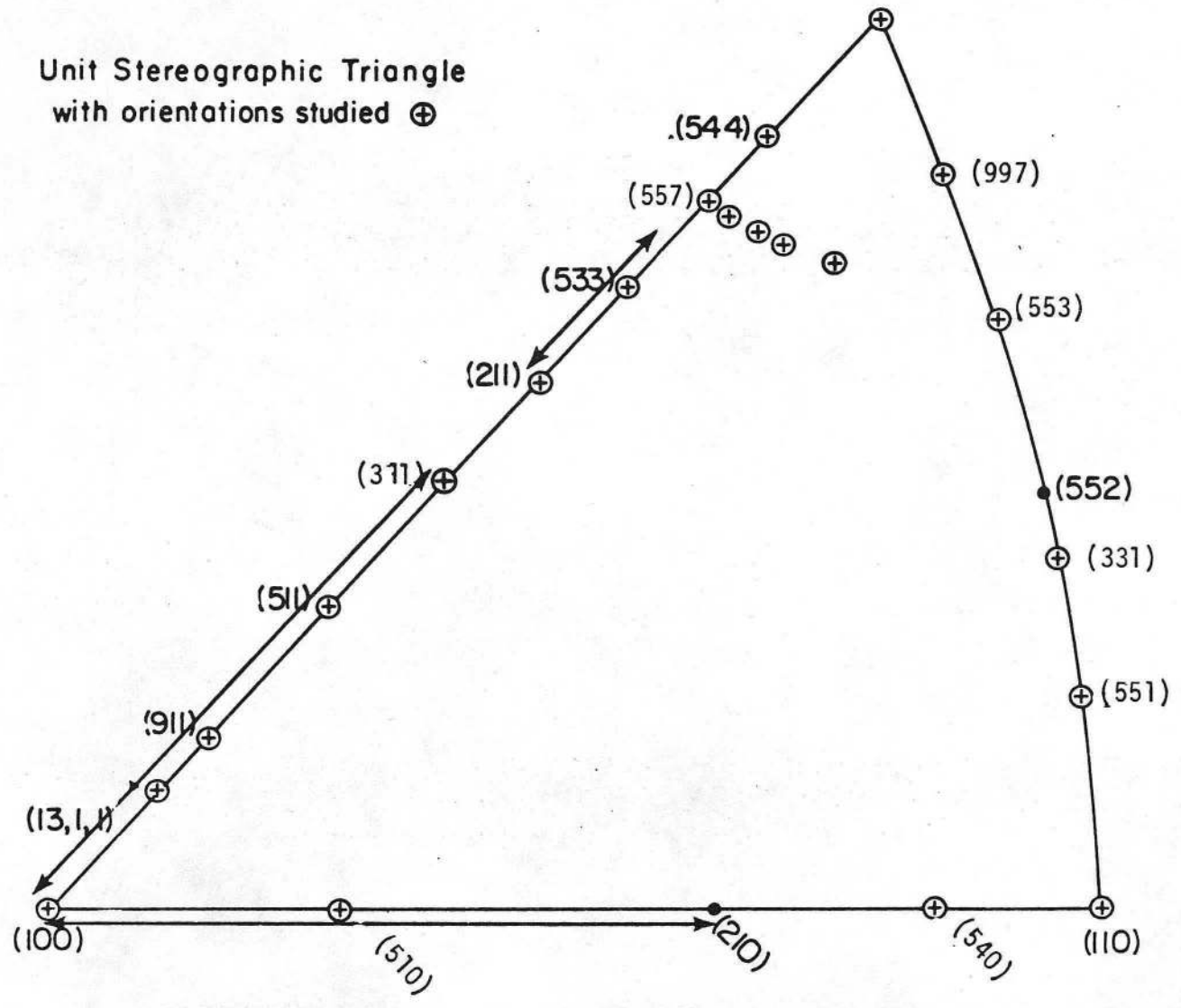
Fig. 2
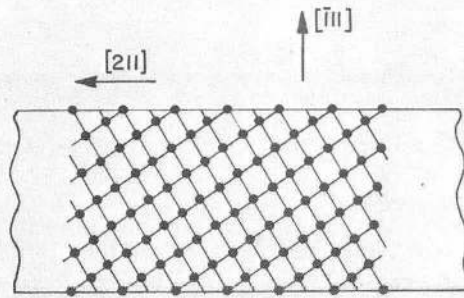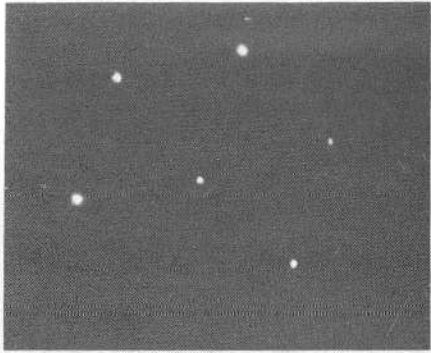
a) Pt - (̄111)
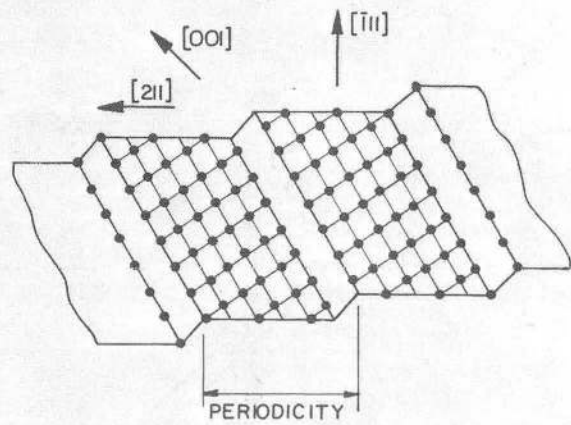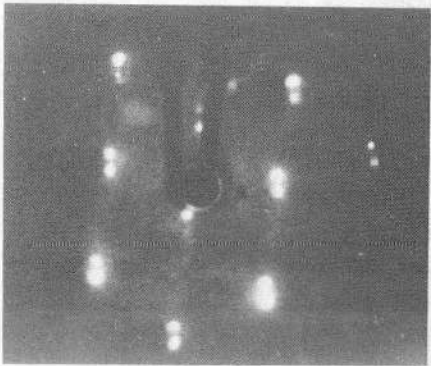
b) Pt - (̄557)
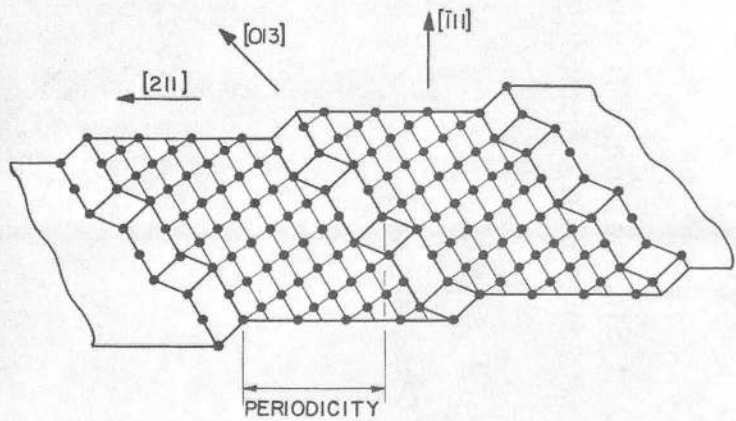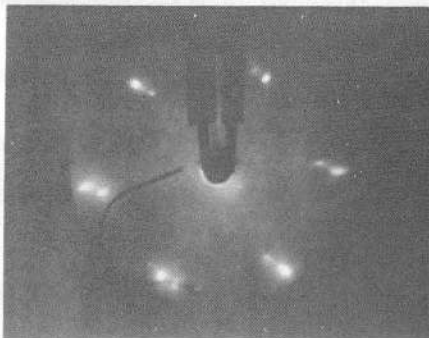
c) Pt - (̄679)

Fig. 3
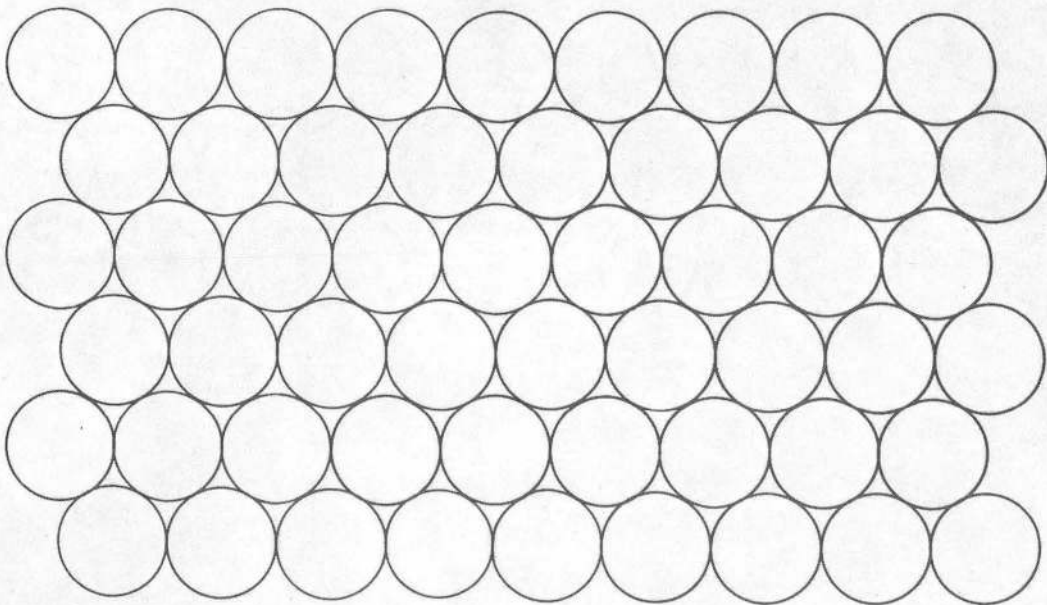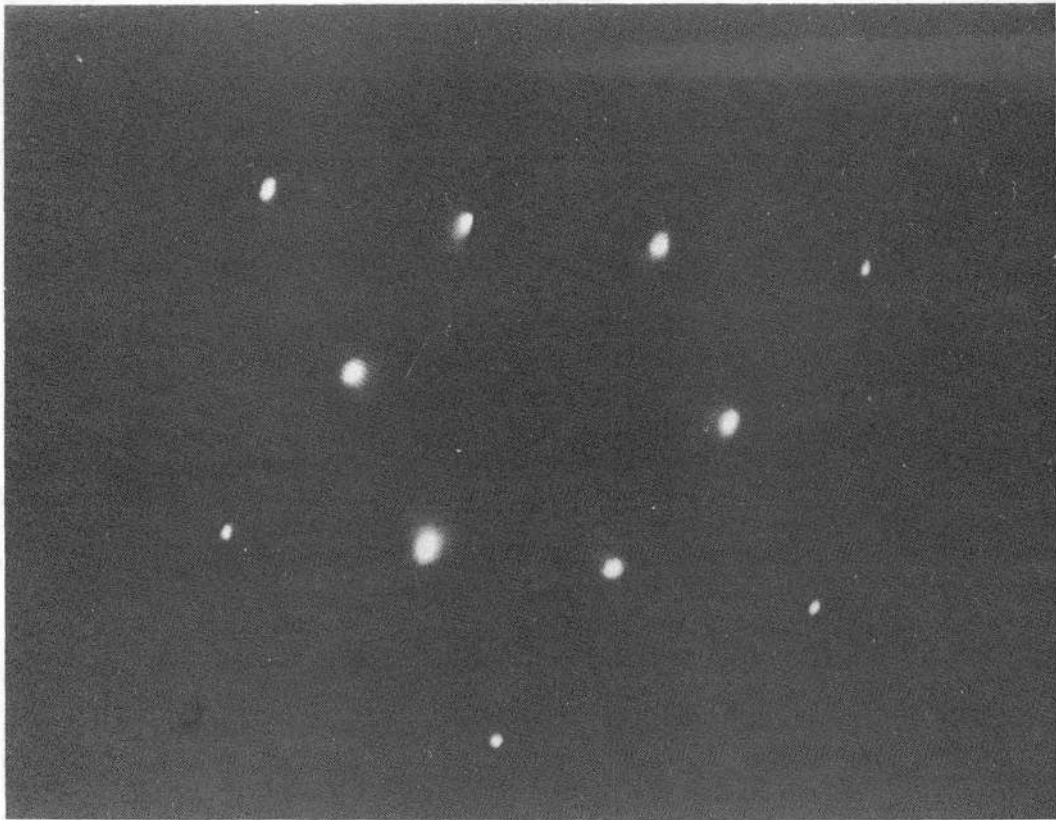
Fig. 4

XBB 725-2327
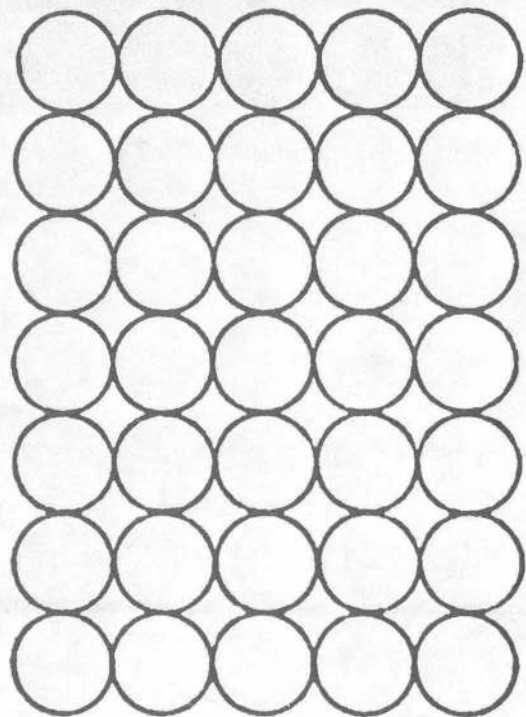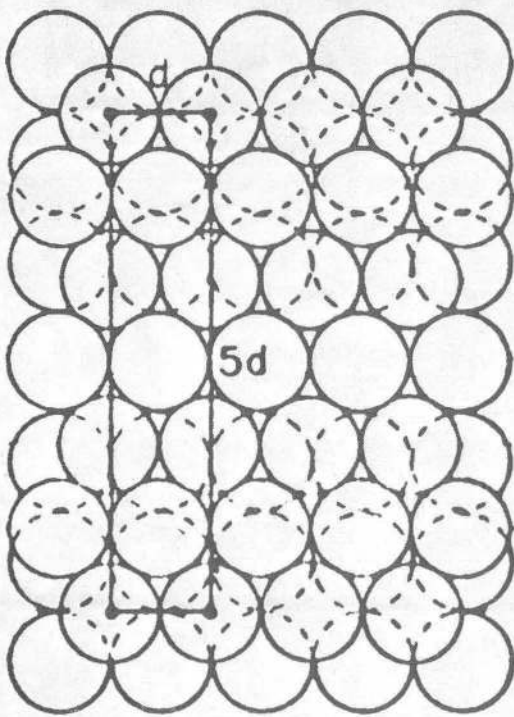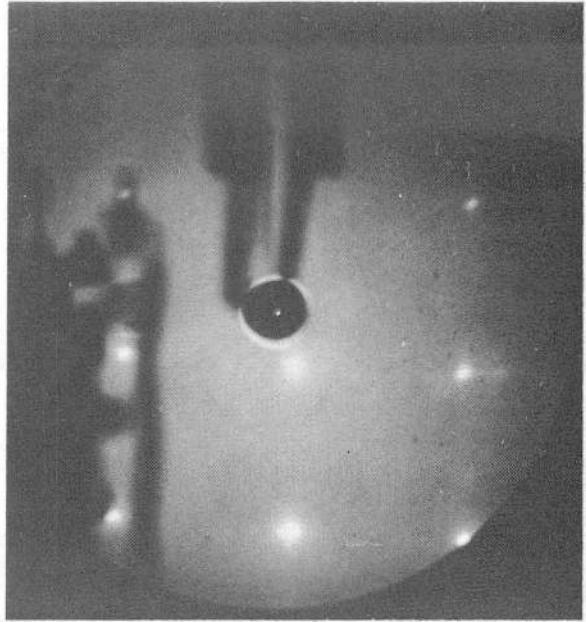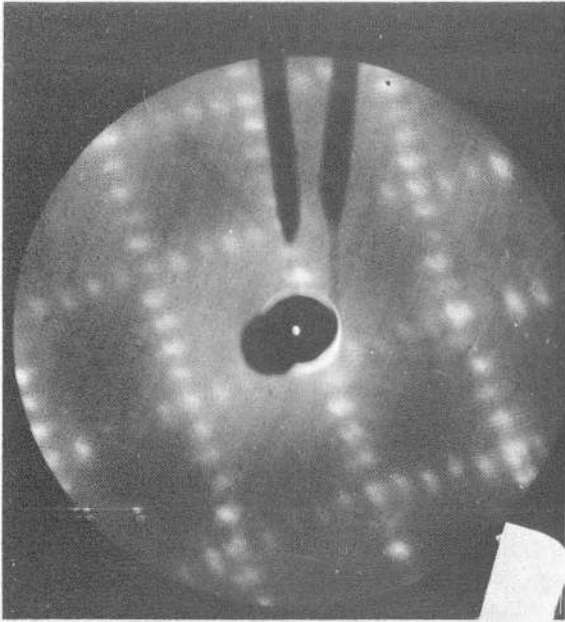
Fig. 5   XBB 7111-5356

Unit Stereographic Triangle
with orientations studied ⊕

(111)

9(111)×(100) ↔ (544)

9(111)×(111) ↔ (997)

6(111)×(100) ↔ (557)

4(111)×(100) ↔ (533)

5(111)×(111) ↔ (553)

3(111)×(100) ↔ (211)

(311)

(552)

3(100)×(111) ↔ (511)

3(111)×(111) ↔
(331)

5(100)×(111) ↔ (911)

5(110)×(111) ↔
(551)

7(100)×(111) ↔
(13,1,1)

(100)

5(100)×(100) ↔ (210)

(110)

5(100)×(100) ↔ (510)

5(110)×(100) ↔ (540)

Fig. 6

Pt(S)-[9(111)X(100)]

Fig. 7a

XBB 733-2188

Pt(S)-[4(111)X(100)]

PERIODICITY
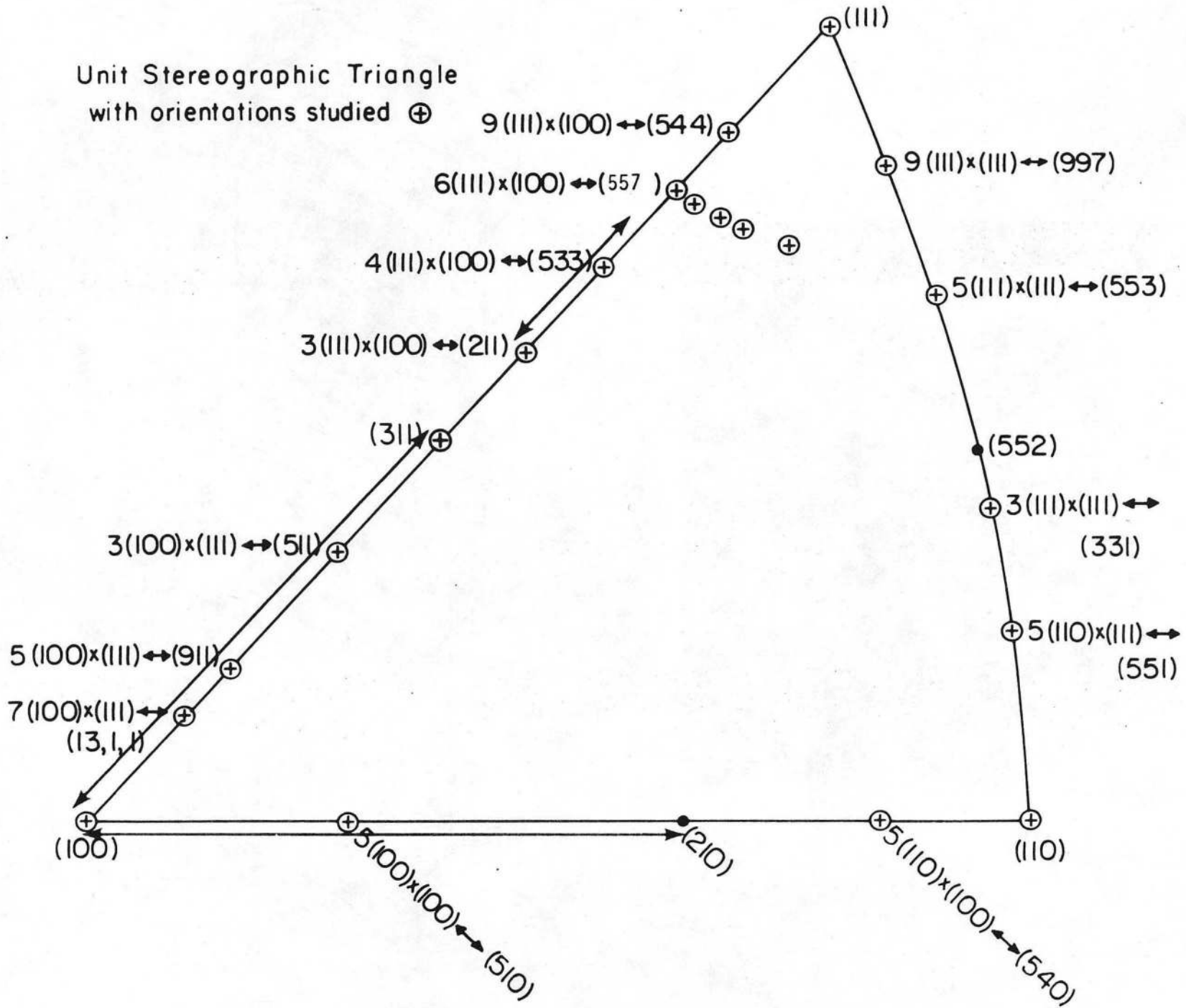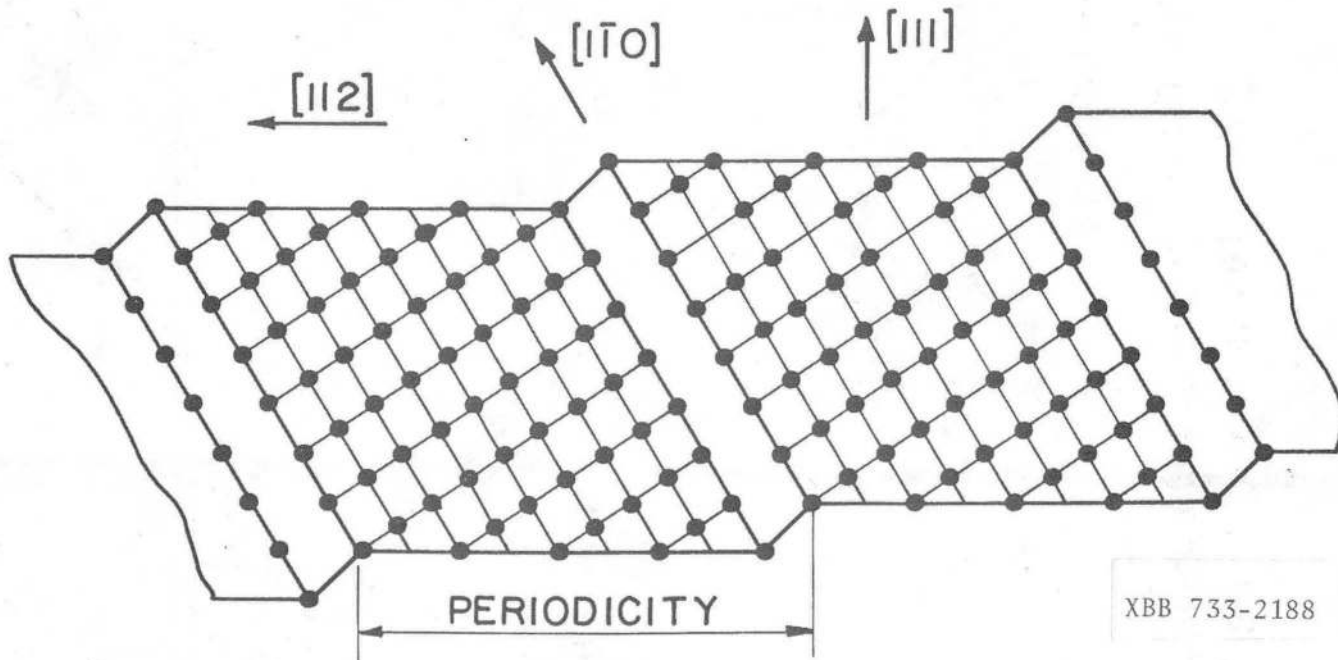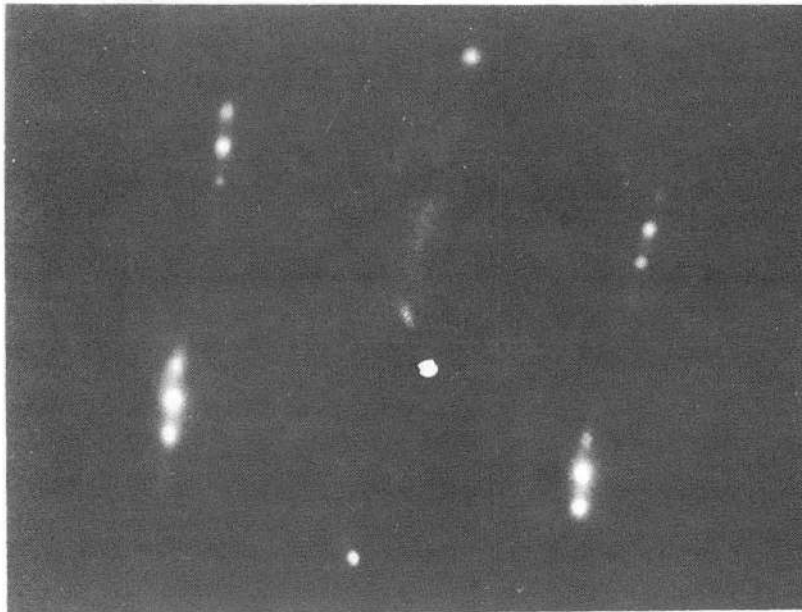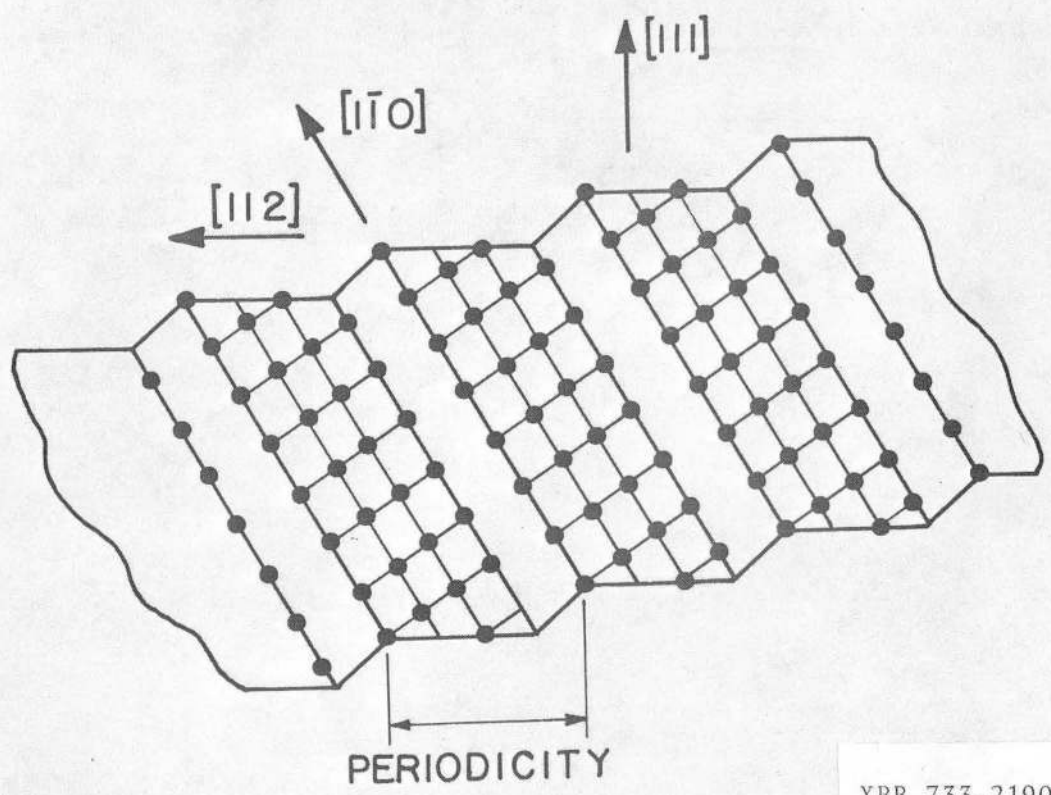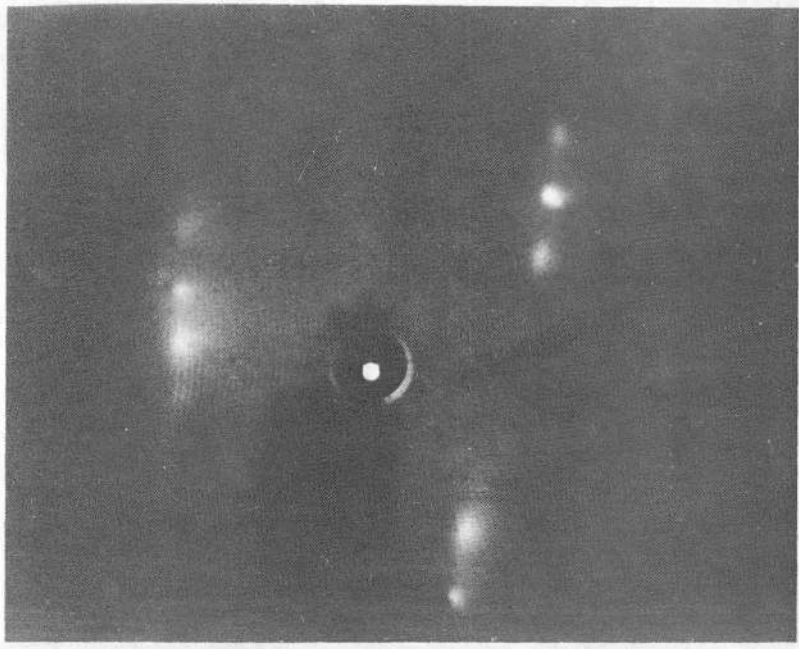
XBB 733-2190

Fig. 7b

P + (S) - [7(111)X(310)]
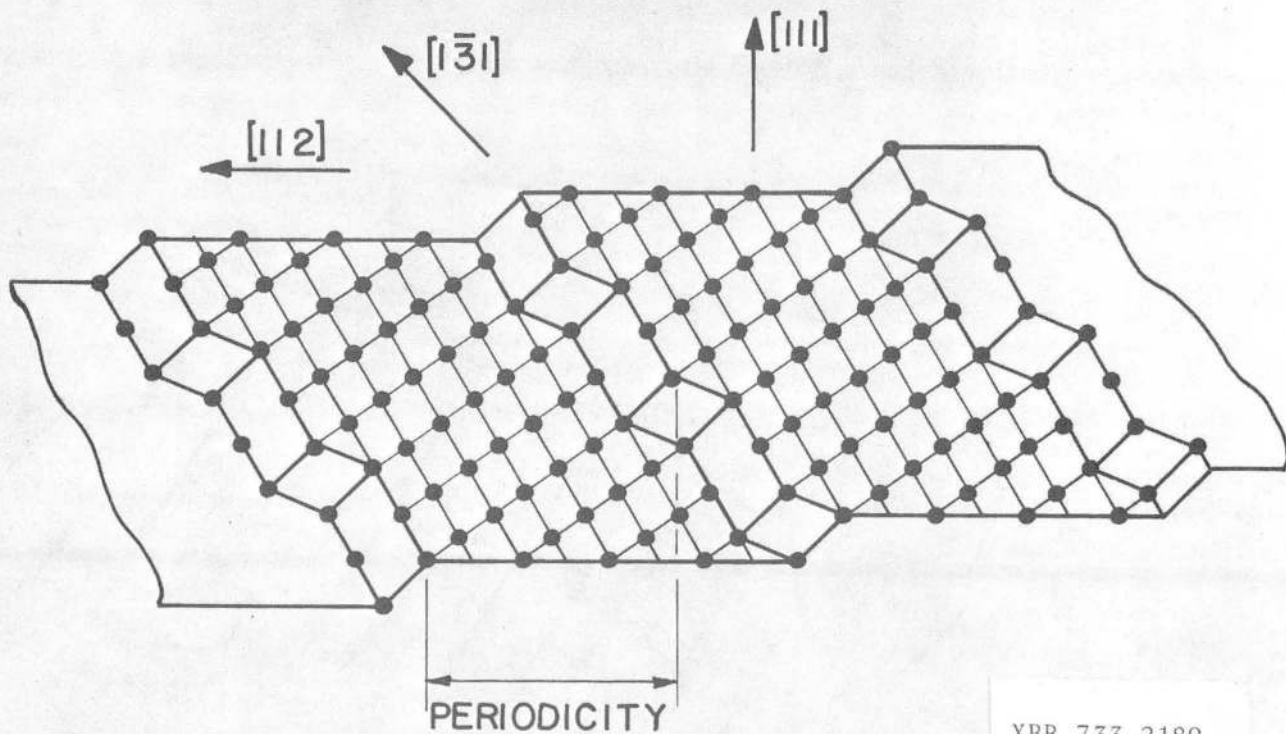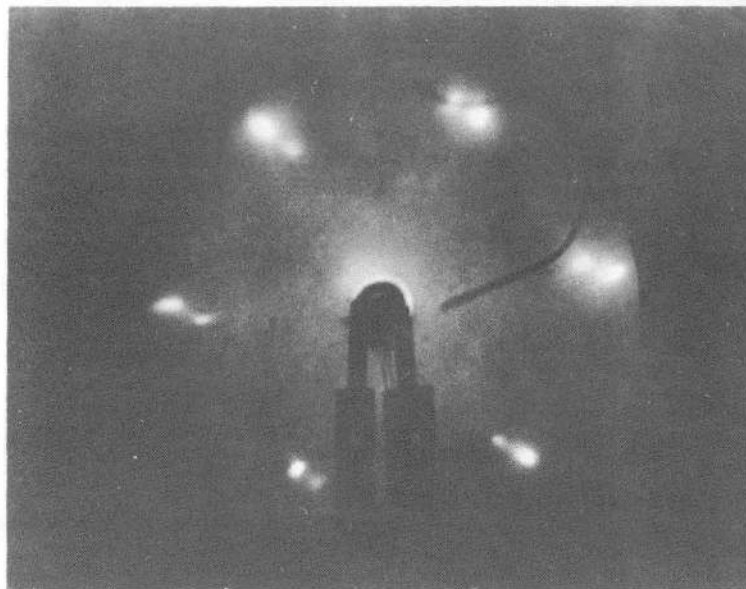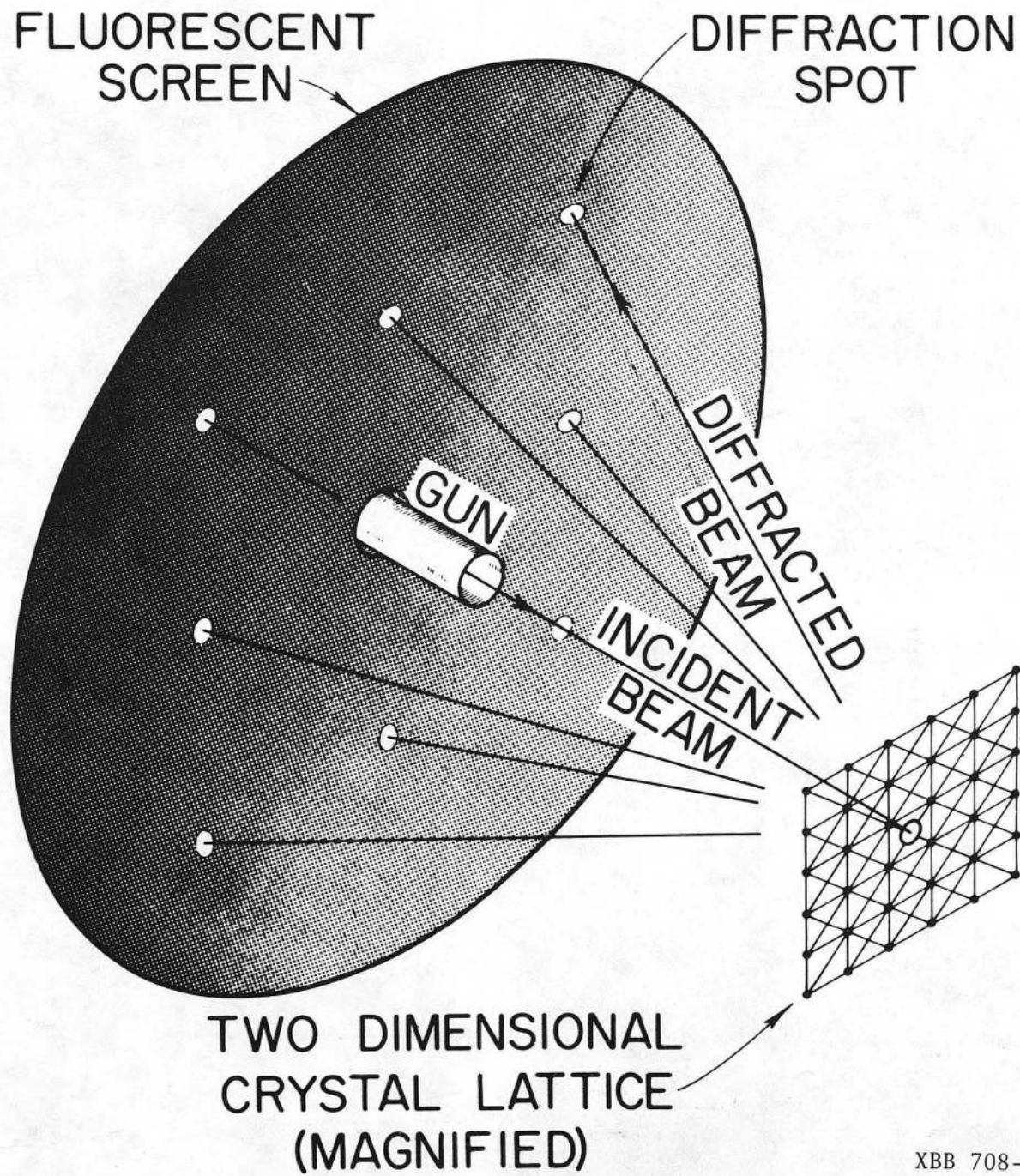
PERIODICITY

XBB 733-2189

Fig. 7c

FLUORESCENT SCREEN
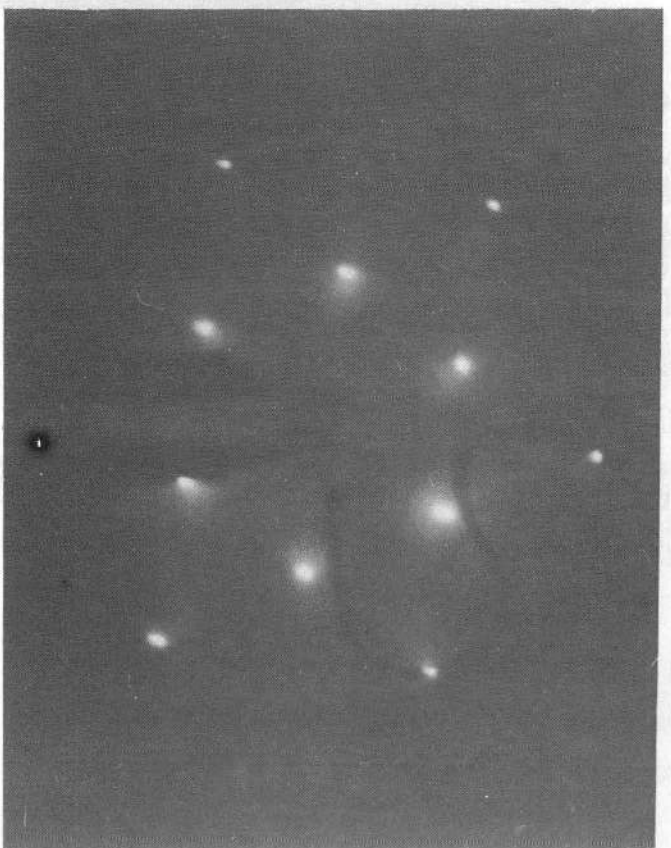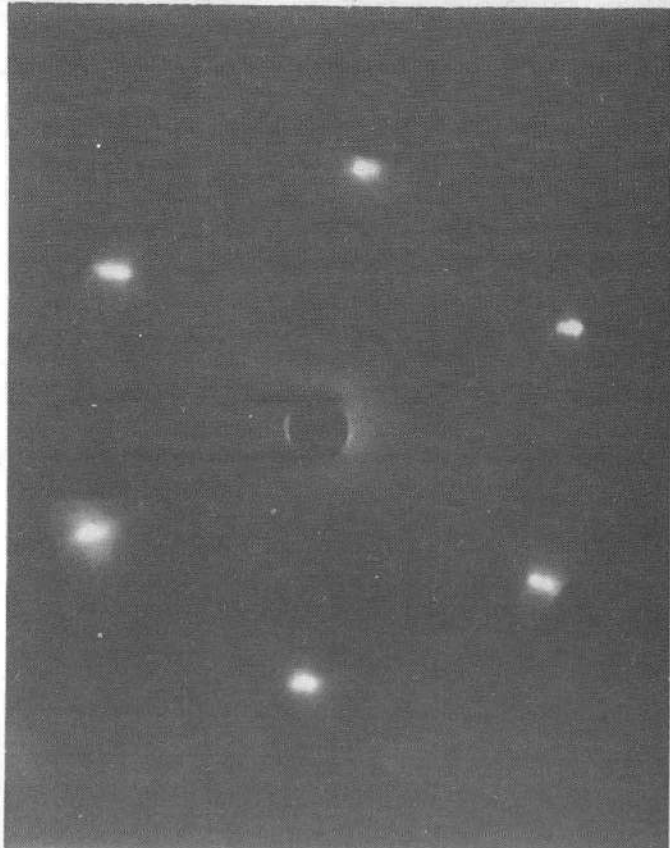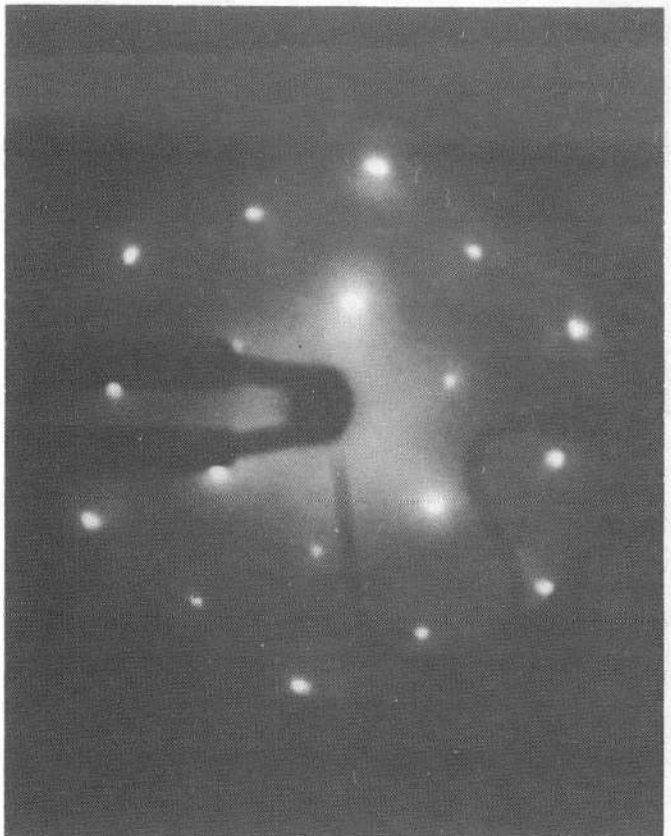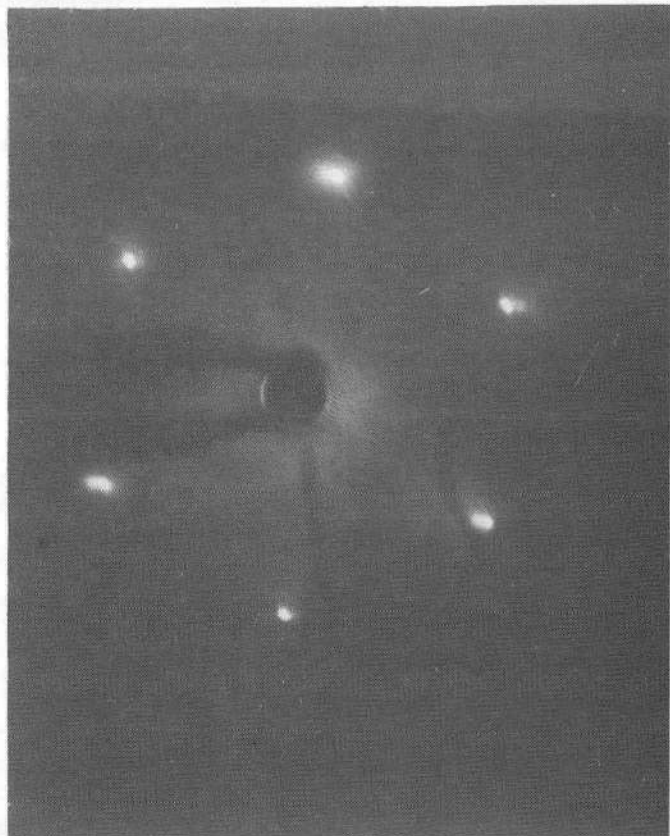
DIFFRACTION SPOT

DIFFRACTED BEAM

GUN

INCIDENT BEAM

TWO DIMENSIONAL CRYSTAL LATTICE (MAGNIFIED)

XBB 708-3583

Fig. 8

Fig. 9

Fig. 10

Fig. 11

Fig. 12

XBL707-3389

(a)   (b)
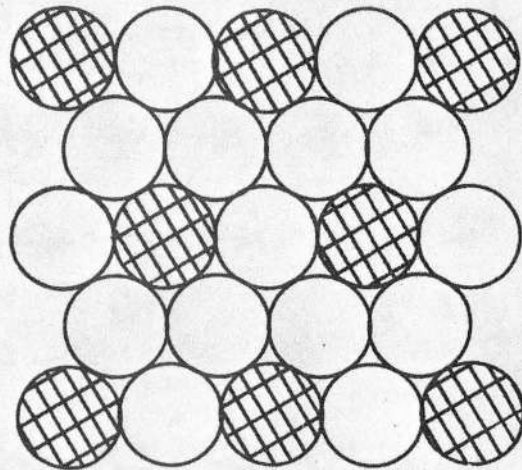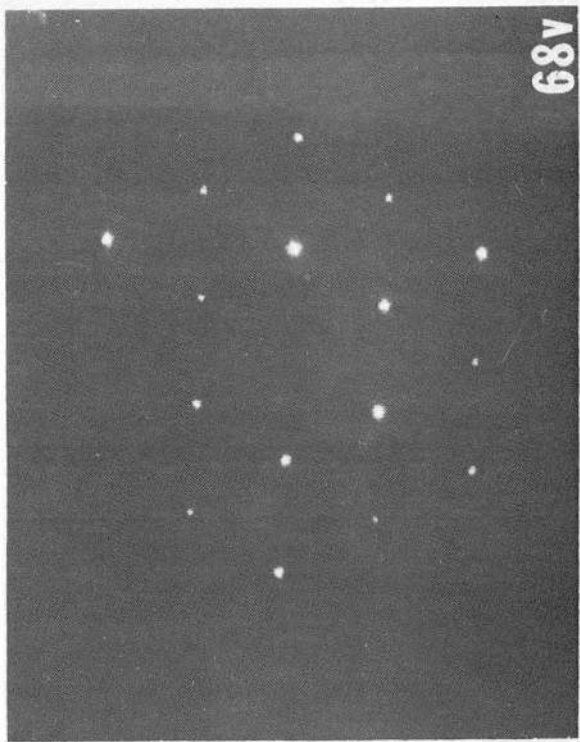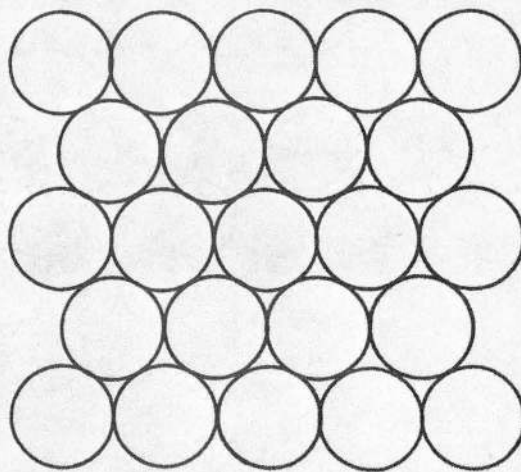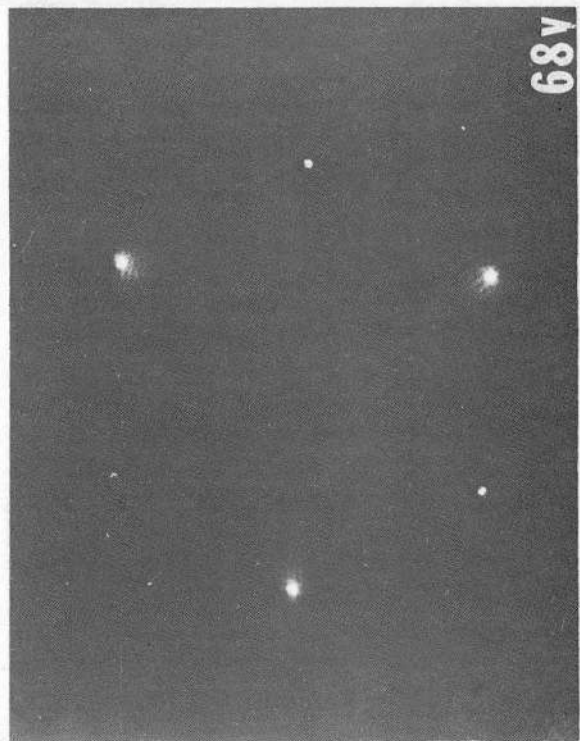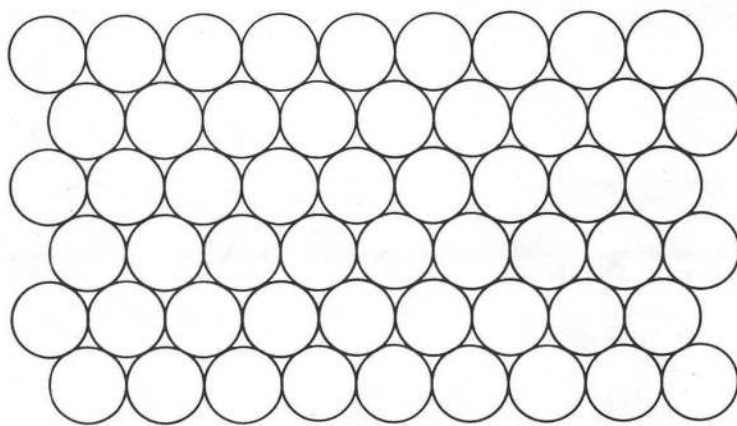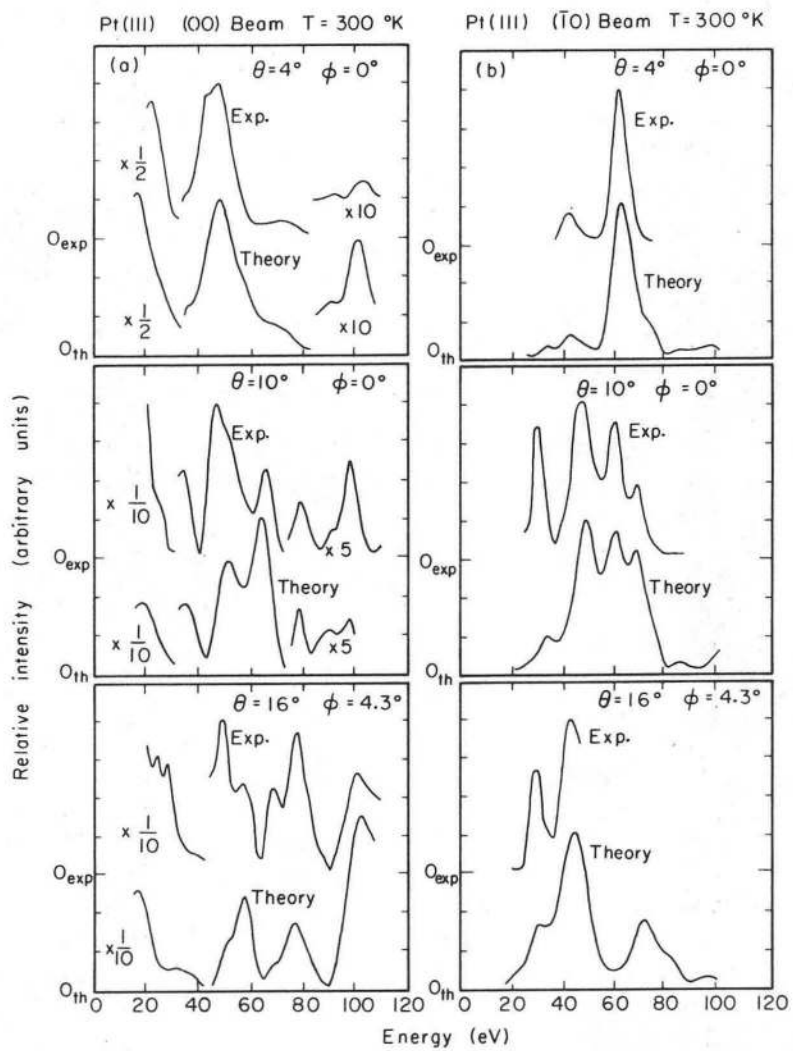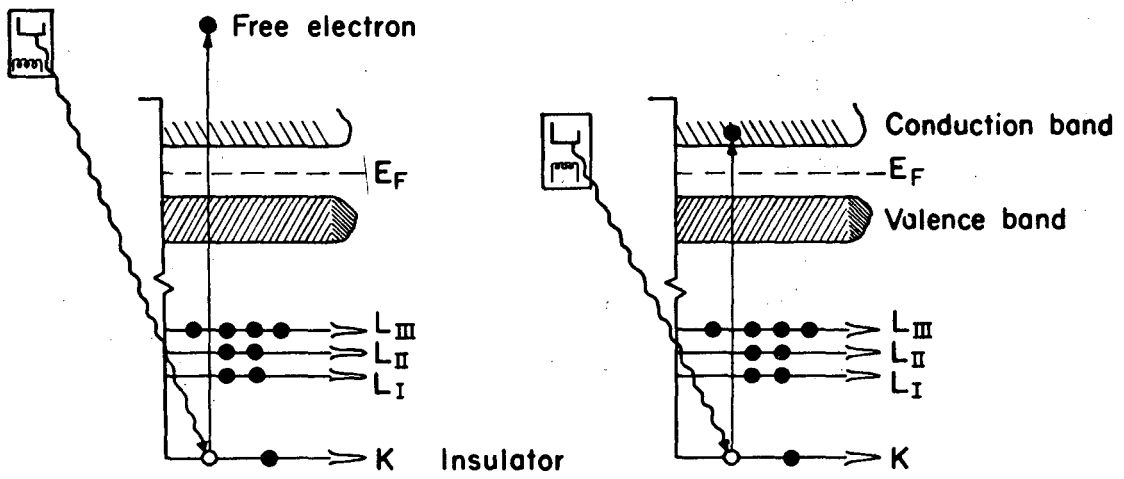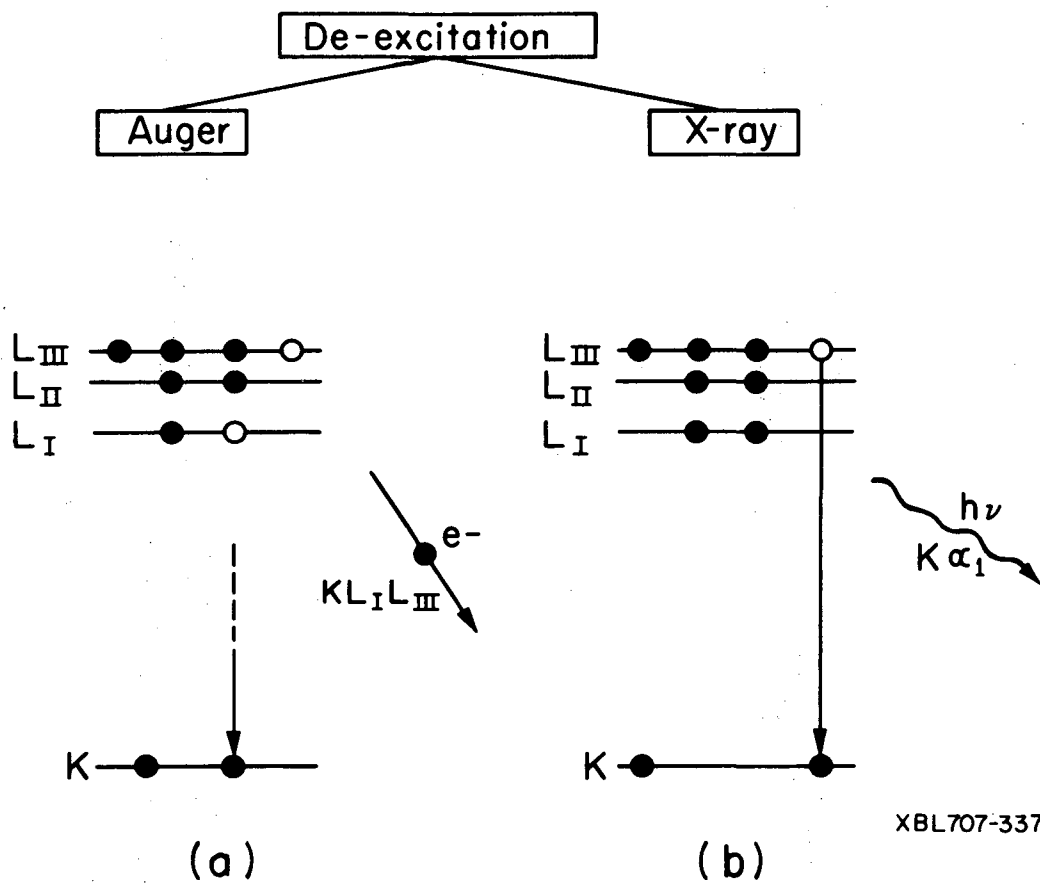
XBL707-3377

XBL712-2764

Fig. 13
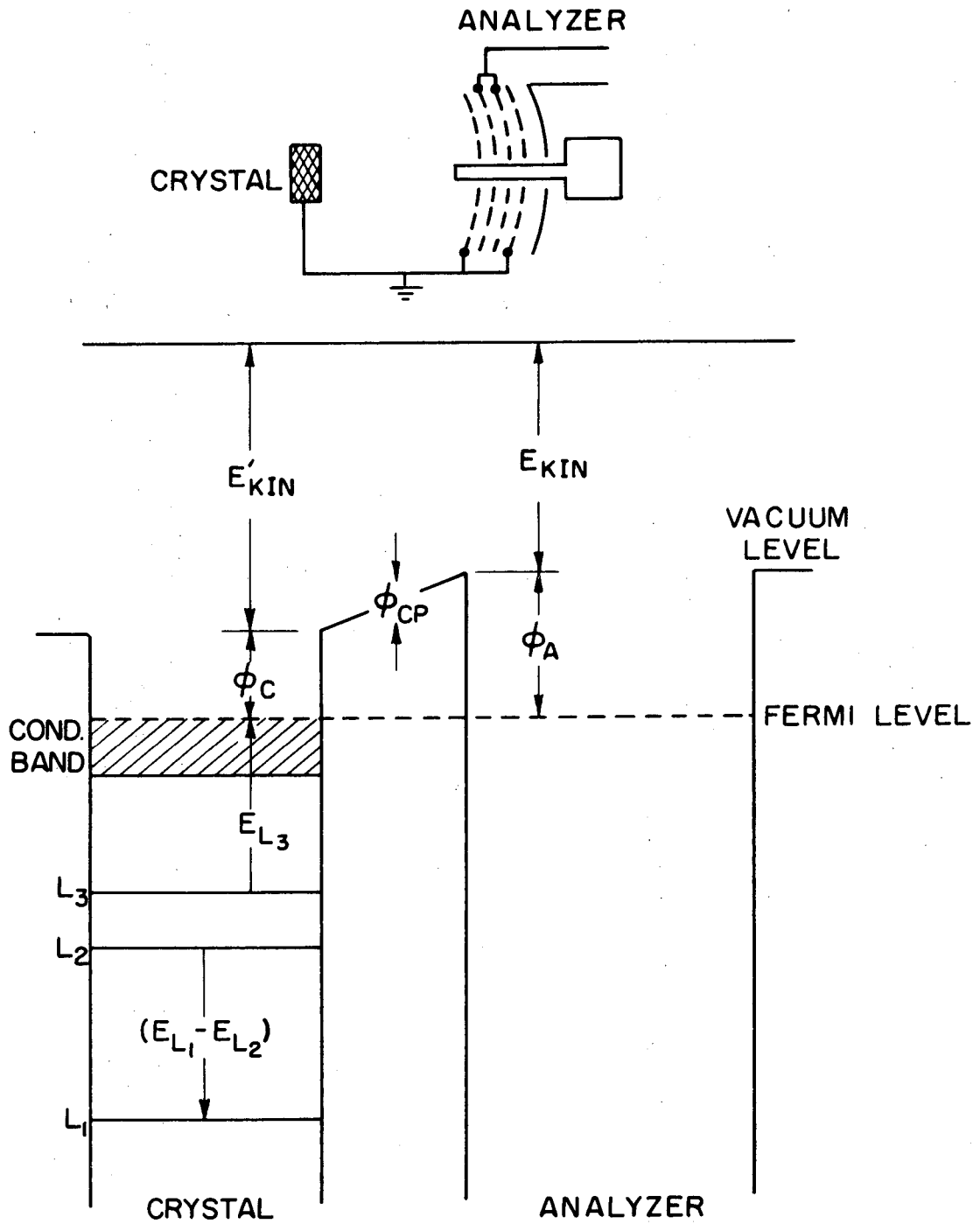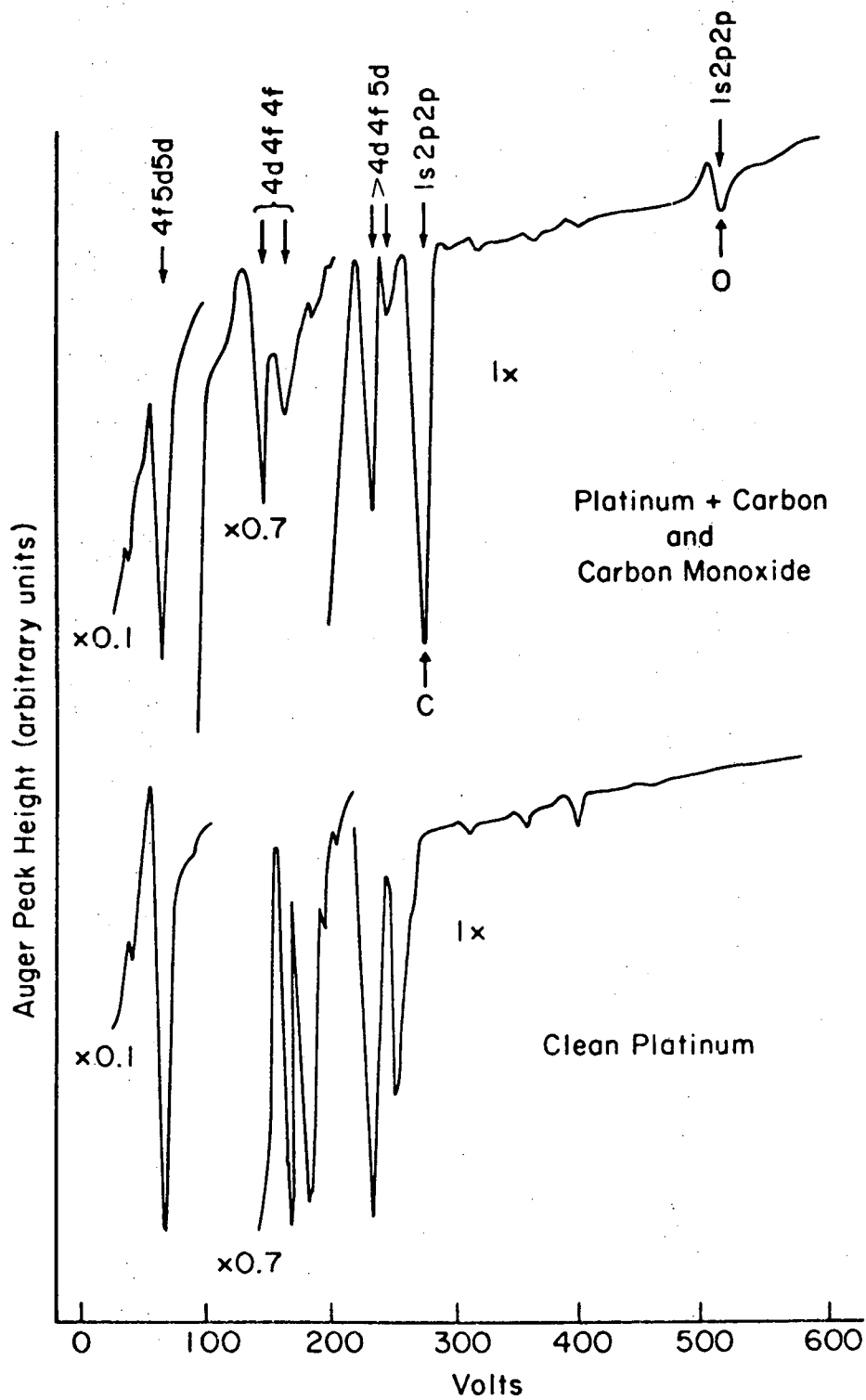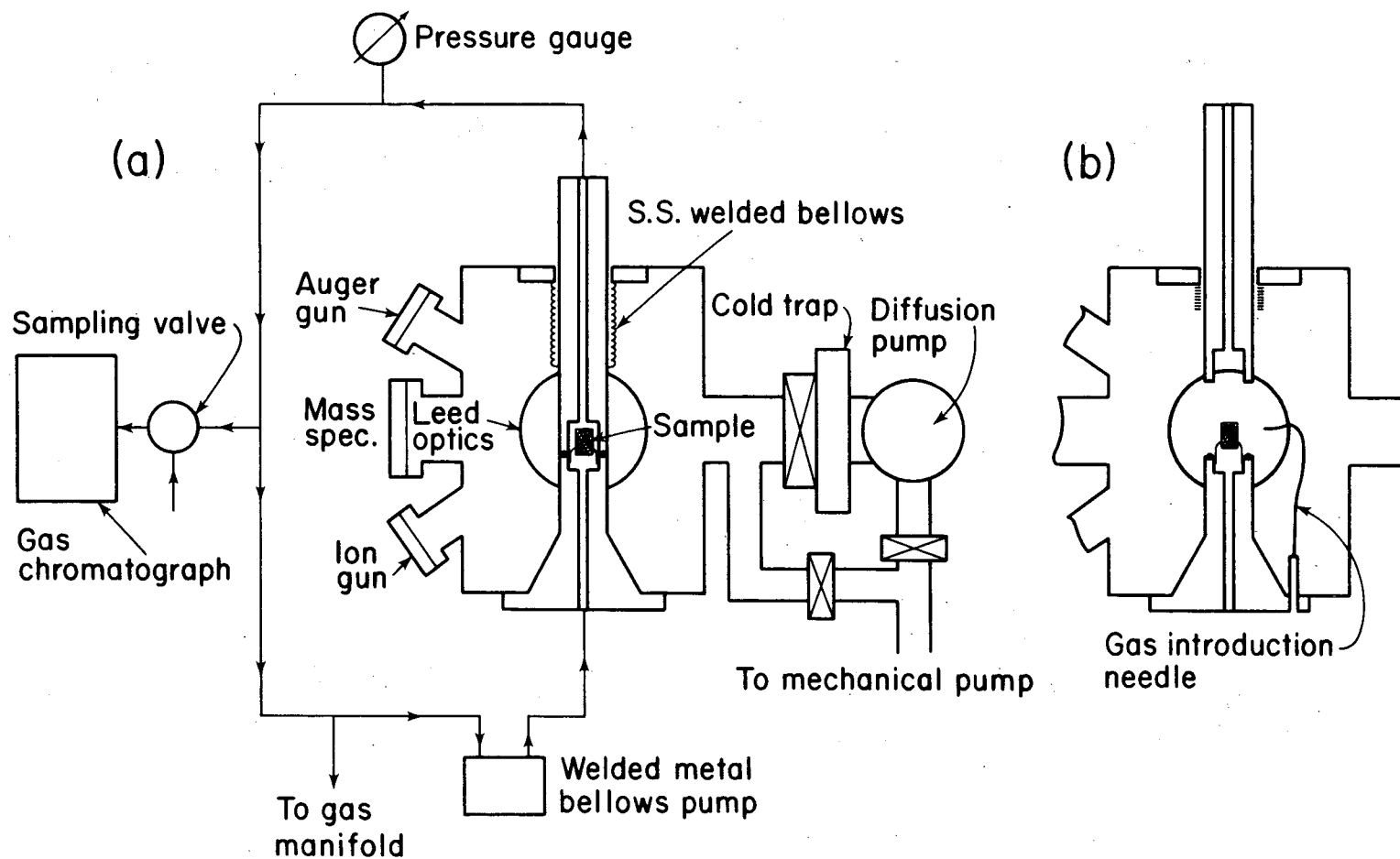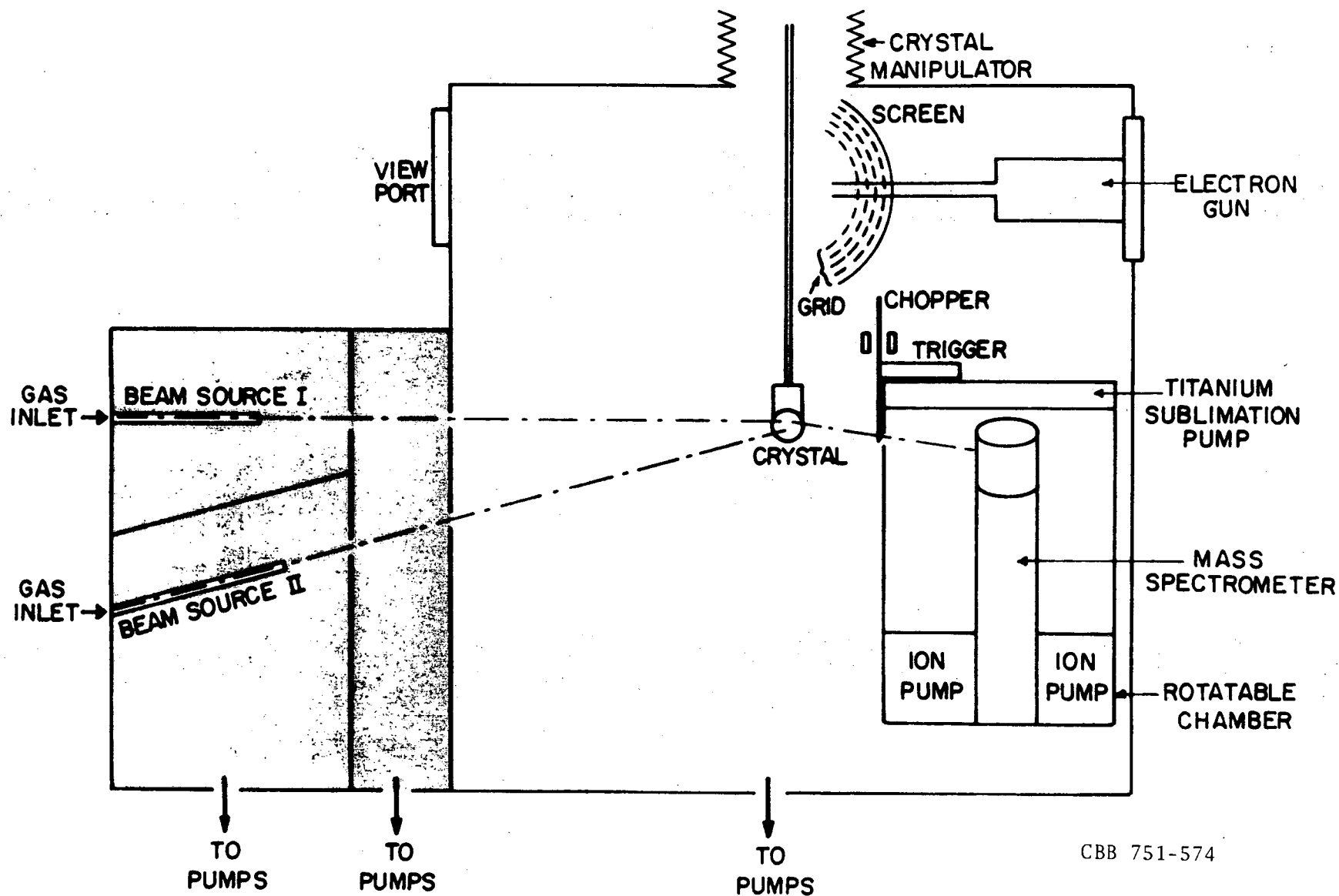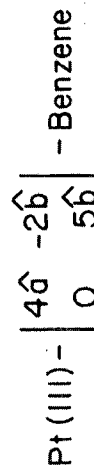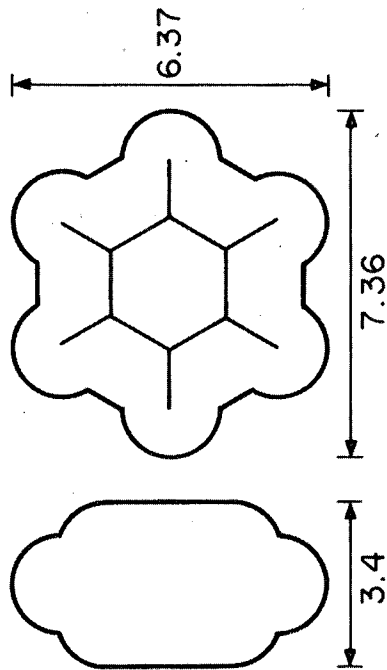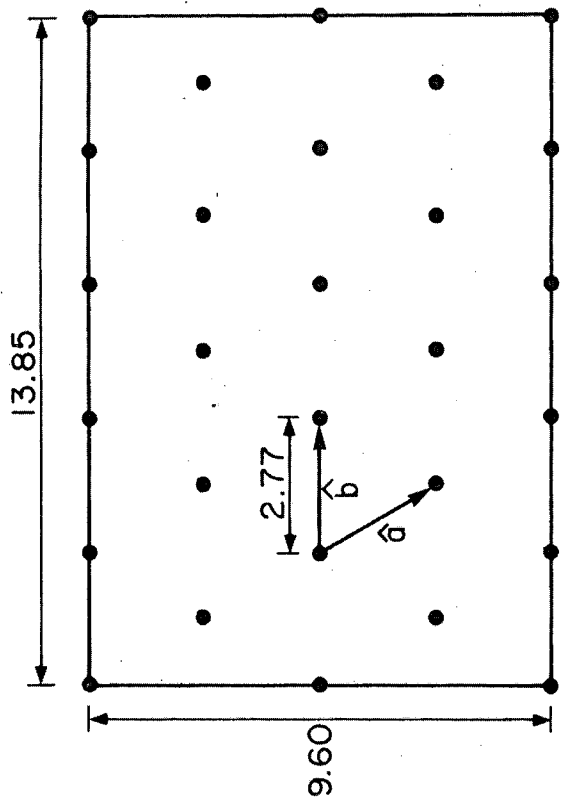
Fig. 14

XBL 733-5928

Fig. 15

XBL 725-6338

Fig. 16

XBL 756-3160

CRYSTAL
MANIPULATOR

SCREEN

VIEW
PORT

ELECTRON
GUN

GRID

CHOPPER

TRIGGER

GAS
INLET

BEAM SOURCE I

TITANIUM
SUBLIMATION
PUMP

CRYSTAL

GAS
INLET

BEAM SOURCE II

MASS
SPECTROMETER

ION
PUMP

ION
PUMP

ROTATABLE
CHAMBER

TO
PUMPS

TO
PUMPS

TO
PUMPS

CBB 751-574

Fig. 17

13.85

9.60

2.77

$\hat{b}$

$\hat{a}$

6.37

7.36

3.4

$Pt(III) - \left|\begin{array}{cc} 4\hat{a} & -2\hat{b} \\ 0 & 5\hat{b} \end{array}\right| - Benzene$

XBB 732-6634

Fig. 18

55V

A

48V

B

29V

C
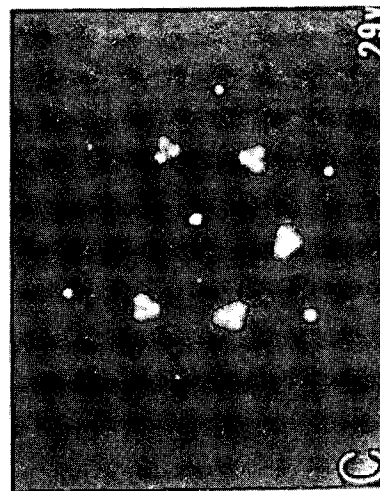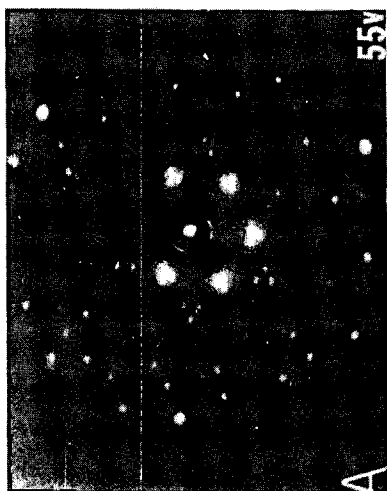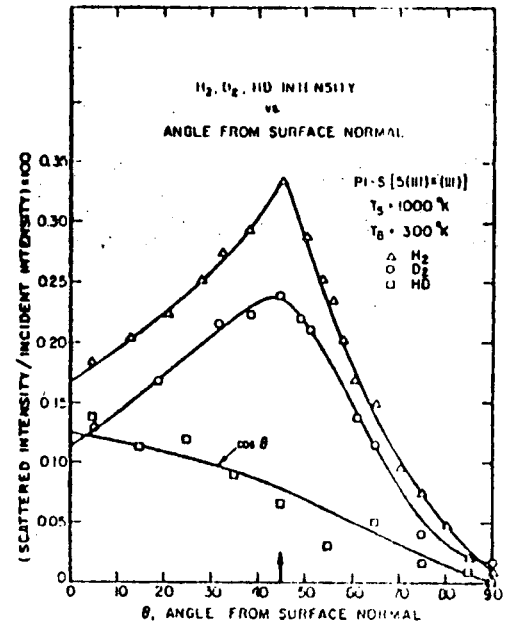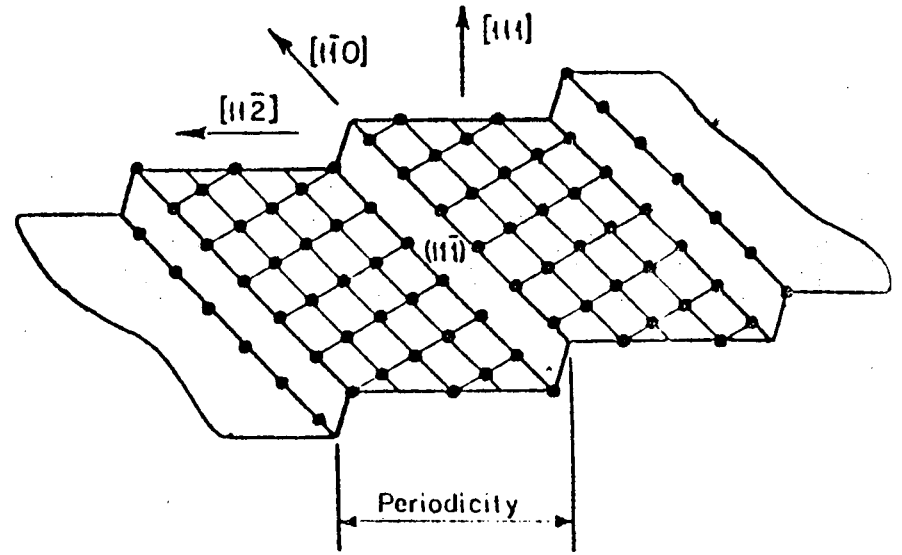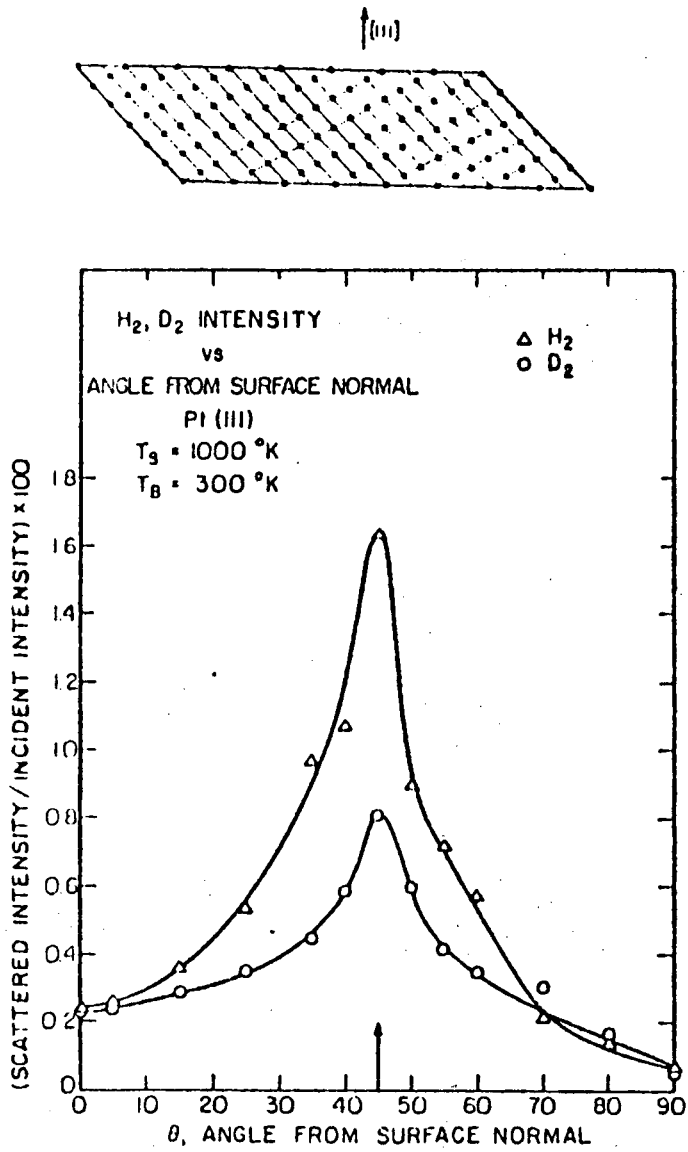
Fig. 19
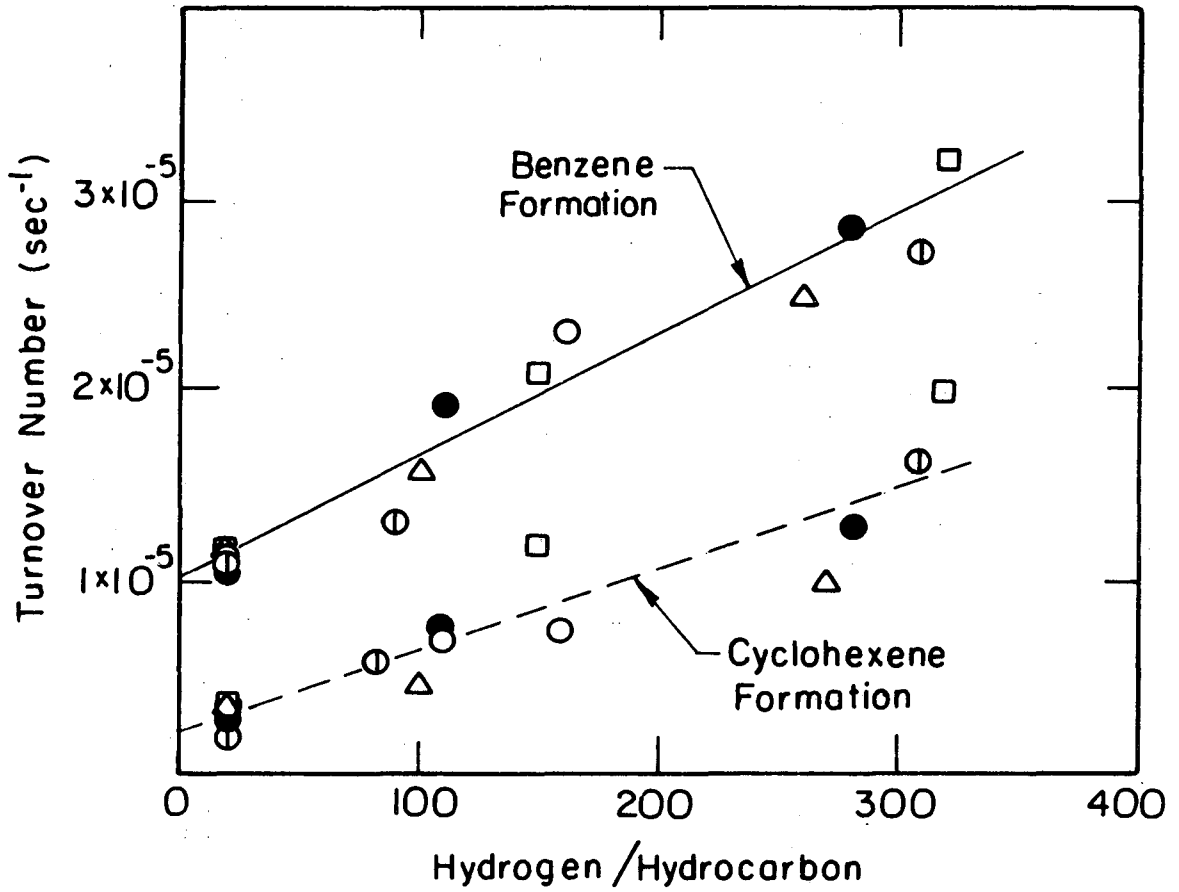
Fig. 20
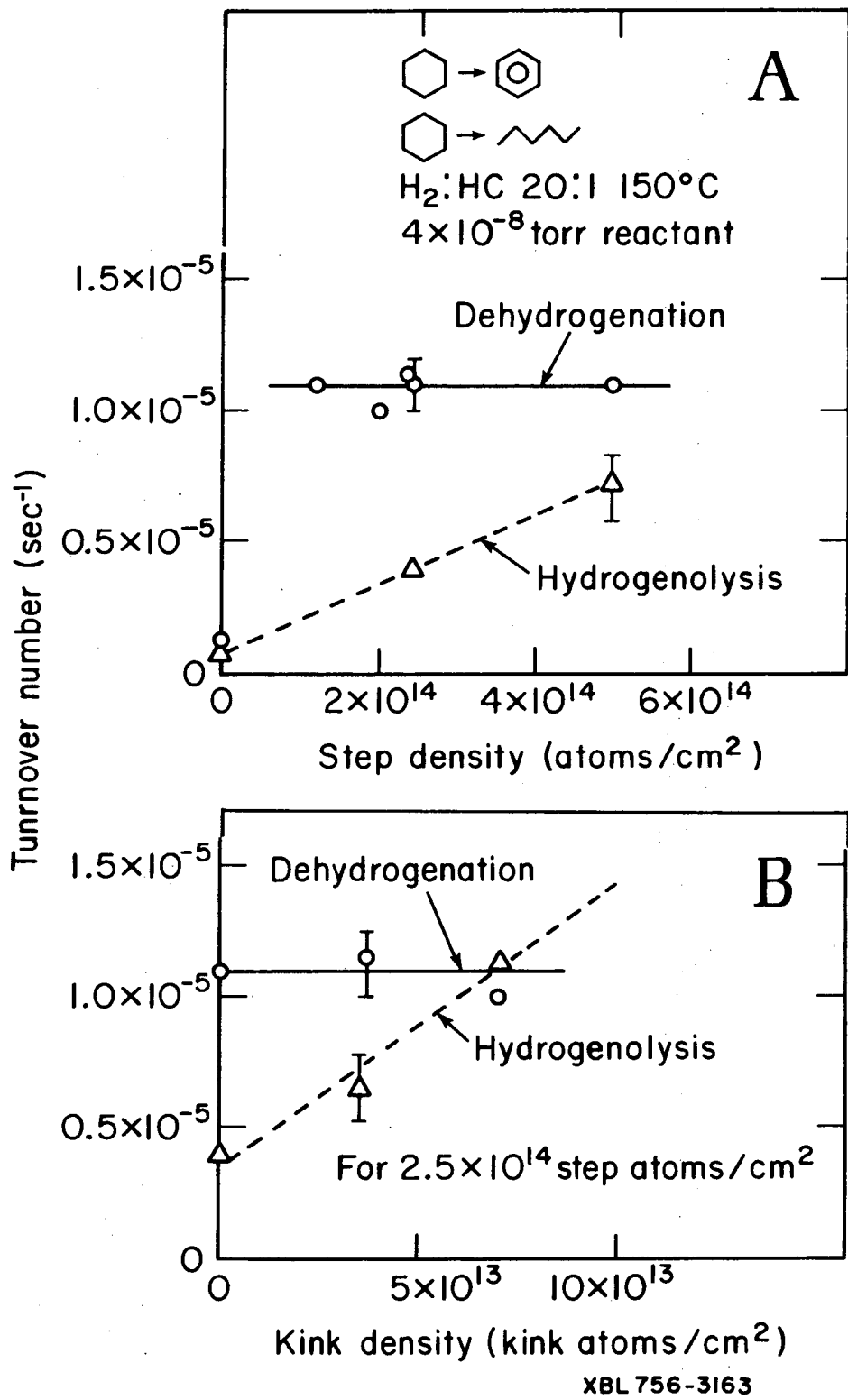
XBL 758-6870

Fig. 21
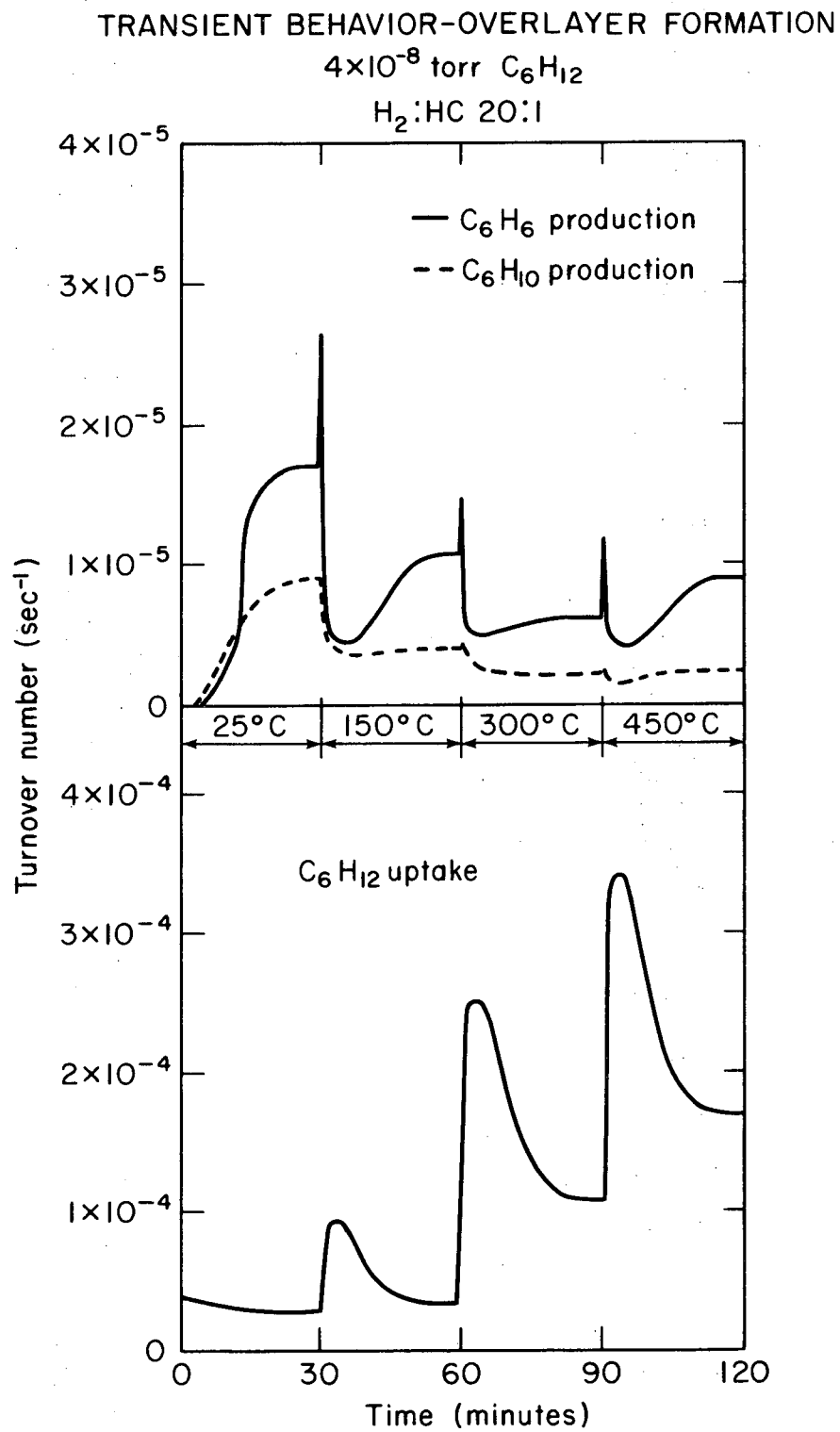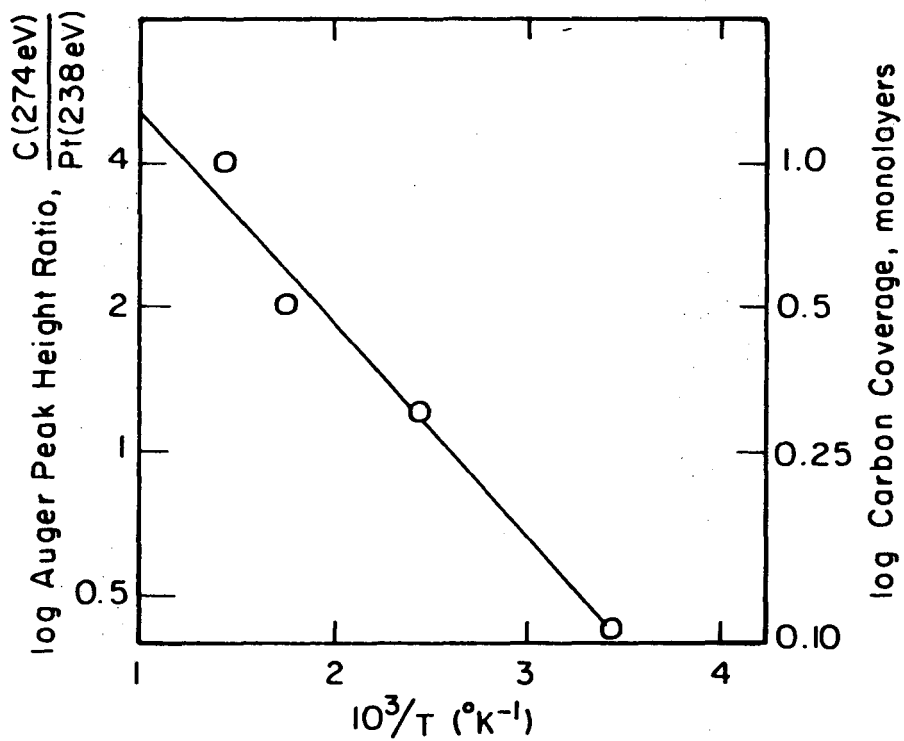
XBL 758-6869

Fig. 23

XBL 758-6868

Fig. 24

Fig. 25

Fig. 26

XBL756-3164

Poisoning of cyclohexene dehydrogenation

$H_2:HC$ 20:1 150°C

4×10^{-8} torr reactant

7(100)×(111) ordered overlayer

13(111)×(310) disordered overlayer

6(111)×(100) disordered overlayer

XBL 756-3165

Fig. 27

Fig. 28

CBB 756-4361

Fig. 29

XBL 756-6454